Příloha 1

KRÁLOVIČOVÁ, J., BARTŮNĚK, A., HOFMANN, J., KŘÍŽEK, T., KOZLÍK, P., ROUŠAROVÁ, J., RYŠÁNEK, P., ŠÍMA, M., SLANAŘ, O. Pharmacokinetic variability in pre-clinical studies: sample study with abiraterone in rats and implications for short-term comparative pharmacokinetic study designs. *Pharmaceutics*, 2022, 14, 3, 643.

pharmaceutics

MDPI

Article

Pharmacokinetic Variability in Pre-Clinical Studies: Sample Study with Abiraterone in Rats and Implications for Short-Term Comparative Pharmacokinetic Study Designs

Jana Královičová [1,*,†], Aleš Bartůněk [1,†], Jiří Hofmann [2], Tomáš Křížek [3], Petr Kozlík [3], Jaroslava Roušarová [1], Pavel Ryšánek [1], Martin Šíma [1] and Ondřej Slanař [1]

[1] Department of Pharmacology, First Faculty of Medicine, Charles University and General University Hospital in Prague, Albertov 4, 12800 Prague, Czech Republic; ales.bartunek@synavia.com (A.B.); jaroslava.rousarova@lf1.cuni.cz (J.R.); pavel.rysanek@lf1.cuni.cz (P.R.); martin.sima@lf1.cuni.cz (M.Š.); ondrej.slanar@lf1.cuni.cz (O.S.)
[2] Zentiva k.s., U Kabelovny 130, 10237 Prague, Czech Republic; jiri.hofmann@zentiva.com
[3] Department of Analytical Chemistry, Faculty of Science, Charles University, Hlavova 8, 12800 Prague, Czech Republic; tomas.krizek@natur.cuni.cz (T.K.); petr.kozlik@natur.cuni.cz (P.K.)
* Correspondence: jana.horinkova@lf1.cuni.cz
† These authors contributed equally to this work.

Abstract: One of the major concerns for all in vivo experiments is intra- and inter-subject variability, which can be a great source of inaccuracy. The aim of this study is, therefore, to estimate the ability of parallel vs. cross-over design studies in order to describe the relative pharmacokinetic performance of the studied drug formulations. We analyzed the data from a drug development program that examined the performance of innovative abiraterone acetate formulations against the identical reference product in three stages. In stages 1–3, groups A–F were dosed with the reference product once in a parallel manner. Stage 4 was performed to evaluate the intra-individual variability (IIV) by repeated administration of the reference product to the same animals. Although the geometric mean (90% CI) values of abiraterone AUC_{last} in groups A–F were similar to the IIV group (24.36 (23.79–41.00) vs. 26.29 (20.56–47.00) mg/mL·min·g), the results generated in the isolated parallel groups provided imprecise estimates of the true AUC_{last} values ranging from 9.62 to 44.62 mg/mL·min·g due to chance. Notably, in 4 out of 15 possible pair comparisons between the parallel groups, the confidence intervals did not include 100%, which is the true ratio for all comparisons tested after identical formulation administration to all groups. A cross-over design can significantly improve the methodology in short-term comparative pre-clinical pharmacokinetic studies, and can provide more precise and accurate results in comparison to more traditional pre-clinical study designs.

Keywords: abiraterone; variability; pharmacokinetics; cross-over design; rat; in vivo study

Citation: Královičová, J.; Bartůněk, A.; Hofmann, J.; Křížek, T.; Kozlík, P.; Roušarová, J.; Ryšánek, P.; Šíma, M.; Slanař, O. Pharmacokinetic Variability in Pre-Clinical Studies: Sample Study with Abiraterone in Rats and Implications for Short-Term Comparative Pharmacokinetic Study Designs. *Pharmaceutics* **2022**, *14*, 643. https://doi.org/10.3390/pharmaceutics14030643

Academic Editor: Antonello Di Paolo

Received: 17 February 2022
Accepted: 13 March 2022
Published: 15 March 2022

1. Introduction

Pre-clinical pharmacokinetic (PK) studies play a key role in several stages of pharmaceutical research, as they are currently an irreplaceable source of basic pharmacokinetic data, and they also allow a relationship to be established between exposure and drug-induced toxicity (toxicokinetics) before a new molecule is administered to humans [1,2]. Furthermore, animal studies are sometimes needed during the development of innovative drug formulations in order to confirm the performance of the drug formulation, estimated from in vitro and modelling studies [3].

Clinical pharmacokinetic trials currently have a rather sophisticated methodology, which is guided by major regulatory agencies worldwide. The methodology of clinical studies has been cultivated for a long time to deliver reliable, accurate and precise data, while minimizing study subjects' exposure to test compounds. Therefore, the methodology

of a clinical pharmacokinetic study is inherently dependent on the hypothesis tested and the aim of the study.

On the other hand, relatively little attention has been paid to the optimal ways of performing the pre-clinical pharmacokinetic studies. When planning these studies, parallel design is usually adopted [4,5]. The limited sampling strategy has also gained popularity in recent years, as it enables pharmacokinetic data to be obtained in a simplified model [6,7]. However, these approaches are often chosen without further considerations and irrespective of the aim of the study.

One of the major concerns for all in vivo experiments is intra- and inter-subject variability, which can be a great source of inaccuracy. Gender, age, weight, hormonal status and eating habits are just a few examples of the factors which introduce variability into the study data [8]. Actual status of the gastrointestinal system, (e.g., gastric and intestinal pH, gastric emptying and intestinal transit, bacterial colonization or surface area [9–11]), renal function, hepatic abundance and drug transporters further contribute to the actual fate of a compound in the body [12]. Furthermore, genetic polymorphisms within the genes which encode for drug-metabolizing enzymes or transporters may further substantially affect drug absorption, distribution, or elimination.

As a result, it is almost impossible to ensure the same inner and outer conditions for each subject enrolled in a study. Previous experiments with mice have shown that animals act differently across laboratories despite strict standardization [13]. It has also been demonstrated that mice phenotypes can fluctuate to the extent that the obtained results may differ between batches [14].

We hypothesized that to obtain precise and accurate results during pre-clinical pharmacokinetic studies aimed at comparing drug formulation PK performance, a parallel study design may not be appropriate, and a cross-over design of the pharmacokinetic experiment that limits the consequences of inter-subject variability should be chosen.

Therefore, our aim was to estimate the ability of parallel vs. cross-over design studies to describe the relative pharmacokinetic performance of the studied drug formulations.

2. Materials and Methods

2.1. Materials

For anesthesia, isoflurane (IsoFlo 250 mL, Zoetis/Pfizer, Prague, Czech Republic), ketamine (Narkamon 100 mg/mL inj sol, Bioveta, Ivanovice na Hané, Czech Republic), and xylazine (Rometar 20 mg/mL inj sol, Bioveta, Ivanovice na Hané, Czech Republic) were used. Amoxicillin with clavulanic acid (Synulox RTU inj 100 mL, Zoetis/Pfizer, Prague, Czech Republic) was used as a perioperative antibiotic, ketoprofen (Ketodolor inj 100 mL, LeVet Pharma b.v., Oudewater, The Netherlands) as an analgesic, and enoxaparin (Clexane inj 4000 IU/0.4 mL, Sanofi-Aventis, Prague, Czech Republic) and heparin (Heparin Léčiva inj 1 × 10 mL/50KU, Zentiva, Prague, Czech Republic) as anticoagulants. Surgical skin glue was obtained from Henry Schein (Brno, Czech Republic). The reference formulation of abiraterone acetate (Zytiga, Janssen-Cilag Spa, Latina, Italy) was provided by Zentiva, k.s. (Prague, Czech Republic). Before dosing, the tablets were crushed and the powder was placed into gelatin capsules containing 4.2 mg of abiraterone acetate.

2.2. Animals

Male Wistar rats were purchased from Velaz (Prague, Czech Republic). They were kept under standard conditions with a 12 h light–dark cycle, 22 ± 2 °C temperature, and 50 ± 10% relative humidity. They had ad libitum access to water and a standard granulated diet, with the exception of 4 h before and after dosing with abiraterone acetate. The rats were treated in compliance with the Guiding Principles for the Use of Animals at Charles University, First Faculty of Medicine, and all measures were taken to minimize animal suffering. The experimental animal project was approved by the Ministry of Education, Youth and Sports, Czech Republic (MSMT-9445/2018-8).

2.3. Experimental Design and Procedures

We analyzed the data from a drug development program that examined the performance of innovative abiraterone acetate formulations against the identical reference product (Zytiga, Janssen-Cilag Spa, Latina, Italy) in 3 stages. Stage 4 was performed to evaluate the intra-individual variability by repeated administration of the reference product to the same animals. For more detailed information about each stage, see Table 1.

Table 1. Summary of formulations administered to rats and number of rats enrolled into each stage and group. R–reference formulation, T1–T3—innovative formulations.

Stage	Group	Formulations	Number of Rats
1	A	R/T1	4
	B	R/T1	4
2	C	R/T2	6
	D	R/T2	4
3	E	R/T3	3
	F	R/T3	3
4	IIV	R/R	6

Each stage was conducted in a randomized, single-dose, single-center, laboratory-blinded, two-period, cross-over design comparing bioavailability between the test and reference formulations. For the present analysis, animals that were dosed with the reference product in stages 1–3 are considered as individual groups A–F (n = 24). These animals were administered the reference product on one occasion only, which allows for a parallel comparison of the reference product bioavailability between the groups A–F.

In stage 4, the identical reference product was administered to animals (n = 6) in both periods in order to investigate the intra-individual variability of abiraterone acetate in a single-dose, single-center, laboratory-blinded, two-period, cross-over design. The group of animals dosed in Stage 4 is labelled as the intra-individual variability (IIV) group.

Prior to dosing, the rats underwent a surgery where *A. carotis* was cannulated with catheters made of medical-grade polyurethane (1.9-3Fr, Instech Laboratories, Plymouth Meeting, PA, USA). Before the surgery, the rats were anesthetized by isoflurane (2.5–5%) following xylazine (5 mg/kg, i.m.) and ketamine (100 mg/kg, i.m.). Amoxicillin with clavulanic acid (140/35 mg/kg, s.c.) was applied to prevent infection during the surgery and ketoprofen (6 mg/kg, s.c.) was used to minimize post-surgery pain. Catheters were flushed with physiological saline (200 µL), heparin (50 µL), and sealed with heparinized glycerol every day after surgery to avoid clogging.

After three days, the rats were randomly placed into groups and a formulation containing abiraterone acetate was administered via oral gavage together with 1 mL of water. To reach a fasted state, access to food was restricted between 4 h before and 4 h after dosing. After drug dosing via gavage, blood samples (100 µL) were collected for 7 h (pre-dose, 0.5, 1, 1.5, 2, 2.5, 3, 4, 5 and 7 h). Blood withdrawn was replaced by physiological saline (100 µL), and catheters were flushed by heparinized saline (1250 IU/mL) and sealed by heparinized glycerol. Centrifugation of blood samples was performed (4500× g, 4 °C, 10 min) and obtained serum aliquots were stored at −80 °C until further analysis. A washout period of at least forty-eight hours was kept between study periods, based on the previously reported half-life in rats (so that there are at least five half-lives between the periods) [15]. Sufficient length of the washout was confirmed by measuring plasma levels of abiraterone below LLOQ before starting the second period.

2.4. Analytical Methods

For the determination of abiraterone, plasma samples were processed as follows. In 25 µL of plasma, proteins were precipitated by the addition of 100 µL of acetonitrile (containing 32 ng/mL abiraterone-d4 as an internal standard). The mixture was vortexed and centrifuged at 9800× g for 10 min. The supernatant was injected into the UHPLC-MS/MS

system. Nexera X3 UHPLC coupled with Triple Quad 8045 MS (Shimadzu, Kyoto, Japan) was used with Kinetex EVO C18 column, 100 × 2.1 mm, 1.7 µm particles (Phenomenex, Torrance, CA, USA), thermostated at 40 °C. The mobile phase (A: 0.1% formic acid in deionized water, B: acetonitrile) was pumped in at a flow rate of 0.35 mL/min, and the following gradient program was applied (min/% B) 0/30, 1.5/90, 3.0/90, 3.5/30, 6.0/30. The autosampler temperature was maintained at 10 °C and the sample injection volume was 2 µL. Effluent from the column was directed to the MS ion source between 2.6 and 3.8 min only. For the rest of the time, the effluent was directed to the waste. The MS was operated with positive electrospray ionization, with ion source settings as follows: a nebulizing gas flow of 3 L/min, a heating gas flow of 10 L/min, an interface temperature of 300 °C, a desolvation line temperature of 250 °C, a heat block temperature of 400 °C, and a drying gas flow of 10 L/min. A multiple reaction monitoring (MRM) mode was used for abiraterone quantification. An MRM transition of 350.3 > 156.1 (Q1 pre-bias—17 V, Q3 pre-bias—27 V, collision energy—57 V) was monitored for abiraterone and transition 354.3 > 160.1 (Q1 pre-bias—17 V, Q3 pre-bias—30 V and collision energy—57 V) was monitored for abiraterone-d4. The method was validated concerning linearity, detection limit, accuracy, precision, recovery, selectivity, and matrix effects. A seven-point calibration curve was constructed using the analyte-to-internal standard peak area ratio. Weighted least-squares linear regression ($1/x^2$ weighting factor) was used. The developed method was linear in the range of 0.5–600 mg/mL ($R^2 > 0.9996$). The detection limit was 0.03 ng/mL (determined as a concentration providing a signal corresponding to 3.3 times blank matrix baseline noise), which was sufficient for the determination of abiraterone in plasma samples. The accuracy expressed as the relative error in % was within ±7.1%. Inter-day and intra-day precision expressed as relative standard deviations in % were between 2.4 and 5.2%. The selectivity of the method was assessed by analysis of six different plasma samples in the scan MS mode. No interfering compounds appeared within the retention time window of abiraterone. It should be noted that the method uses tandem MS in the MRM mode, which further increases the selectivity. Recovery of the method was checked by a comparison between the abiraterone concentration found in a plasma sample spiked with the standard before precipitation of proteins and the concentration found in a plasma sample spiked after precipitation of proteins, at three concentration levels (1, 50 and 250 ng/mL). The matrix effect was evaluated with six different plasma samples spiked with abiraterone standard after precipitation of proteins at two concentration levels (1 and 100 ng/mL). Abiraterone concentrations found in the plasma samples were between 80 and 108% of the concentration found in the spiked 80% acetonitrile. Calibration was performed every day and quality control samples were injected after every seven samples.

2.5. Data Analysis and Statistics

Phoenix WinNonlin® 8.3 (Certara, Princeton, NJ, USA) was used to analyze statistics and pharmacokinetics. For AUC_{last}, natural logarithmic transformation was used for all statistical inference. For AUC_{last}, non-compartmental analysis using linear trapezoidal rule with linear interpolation was employed. For parallel comparisons of groups A–F, the two-one-sided t-tests rely on the assumption that the observations for the groups come from distributions that have equal variances. This assumption is taken since an identical reference formulation was administered to all groups. For the cross-over comparison in the paired design in stage 4, the ANOVA model with the fixed effects subject and period was used. The residual variance from the model was used to construct a 90% confidence interval (CI). For all pharmacokinetic calculations, actual sampling times and ln-transformed concentration data normalized by animal weight were used. All figures and histograms were constructed using GraphPad Prism 9.3.1 (GraphPad Software, San Diego, CA, USA).

2.6. Simulation Methods

All simulations were performed in R [16], version 4.0.2, by using the Mersenne Twister algorithm for random number generation. In brief, individual test-to-reference ratios were simulated on the basis of log-normal distribution, where the simulated geometric means ratio (GMR) was 1 and the coefficient of variation was 0.73 and 0.96 for cross-over and parallel design, respectively. These variations were observed in our program for the reference formulation Zytiga. In the case of parallel design, homoscedasticity and balanced treatment groups were respected. The total sample size corresponded to 24 for both designs. For each design, 10,000 simulations were conducted, and the proportion of ratios falling within the standard bioequivalence acceptance range 0.8 to 1.25 was expressed in percentage.

3. Results

In stages 1–3, groups A–F were dosed with the reference product once in a parallel manner. The geometric mean AUC_{last} values of the groups A–F ranged from 9.62 to 44.62 mg/mL·min·g. In stage 4, the group labelled IIV was administered with the same reference product in two periods, described as IIV1 and IIV2. The geometric means of AUC_{last} values are presented for all the groups in Figure 1. The geometric mean (90% CI) AUC_{last} value of groups A–F was 24.36 (23.79–41.00) mg/mL·min·g, and the geometric mean (90% CI) AUC_{last} value of IIV groups was 26.29 (20.56–47.00) mg/mL·min·g.

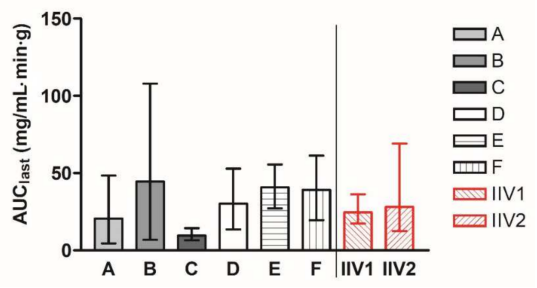

Figure 1. Geometric mean AUC_{last} (90% CI) of individual parallel groups A–F within the program with abiraterone acetate reference product in fasted state. To the right of the division line, AUC_{last} values of group IIV are presented for periods 1 and 2 separately.

All possible parallel comparisons between groups A–F were calculated, as well as the comparison of period 2 against period 1 for the IIV study. AUC_{last} ratios and 90% CI are presented in Figure 2.

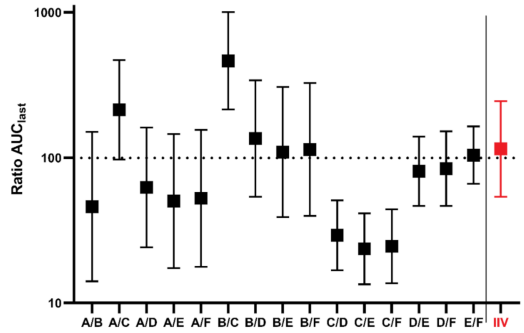

Figure 2. Results of bioequivalence evaluations, and AUC_{last} ratios with 90% CI between groups A–F in parallel design. To the right of the division line is the group IIV AUC_{last} ratio to compare periods from cross-over design. Log scale was used on y axis.

Simulations of the probability that the resulting ratio would fall into the range of 80–125% (standard bioequivalence acceptance range), based on the observed inter-

individual variability from groups A–F or IIV in parallel or cross-over design and a sample size of 24 animals, are summarized in Table 2. Histograms showing the distribution of the resulting ratios in cross-over and parallel designs are presented in Figure 3.

Table 2. Parameters used in simulations with calculated probability that the resulting ratio would fall into the range of 80–125%. CV: intra-subject for cross-over, total for parallel.

	Cross-Over	Parallel
Simulations	10,000	10,000
Sample size	24	24
CV	73%	96%
Ratios 80–125%	76%	49%

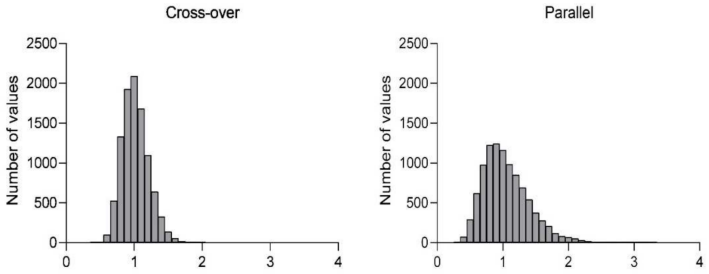

Figure 3. Histograms showing distribution of the resulting ratios in cross-over and parallel designs.

4. Discussion

When any pre-clinical study is being planned or performed, the 3R principles must be followed. These principles include a reduction in animal use, a replacement of other methods whenever feasible, and minimized pain felt by the animals to the greatest possible extent [17]. In parallel with the 3R principles, more attention has been paid in recent years to the design of pre-clinical pharmacokinetic studies [18,19]. Some attempts to standardize the procedures used in these studies are emerging to improve the quality of the obtained data [3,20]. Our work was conducted to elaborate on the impact of inter- and intra-subject variability within comparative pre-clinical studies, which is an important factor that may substantially affect the obtained results. Abiraterone has been selected as a model compound belonging to BCS class IV, which is a class with reported high inter- as well as intra-animal pharmacokinetic variability [9].

Our analysis indicates that, although the geometric mean (90% CI) values of abiraterone AUC_{last} in the parallel groups A–F were similar to the IIV group (24.36 (23.79–41.00) vs. 26.29 (20.56–47.00) mg/mL·min·g) after the administration of the identical reference formulation, the results generated in the isolated parallel groups provided likely imprecise estimates of the true AUC_{last} values ranging from 9.62 to 44.62 mg/mL·min·g only due to chance. The differences between individual groups were extensive, with a maximum value of geometric means more than 4 times higher than the minimum value. Notably, in 4 out of 15 possible pair comparisons between the parallel groups, the confidence intervals did not include 100%, which is the true ratio for all comparisons tested after identical formulation administration to all groups. That means that in 27% of the studies, identical formulations would be claimed to provide different absorption characteristics compared to the reference formulation. This observation represents a practical example of false positive results that may be generated in studies in parallel design with a limited number of animals enrolled, where it is not feasible to keep all factors standardized and balanced.

It has been described that, despite maximum efforts to standardize the conditions of animal experiments, there is still high variability between various batches in parallel design [13]. Within our work, the same conditions were maintained for all rats throughout their housing and experiments, and identical methodology, analysis, and other processes have been applied.

However, there was still high variability in response between the parallel groups, which can be explained by differences between the subjects and their behaviors: individual genetic background, susceptibility to stress, eating habits that may differ even when all rats are fed the same way, physical activity, and the number of physiological conditions. Many of these factors cannot be measured or controlled during the experiments.

Stage 4 of our program was designed as a cross-over study to investigate intra-subject variability. In this study, all animals received the same formulation in both periods, and the extent of absorption (AUC_{last}) from period 2 was compared to period 1 in a paired design. There was no huge difference between the periods, showing that the intra-subject variability was rather low. The coefficient of variability (CV) decreased from 96% in the parallel setting to 73% in the cross-over design. A decrease in variability of this magnitude is a significant factor for the sample size calculation of any planned experiment. For example, to test the significance of a 1.5-fold difference between groups with 80% ($\beta = 0.2$) power and $\alpha = 0.05$, a minimal sample size of 116 and 66 probands was estimated when the CV is 96% and 73%, respectively. The use of a cross-over design would, therefore in such a case, allow the number of animals to be reduced by almost one half.

Additionally, for both parallel and cross-over design, simulations of probability to obtain accurate results confirming equivalence were created. For both designs, the same sample size ($n = 24$) was tested, with the CV obtained from our current work presented. The results show that 76% of runs generated ratios within 80–125% in cross-over design. In the case of parallel design with the same total number of animals, the number of ratios within the 80–125% range falls to 49%. In other words, for comparative studies of this size, there is almost 80% probability of achieving the correct conclusion of similar PK performance between both administrations of identical formulation, while only 50% of studies will generate the same true conclusion in the parallel group design.

Our observation corresponds to the known consequences of variability in human comparative pharmacokinetic studies. For human comparative studies, cross-over design has been recommended as the gold-standard methodology by both the Food and Drug Administration (FDA) and the European Medicines Agency (EMA) for several decades [21–23].

The cross-over design brings an indisputable advantage, as a smaller sample size is sufficient to provide reliable results because each subject serves also as its own control. In such a design, a large component of variability that is related to inter-individual differences is eliminated. The choice of such a design in comparative pre-clinical study also fits in with attempts to minimize the number of experimental animals (e.g., the Animal Welfare Act originally from 1966 [17] or Directive 2010/63/EU of the European Parliament and of the Council from 2010 [24]). On the other hand, there is a disadvantage to the cross-over methodology in small animals such as rats, i.e., the need for mature surgical techniques and advanced peri-operative care of the animals in order to minimize blood loss and maintain the animals in good overall status throughout the study.

Contrary to our findings, Daublain et al. reported the rather surprising observation that intra-animal exposures were found to be more variable than inter-animal exposures in their analysis of PK studies with more than 16,000 research compounds [9]. However, this observation is likely to be a consequence of the long duration of the PK studies included in the analysis by Daublain et al., such as toxicokinetic studies, which also introduce the factor of rapid ontogenesis in rats likely to override a single-time-point variability. Therefore, our findings only apply to short-term animal experiments, where the ontogenetic changes of animals do not substantially affect the study animals.

5. Conclusions

To conclude, the traditional approach to comparative pre-clinical pharmacokinetic studies brings neither the required accuracy nor precision, if the 3R principles are followed and the number of animals is kept acceptably small. Adopting a cross-over design is one solution to ensure a high quality of data while reducing the number of animals needed for the study. There are a few technical disadvantages of this more complicated study design,

especially the need for more advanced care of the animals and the necessity to minimize the blood sample volumes. Despite this, a cross-over design can significantly improve the methodology in short-term comparative pre-clinical pharmacokinetic studies, and can provide more precise and accurate results in comparison to more traditional pre-clinical study designs.

Author Contributions: Investigation, J.K., J.R., P.R. and M.Š.; formal analysis, A.B., J.H., J.K., M.Š., T.K. and P.K.; methodology, J.K., T.K., P.K., J.R., P.R., M.Š. and O.S.; software, J.H.; supervision, O.S.; visualization, J.K. and A.B.; writing—original draft, J.K., A.B., J.H., T.K. and P.K.; writing—review & editing, J.R, P.R., M.Š. and O.S.; funding acquisition, O.S. All authors have read and agreed to the published version of the manuscript.

Funding: The work was supported by the Charles University Cooperatio Program (research area PHAR) and grant no. SVV 260 523.

Institutional Review Board Statement: The animals were treated in compliance with the Guiding Principles for the Use of Animals in Charles University, First Faculty of Medicine. The experimental animal project was approved by the Ministry of Education, Youth and Sports, Czech Republic (MSMT-9445/2018-8) on 01 June 2018.

Data Availability Statement: Data supporting the findings of this study are available from the corresponding author upon reasonable request.

Acknowledgments: J.K., J.R. and P.R. wish to acknowledge the support provided by the Pharmaceutical Applied Research Centre (the PARC) for their scientific work.

Conflicts of Interest: The authors declare that they have no known competing financial interests or personal relationships that have appeared to influence the work reported in this paper.

References

1. Singh, S.S. Preclinical pharmacokinetics: An approach towards safer and efficacious drugs. *Curr. Drug Metab.* **2006**, *7*, 165–182. [CrossRef] [PubMed]
2. Buchanan, J.R.; Burka, L.T.; Melnick, R.L. Purpose and guidelines for toxicokinetic studies within the National Toxicology Program. *Environ. Health Perspect.* **1997**, *105*, 468–471. [CrossRef] [PubMed]
3. Jaiswal, S.; Sharma, A.; Shukla, M.; Vaghasiya, K.; Rangaraj, N.; Lal, J. Novel pre-clinical methodologies for pharmacokinetic drug-drug interaction studies: Spotlight on "humanized" animal models. *Drug Metab. Rev.* **2014**, *46*, 475–493. [CrossRef] [PubMed]
4. Lin, L.C.; Pai, Y.F.; Tsai, T.H. Isolation of Luteolin and Luteolin-7-O-glucoside from *Dendranthema morifolium* Ramat Tzvel and Their Pharmacokinetics in Rats. *J. Agric. Food Chem.* **2015**, *63*, 7700–7706. [CrossRef] [PubMed]
5. Vrublova, E.; Vostalova, J.; Vecera, R.; Klejdus, B.; Stejskal, D.; Kosina, P.; Zdarilova, A.; Svobodova, A.; Lichnovsky, V.; Anzenbacher, P.; et al. The toxicity and pharmacokinetics of dihydrosanguinarine in rat: A pilot study. *Food Chem. Toxicol.* **2008**, *46*, 2546–2553. [CrossRef] [PubMed]
6. Zhu, X.H.; Jiao, J.J.; Zhang, C.L.; Lou, J.S.; Liu, C.X. Limited sampling strategy in rats to predict the inhibited activities of hepatic CYP3A. *Lab. Anim.* **2009**, *43*, 284–290. [CrossRef] [PubMed]
7. Wittenburg, L.A.; Thamm, D.H.; Gustafson, D.L. Development of a limited-sampling model for prediction of doxorubicin exposure in dogs. *Vet. Comp. Oncol.* **2014**, *12*, 114–119. [CrossRef] [PubMed]
8. Nicolas, J.M.; Espie, P.; Molimard, M. Gender and interindividual variability in pharmacokinetics. *Drug Metab. Rev.* **2009**, *41*, 408–421. [CrossRef] [PubMed]
9. Daublain, P.; Feng, K.I.; Altman, M.D.; Martin, I.; Mukherjee, S.; Nofsinger, R.; Northrup, A.B.; Tschirret-Guth, R.; Cartwright, M.; McGregor, C. Analyzing the Potential Root Causes of Variability of Pharmacokinetics in Preclinical Species. *Mol. Pharm* **2017**, *14*, 1634–1645. [CrossRef] [PubMed]
10. Yu, G.; Zheng, Q.S.; Li, G.F. Similarities and Differences in Gastrointestinal Physiology between Neonates and Adults: A Physiologically Based Pharmacokinetic Modeling Perspective. *AAPS J.* **2014**, *16*, 1162–1166. [CrossRef] [PubMed]
11. Lu, C.X.; An, X.X.; Yu, Y.; Jiao, L.R.; Canarutto, D.; Li, G.F.; Yu, G. Pooled Analysis of Gastric Emptying in Patients with Obesity: Implications for Oral Absorption Projection. *Clin. Ther.* **2021**, *43*, 1768–1788. [CrossRef] [PubMed]
12. Li, G.F.; Zheng, Q.S.; Yu, Y.; Zhong, W.; Zhou, H.H.; Qiu, F.; Wang, G.; Yu, G.; Derendorf, H. Impact of Ethnicity-Specific Hepatic Microsomal Scaling Factor, Liver Weight, and Cytochrome P450 (CYP) 1A2 Content on Physiologically Based Prediction of CYP1A2-Mediated Pharmacokinetics in Young and Elderly Chinese Adults. *Clin. Pharmacokinet.* **2019**, *58*, 927–941. [CrossRef] [PubMed]
13. Crabbe, J.C.; Wahlsten, D.; Dudek, B.C. Genetics of Mouse Behavior: Interactions with Laboratory Environment. *Science* **1999**, *284*, 1670–1672. [CrossRef] [PubMed]

14. Karp, N.A.; Speak, A.O.; White, J.K.; Adams, D.J.; de Angelis, M.H.; Hérault, Y.; Mott, R.F. Impact of temporal variation on design and analysis of mouse knockout phenotyping studies. *PLoS ONE* **2014**, *9*, e111239. [CrossRef] [PubMed]
15. Gurav, S.; Punde, R.; Farooqui, J.; Zainnudin, M.; Rajagopal, S.; Mullangi, R. Development and validation of a highly sensitive method for the determination of abiraterone in rat and human plasma by LC-MS/MS-ESI: Application to a pharmacokinetic study. *Biomed. Chromatogr.* **2011**, *26*, 761–768. [CrossRef] [PubMed]
16. R Core Team. R: A language and environment for statistical computing. In *R Foundation for Statistical Computing*; R Core Team: Vienna, Austria, 2020. Available online: https://www.R-project.org/ (accessed on 30 August 2021).
17. Animal Welfare Act. Available online: https://www.govinfo.gov/content/pkg/USCODE-2013-title7/pdf/USCODE-2013-title7-chap54.pdf (accessed on 9 September 2021).
18. Aarons, L.; Ogungbenro, K. Optimal design of pharmacokinetic studies. *Basic Clin. Pharmacol. Toxicol.* **2010**, *106*, 250–255. [CrossRef] [PubMed]
19. Takemoto, S.; Yamaoka, K.; Nishikawa, M.; Yano, Y.; Takakura, Y. Bootstrap method-based estimation of the minimum sample number for obtaining pharmacokinetic parameters in preclinical experiments. *J. Pharm. Sci.* **2010**, *99*, 2176–2184. [CrossRef] [PubMed]
20. Valic, M.S.; Halim, M.; Schimmer, P.; Zheng, G. Guidelines for the experimental design of pharmacokinetic studies with nanomaterials in preclinical animal models. *J. Control. Release* **2020**, *323*, 83–101. [CrossRef] [PubMed]
21. FDA. Guidance for Industry: Bioavailability and Bioequivalence Studies Submitted in NDAs or INDs—General Considerations. Available online: https://www.fda.gov/files/drugs/published/Bioavailability-and-Bioequivalence-Studies-Submitted-in-NDAs-or-INDs-%E2%80%94-General-Considerations.pdf (accessed on 9 September 2021).
22. FDA. Guidance for industry: Bioequivalence Studies with Pharmacokinetic Endpoints for Drugs Submitted under an ANDA. Available online: https://www.fda.gov/regulatory-information/search-fda-guidance-documents/bioequivalence-studies-pharmacokinetic-endpoints-drugs-submitted-under-abbreviated-new-drug (accessed on 9 September 2021).
23. EMA. Guideline on the Investigation of Bioequivalence. Available online: https://www.ema.europa.eu/en/documents/scientific-guideline/guideline-investigation-bioequivalence-rev1_en.pdf (accessed on 9 September 2021).
24. Directive 2010/63/EU of the European Parliament and of the Council on the Protection of Animals Used for Scientific Purposes. Available online: https://eur-lex.europa.eu/legal-content/EN/TXT/?uri=CELEX:02010L0063-20190626 (accessed on 11 September 2021).

Příloha 2

BOLESLAVSKÁ, T., RYCHECKÝ, O., KROV, M., ŽVÁTORA, P., DAMMER, O., BERÁNEK, J., KOZLÍK, P., KŘÍŽEK, T., HOŘÍNKOVÁ, J., RYŠÁNEK, P., ROUŠAROVÁ, J., KUTINOVÁ CANOVÁ, N., ŠÍMA, M., SLANAŘ, O., ŠTĚPÁNEK, F. Bioavailability enhancement and food effect elimination of abiraterone acetate by encapsulation in surfactant-enriched oil marbles. *AAPS J*, 2020, 22, 6, 1-12.

The AAPS Journal (2020) 22: 122
DOI: 10.1208/s12248-020-00505-5

Research Article

Bioavailability Enhancement and Food Effect Elimination of Abiraterone Acetate by Encapsulation in Surfactant-Enriched Oil Marbles

Tereza Boleslavská,[1,2] Ondřej Rychecký,[1,2] Martin Krov,[2] Pavel Žvátora,[1] Ondřej Dammer,[1] Josef Beránek,[1] Petr Kozlík,[3] Tomáš Křížek,[3] Jana Hořínková,[4] Pavel Ryšánek,[4] Jaroslava Roušarová,[4] Nikolina Kutinová Canová,[4] Martin Šíma,[4] Ondřej Slanař,[4] and František Štěpánek[2,5]

Received 29 June 2020; accepted 27 August 2020; published online 25 September 2020

Abstract. Abiraterone acetate has limited bioavailability in the fasted state and exhibits a strong positive food effect. We present a novel formulation concept based on the so-called oil marbles (OMs) and show by *in vitro* and *in vivo* experiments that the food effect can be suppressed. OMs are spherical particles with a core-shell structure, formed by coating oil-based droplets that contain the dissolved drug by a layer of powder that prevents the cores from sticking and coalescence. OMs prepared in this work contained abiraterone acetate in the amorphous form and showed enhanced dissolution properties during *in vitro* experiments when compared with originally marketed formulation of abiraterone acetate (Zytiga®). Based on *in vitro* comparison of OMs containing different oil/surfactant combinations, the most promising formulation was chosen for *in vivo* studies. To ensure relevance, it was verified that the food effect previously reported for Zytiga® in humans was translated into the rat animal model. The bioavailability of abiraterone acetate formulated in OMs in the fasted state was then found to be enhanced by a factor of 2.7 in terms of AUC and by a factor of 4.0 in terms of C_{max}. Crucially, the food effect reported in the literature for other abiraterone acetate formulations was successfully eliminated and OMs showed comparable extent of bioavailability in a fed-fasted study. Oil marbles therefore seem to be a promising formulation concept not only for abiraterone acetate but potentially also for other poorly soluble drugs that reveal a positive food effect.

KEY WORDS: bioavailability; bioequivalence; food effect; formulation; liquid marble.

INTRODUCTION

Poorly soluble drugs (i.e., drugs belonging to BCS groups II and IV) and their limited oral bioavailability currently present a major challenge to pharmaceutical scientists (1). An example of such a hard-to-formulate drug is abiraterone acetate, a prodrug of androgen biosynthesis inhibitor abiraterone, marketed under the original brand name Zytiga® and used as a medication for the treatment of metastatic castration–resistant prostate cancer (2). Abiraterone acetate has an extremely low bioavailability in the fasted state (estimated to be less than 10%) and exhibits a highly variable increase in bioavailability in the fed state (3–5). It has been reported that intake with high-fat meal leads to increase in overall exposures by approximately 17- and 10-fold, in terms C_{max} and AUC, respectively. The original formulation must therefore be taken on a fasting stomach in high doses, 1000 mg daily (2). This not only is inconvenient for the patients, but also presents a risk of accidental overdose. Attempts have been made to establish safe dosing regimen for lower doses of Zytiga® administered with food—these attempts have however been unsuccessful so far

Tereza Boleslavská and Ondřej Rychecký contributed equally to this work.

Electronic supplementary material The online version of this article (https://doi.org/10.1208/s12248-020-00505-5) contains supplementary material, which is available to authorized users.

[1] Zentiva, k.s., U Kabelovny 130, 102 37, Prague, Czech Republic.
[2] Department of Chemical Engineering, University of Chemistry and Technology, Prague, Technická 5, 166 28, Prague, Czech Republic.
[3] Department of Analytical Chemistry, Faculty of Science, Charles University, Prague, Czech Republic.
[4] Institute of Pharmacology, First Faculty of Medicine, Charles University and General University Hospital in Prague, Prague, Czech Republic.
[5] To whom correspondence should be addressed. (e–mail: Frantisek.Stepanek@vscht.cz)

Abbreviations: *API,* active pharmaceutical ingredient; *ASD*, amorphous solid dispersions; *AUC*, area under the curve; *ODP*, original drug product; *OM*, oil marble; *SEDDS*, self-emulsifying drug delivery system; *SMEEDS*, self-microemulsifying drug delivery system;

(3). This implies a need for the development of novel formulation strategies that would allow food effect elimination and thus safe dosing regimen for abiraterone acetate.

Therefore, it can be hypothesized that by using advanced formulation approaches to increase the bioavailability of abiraterone acetate on a fasting stomach, the dangerous food effect can be suppressed (6). Administration of the crystalline drug in the form of nanoparticles allowed dose reduction to 500 mg (7,8). Solymosi *et al.* reported a negligible food effect for a novel formulation based on continuous flow precipitation with Soluplus (9,10). Finally, we have shown in a recent study that amorphous solid dispersion (ASD) formulation based on precipitation inhibitor allowed 2.5-fold bioavailability enhancement in fasted rats (11).

Alternatively, lipid-based formulations of abiraterone acetate have been investigated recently (12). Complex lipid-based formulations can contain various oils, surfactants, and co-solvents. These systems can be categorized based on the Lipid Formulation Classification System (LFCS) into several groups among which the self-emulsifying drug delivery systems (SEDDS) and the self-microemulsifying drug delivery systems (SMEDDS) are of particular significance (13–15). These liquid formulations are usually filled into soft gelatin capsules. Even though these systems can be highly effective in bioavailability enhancement, they also have some drawbacks when compared with solid dosage forms.

As SEDDS and SMEDDS are essentially liquid formulations, it is not easily possible to alter their dissolution kinetics as such (16). Once the soft gelatin capsule is opened, it releases the whole content at once, forming a fine emulsion. The lipids are then available for enzymatic digestion (lipolysis), which is believed to be the critical step for drug absorption (15,17). Moreover, there are several challenges associated with soft gelatin capsules—e.g., cross-linking to the gelatin (which can result in poor dissolution) or the necessity to employ a special production line (18). Due to these aspects of liquid oil–based drug delivery systems, there have been efforts towards the solidification of these types of formulations (15). SEDDS solidification techniques have been reviewed recently by Joyce *et al.* (19) In the present work, we are introducing a novel approach towards the preparation of solidified oil-based formulations of abiraterone acetate based on the so-called oil marbles.

The general term "liquid marble" refers to a droplet covered by a layer of non-wetting solid particles that stabilize the interface and cause the droplet to behave and roll as if it were a rigid sphere. (20,21) Most of the existing literature on pharmaceutical applications of liquid marbles is concerned with water-based systems covered by hydrophobic powders (22). Such marbles typically contain about 90% w/w of the liquid core, depending on the interfacial tension, the droplet diameter, and the particle size. Solid particles on the surface prevent the encapsulated liquid from evaporation or leakage and protect the marbles from agglomeration, thus improving their handling properties (20,21). Although oil-based liquid marbles can be prepared as well, they are not so well documented in the literature and their practical application has so far been hindered by a limited choice of sufficiently oleophobic powders for coating (23). A fully liquid oil core combined with an insufficiently oleophobic powder leads to an unfavorable ratio between the oily core and the shell material, which ultimately limits the achievable drug load in the formulation.

Therefore, the aim of the present work was to overcome this limitation by formulating the oil-based core in such way that it can be combined even with wettable powders without their excessive absorption into the core. The resulting oil marbles (OMs) combine the advantages of oil-based formulations in terms of bioavailability enhancement and those of solid dosage forms in terms of handling the product. It will be shown that OMs can be filled into hard gelatin capsules and handled similarly as a solid material once they are prepared. We will demonstrate that unlike fully liquid formulations, OMs can provide a range of dissolution profiles depending on the matrix composition and OM size. Crucially, it will be shown that OM formulation of abiraterone acetate leads not only to improved dissolution *in vitro* but also to significant bioavailability enhancement *in vivo* and ultimately successful elimination of the food effect.

MATERIALS AND METHODS

Materials

Abiraterone acetate was provided by Zentiva, k.s. (Prague, Czech Republic). Capmul oil MCM NF was purchased from Abitec (Columbus, USA); Capryol PGMC was kindly donated by Gattefossé (Saint-Priest, France). Surfactants (summarized in Supplementary Material, Table S1) were purchased from Sigma-Aldrich. Natural oils (olive oil, rapeseed oil, and castor oil) were purchased from Merck (Germany). Hydroxypropyl methylcellulose (HPMCAS-LF) was bought from Shin-Etsu Chemical. Powders for biorelevant media were purchased from Biorelevant.com Ltd. (London, UK). The biorelevant dissolution media were prepared according to the manufacturer's protocol. All solvents used were at least of HPLC grade.

Solubility Measurements

In order to select the most appropriate oil for the OMs, the solubility of abiraterone acetate in several candidate oils was determined using the shake flask method. Briefly, an excess of abiraterone acetate was added to an Eppendorf vial containing 1 mL of the oil and the resulting suspension was shaken at 37°C for 24 h. At the end of the experiment, the vials were centrifuged at 10,000 RPM for 10 min, the supernatant was diluted ten times into isopropyl alcohol, and the concentration of abiraterone acetate in the resulting solution was determined by HPLC (method adapted from our previous study) (11).

As an additional component of the OM formulation, surfactants were screened for their ability to enhance the solubility of abiraterone acetate in aqueous media. The solubility was determined using the shake flask method described above. Surfactants with relatively higher melting point (around 50°C) were selected along with several commonly used non-ionic surfactants such as Tween. The full list of surfactants is provided in Supplementary Material, Table S1. Phosphate buffer pH 6.8 supplemented with these surfactants at different concentrations (namely 1.0, 0.5, 0.25,

and 0.125 mg/L) was used as the dissolution media in the shake flask method.

Preparation of Oil Marbles

All components of the oil core (abiraterone acetate, oil, surfactant) were weighted and placed into a flask. The mixture was heated in a bath at 56°C and stirred for 20 min at 250 RPM to allow complete dissolution and homogenization of the mixture. Oil Marbles were created by dripping the liquid at a rate of 2 Hz using a 30G needle connected to a precise syringe pump, into a powder bed placed in Petri dish that moved underneath the needle tip at a velocity or approximately 10 mm/s in order to allow sufficient distance between the individual OMs. The powder bed was maintained at room temperature (approximately 20°C); HPMCAS-LF was used as the covering powder material. After 3 min (time necessary for the droplets to cool down and partially solidify), the Petri dish was shaken to fully cover the droplets by the powder. Thanks to the surface cooling of the droplets, the HPMCAS powder remained just on the surface even though it is not fully oleophobic. The final product—the oil marble—therefore behaves as a non-sticking solid sphere regardless of the physical consistency of the oily core.

Physicochemical Characterization

Sieve Analysis

After preparation, the OMs were separated by sieving to obtain size classes with a defined diameter. To assess the effect of OM size on *in vitro* dissolution properties of the formulation, the following size fractions were collected: 1.4–2 mm, 2–3 mm, 3–4 mm, 4–5 mm, 5–6 mm, and > 6 mm. Since the rat capsules intended for an *in vivo* study have an inner diameter of 2 mm, only the smallest fraction (1.4 to 2 mm) of OMs was used for the *in vivo* study.

X-ray Powder Diffraction Analysis

X-ray powder diffraction (XRPD) patterns were obtained with the laboratory X-ray diffractometer X'PERT PRO MPD PANalytical with copper radiation CuKα (λ = 1.542 Å, 45 kV/40 mA), 2-theta range 2–40°, with step size 0.02° 2θ and time per step 300 s. Primary optics setting is as follows: Soller slits 0.02 rad, automatic PDS, 10 mm mask, 1/4° anti-scatter slit, irradiated sample area 10 mm. Secondary optics setting is as follows: 5.0 mm anti-scatter slit, Soller slits 0.02 rad, detector X'Celerator with maximal active length. Silicon zero background holders were used for measurement. A few OMs were placed on the holder and gently pressed by a Petri dish to obtain a flat surface. All samples of OM were measured on XRPD to confirm if abiraterone acetate inside the marbles was present in the crystalline or amorphous form.

Drug Load Analysis

The actual drug load in the oil marbles was determined by extraction into methanol. Approximately 80 mg of OMs was weighted into a 20-mL volumetric flask and extracted into methanol. The resulting solution was diluted 10 times, and the concentration of abiraterone acetate was determined on HPLC using a method adapted from our previous study (11).

In Vitro Dissolution Testing

Dissolution experiments were conducted using standard USP 2 dissolution bath equipped with a mini-paddle apparatus (Sotax, Switzerland). The dissolution media were preheated to 37°C and the stirrer speed was set to 125 RPM; these conditions were kept constant throughout the experiment. OMs were placed into a weighing boat and administered directly into the dissolution vessel. The weight of abiraterone acetate corresponded to 20 mg in all dissolution experiments. Liquid samples (500 μL) were collected in predefined time points, filtered through a 0.45-μm filter, immediately diluted with 500 μL of MeOH, and analyzed on HPLC. Unlike the dissolution medium, the filtrate was clear, suggesting the absence of any particles or droplets that would scatter light.

As dissolution media simulating fasted and fed conditions, biorelevant buffers were used—FeSSIF v2 pH 5.8, FaSSIF pH 6.5, and FaSSIF pH 6.5 supplemented with pancreatin (10 mg/mL) (24). Furthermore, pH shift experiment was designed. Briefly, 130 mL of 10 mM HCl pH 2 was used to simulate gastric conditions. After 30 min, concentrated FaSSIF buffer was added to the dissolution vessel to obtain 195 mL of FaSSIF buffer pH 6.5.

In Vivo Bioequivalence Study

Chemicals

Ketamine (Narkamon 100 mg/mL inj. sol.; Bioveta, Ivanovice na Hané, Czech Republic), xylazine (Rometar 20 mg/mL inj. sol.; Bioveta, Ivanovice na Hané, Czech Republic), and isoflurane (IsoFlo 250 mL; Zoetis/Pfizer, Czech Republic) were used for anesthetization. Enoxaparin (Clexane inj. 4000 IU/0.4 mL; Sanofi-Aventis, Czech Republic), heparin (Heparin Léčiva inj. 1 × 10 mL/50KU; Zentiva, Czech Republic), amoxicillin with clavulanic acid (Synulox RTU inj. 100 mL; Zoetis/Pfizer, Czech Republic), and ketoprofen (Ketodolor inj. 100 mL; LeVet Pharma b.v., Netherlands) were used for peri-operative anti-coagulant, antibiotic, and analgesic treatments, respectively. Surgical Skin Glue was purchased from Henry Schein (Brno, Czech Republic). For dosing, mini gelatin drug delivery capsules, size 9el (Harvard Apparatus, USA), were used.

Animals

Male Wistar rats purchased from Velaz (Prague, Czech Republic) were housed under standard conditions (12-h light-dark cycle, 22 ± 2°C temperature and 50 ± 10% relative humidity) and fed on water and standard granulated diet *ad libitum*. All experiments were performed in accordance with the Guiding Principles for the Use of Animals in Charles University, First Faculty of Medicine, and every effort was made to minimize animal suffering. The experimental animal project was approved by the Ministry of

Education, Youth and Sports, Czech Republic (MSMT-9445/2018-8).

Preparation of Capsules for In Vivo Dosing

The mini capsules containing reference formulation were filled with the crushed original drug product Zytiga® to contain approximately 4.2 mg of abiraterone acetate. For the test formulation, two capsules were filled with OM formulation pre-selected on the basis of previous *in vitro* studies. Each capsule contained approximately 2.1 mg of abiraterone acetate—two capsules containing the test formulation were given to each animal by oral gavage.

Experimental Design and Procedure

A randomized, single-dose, laboratory-blinded, 2-period, 2-sequence, crossover bioequivalence study was conducted under fasting conditions in rats to compare the bioavailability of abiraterone after oral administration of test and reference (Zytiga®, Janssen-Cilag SpA, Latina, Italy) formulations (Table I part A). Another randomized, single-dose, laboratory-blinded, 2-period, 4-sequence, crossover comparative bioavailability study was conducted in rats to compare the effect of food on bioavailability of abiraterone after oral administration of test and reference formulations (Table I part B).

All rats underwent cannulation of *a. carotis* with catheters made from medical-grade polyurethane (1.9-3Fr, Instech Laboratories, Plymouth Meeting, USA). Prior to the surgery, 2.5–5% isoflurane was used to anesthetize the rats, continued with ketamine (100 mg/kg, i.m.) and xylazine (5 mg/kg, i.m.). Prophylactic amoxicillin with clavulanic acid (1 mL/kg, s.c.) was administered prior to the surgery to minimize the risk of an infection. After the cannulation, ketoprofen (5 mg/kg, s.c.) was applied. Catheters were flushed with 200 μL of physiological saline and 50 μL of heparin and sealed by 20 μL of glycerol with heparin every day. Peri-procedural thromboembolism prophylaxis with enoxaparin (10 mg/kg, s.c. q.d.) was applied from 12 h prior to surgery until the end of study. The third day after the cannulation, rats were randomly assigned into study groups and dosing of abiraterone acetate containing formulation was performed.

For dosing under fasted state, the access of the animals to food was restricted between 4 h prior to dosing and 4 h after that, and capsule was administered by X-9el dosing syringe (Torpac Inc., Fairfield, USA) followed by 1 mL of water via oral gavage. For dosing under fed state, administered capsule was immediately followed by 1 mL of homogenized mixture (1:1) of olive oil with Nutridrink (Nutricia, Danone, Amsterdam, Netherlands) via oral gavage and the access of the animals to food was not restricted. Total dose of abiraterone acetate was measured in each capsule and ranged between 4.18–4.53 mg and 4.00–4.27 mg for reference and test formulations, respectively. Therefore, all concentration data has been normalized to body weight of each animal. Blood samples (100 μL) were then collected for 7 h (0, 0.5, 1, 1.5, 2, 2.5, 3, 4, 5, and 7 h) after the dosing. Volume replacement with 100 μL of saline was provided after each sampling and 50 μL of heparinized saline flush (1250 IU/mL) of the catheter together with sealing by heparinized glycerol used to secure the catheter patency. Blood samples were centrifuged for 10 min (4500×*g*, 4°C) and serum aliquots were stored at −80°C until analyses. A wash-out period of 48 h between consecutive doses was applied.

Table I. Experimental Design of *In Vivo* Studies

A	**Group no.**	**Formulation sequence**
	1	R–T
	2	T–R
B	**Group no.**	**Formulation/condition sequence**
	1	R (fasted)–R (fed)
	2	T (fasted)–T (fed)
	3	R (fed)–R (fasted)
	4	T (fed)–T (fasted)

R reference, *T* tested formulation

Analytical Methods

Determination of abiraterone in plasma samples was carried out on the Shimadzu UHPLC Nexera X3 coupled with a Triple Quad 8045 tandem mass spectrometer (Shimadzu, Kyoto, Japan). Kinetex EVO C18 column (100 mm × 2.1 mm, 1.7 μm particle size) from Phenomenex (Torrance, USA), thermostatted at 40°C, was used for the analysis. The mobile phase consisted of 0.1% formic acid in deionized water (solvent A) and acetonitrile (solvent B). The flow rate of the mobile phase was maintained at 0.35 mL/min. The optimized gradient program (min/% B) was 0/30, 1.5/90, 3.0/90, 3.5/30, and 6.0/30. The injection volume was 2 μL, and samples were kept at 10°C. To reduce the cleaning time of the ion source, we switched the MS six-port valve to waste for the first 2.6 min and for the last 2.2 min of analysis. The tandem mass spectrometry measurement was performed in multiple reaction monitoring (MRM) mode using positive electrospray ionization. MRM transitions of 350.3 > 156.1 (Q1 pre-bias −17 V, Q3 pre-bias −27 V, and collision energy −57 V) and 354.3 > 160.1 (Q1 pre-bias −17 V, Q3 pre-bias −30 V, and collision energy −57 V) were monitored for abiraterone and abiraterone-d4 (internal standard), respectively. The ion source was set as follows: nebulizing gas flow: 3 L/min, heating gas flow: 10 L/min, interface temperature: 300°C, desolvation line temperature: 250°C, heat block temperature: 400°C, and drying gas flow: 10 L/min. A total of 100 μL of 100% acetonitrile (containing abiraterone-d4; $c = 32$ ng/mL) was added to 25 μL of plasma, shaken (vortex), and centrifuged (10 min/9800×*g*). A total of 70 μL of supernatant was transferred into a chromatographic vial.

The method was validated in terms of linearity, LOD, accuracy, precision, selectivity, recovery, and matrix effects. The calibration curve was constructed in the blank plasma with seven concentrations by plotting the ratio of the peak area of the analyte to that of deuterium-labeled IS against analyte concentration. The calibration curve was statistically analyzed by $1/x^2$ weighted linear regression analysis using the least squares regression method, which improved the accuracy in low concentrations. The developed method was linear (coefficients of determination (R^2) higher than 0.9996) in the concentration range of 0.5–600 ng/mL with the

accuracy (relative error %) within ± 7.1%, and the interday and intraday precisions (RSD %) ranged from 2.4 to 5.2%. LOD value was determined as $3.3 \times \sigma/S$ ratio, where σ is the baseline noise obtained from the blank matrix and S is the slope of the regression line (based on peak heights) obtained from the linearity data. The mean of LOD value was 0.03 ng/mL, which showed satisfactory sensitivity for abiraterone determination in plasma samples. Recovery was evaluated by comparing concentration of abiraterone found in the pre-protein-precipitation spiked plasma sample with the concentration found in the corresponding post-protein-precipitation spiked sample at three concentrations (1, 50, and 250 ng/mL). Method selectivity was monitored by injecting six plasma samples (mass spectrometer was set in scan mode). These chromatograms showed no interfering compound within the retention time window of abiraterone. Moreover, the developed method uses a tandem mass spectrometer in specific SRM mode, which ensures high selectivity. Matrix effect was evaluated at two concentration levels (1 and 100 ng/mL) of six plasma samples. It was determined by comparing the concentration of abiraterone found in the post-protein-precipitation spiked plasma sample with that found in the 80% acetonitrile spiked with abiraterone (without matrix effect). The matrix effect ranged from 80 to 108%. To assess the validity of the analytical method, calibration was performed every day before measuring samples and quality control samples were injected after each 7th sample.

Data Analysis and Statistics

Statistical and pharmacokinetic analysis was performed using Phoenix WinNonlin® (Certara, Princeton, USA). C_{max}, T_{max}, and AUC were evaluated. The natural logarithmic transformation of C_{max} and AUC was used for all statistical inference. AUC was calculated using the trapezoidal rule, and C_{max} and T_{max} were taken directly from the observed data. The pharmacokinetic parameters were analyzed using an ANOVA model. The fixed factors included in this model were the effects of subject, treatment, period, and sequence. The 90% confidence interval for the ratio of geometric least squares means between the test and reference products was calculated. Actual sampling times were used for all pharmacokinetic calculations, while scheduled sampling times were used only for plotting of mean pharmacokinetic profiles. The maximum difference between actual and per-protocol sampling times was 5 min. GraphPad Prism version 8.00 for Windows (GraphPad Software, La Jolla, USA) was used to plot mean pharmacokinetic profiles.

RESULTS

Selection of Formulation Components Based on Solubility

Based on recently published SMEDDS formulations of abiraterone acetate that contained mixtures of castor oil and artificial oils (12), it was decided to explore the solubility of abiraterone acetate in other natural oils (rapeseed oil and olive oil) compared with castor oil, as well as in several artificial oils (Capmul MCM NF and Capryol PGMC). The results are summarized in Fig. 1a (the underlying values can be found in Supplementary Material, Table S2). From the natural oils, castor oil with solubility of abiraterone acetate 137.7 mg/L was chosen for the preparation of oil marbles due to its highest solubility. For the artificial oils (Capmul MCM NF dissolved 53.3 m/L and Capryol PGMC 735.1 mg/L), both were used in combination with different surfactants as described in "Preparation of Oil Marbles and Their Physicochemical Characterization." Surfactants for the formulation were selected based on their solubilization effect for abiraterone acetate and their physical consistency. The preparation of OMs coated by HPMCAS powder requires the usage of solid or semi-solid excipients. Thus, surfactants with a melting point around 50°C (based on manufacturer and literature data) (25–30) were included in the list of possible surfactants (Supplementary Material, Table S1). Along with these, the solubilization capacity of some commonly used non-ionic surfactants (such as Tweens) was tested. The ability of selected surfactants to enhance the solubility of abiraterone acetate was assessed in a phosphate buffer pH 6.8. The solubility of abiraterone acetate alone was under the detection limit of the UPLC method. The highest enhancements were occurred for Kolliphor RH40, Tween 80, Tween 20, and Pluronic F127 (see Fig. 1b).

Preparation of Oil Marbles and Their Physicochemical Characterization

Based on the solubility data, we prepared four types of OMs with a different composition of the inner core, as summarized in Table II. We focused mainly on the manufacturability of the marbles while using surfactants that provided the highest solubility for abiraterone acetate. Some of the surfactants that provided good solubility were found to be unsuitable for the preparation of oil marbles, namely Tween 20 and Tween 80. Both are liquid at room temperature, and we were not able to prepare a mixture that would allow the formation of stable OMs coated by a thin layer of HPMCAS powder. Butylated hydroxyanisole (BHA) was added to all formulations in order to decrease undesired oxidation processes.

For mixture A, solid surfactant Pluronic F-127 was used as the main solubilizing agent (this surfactant showed good solubility for abiraterone acetate in phosphate buffer). Tween 65 was used as a solidifying agent. The resulting mixture thus formed a rather solid core. For mixture B, both used surfactants (solid Pluronic F-127 and liquid Kolliphor RH40) showed the ability to solubilize abiraterone acetate. Their mixture also allowed formation of a solid oil core at room temperature although softer than when using mixture A. Mixture C was prepared using surfactants that have a high melting point, but they did not perform well in the solubility measurements. We therefore assumed that this mixture would not perform well in the dissolution studies although the solid core could still contain molecularly dispersed abiraterone acetate (see Fig. 3). For mixture D, both used surfactants (Pluronic F-127 and Span 40) are solid materials but only Pluronic F-127 showed solubility enhancement.

As a covering material, HPMCAS-LF, a polymeric excipient with pH-dependent solubility, was used. This covering material was chosen for two main reasons: (i) pH-dependent solubility of this polymer allows pH-controlled

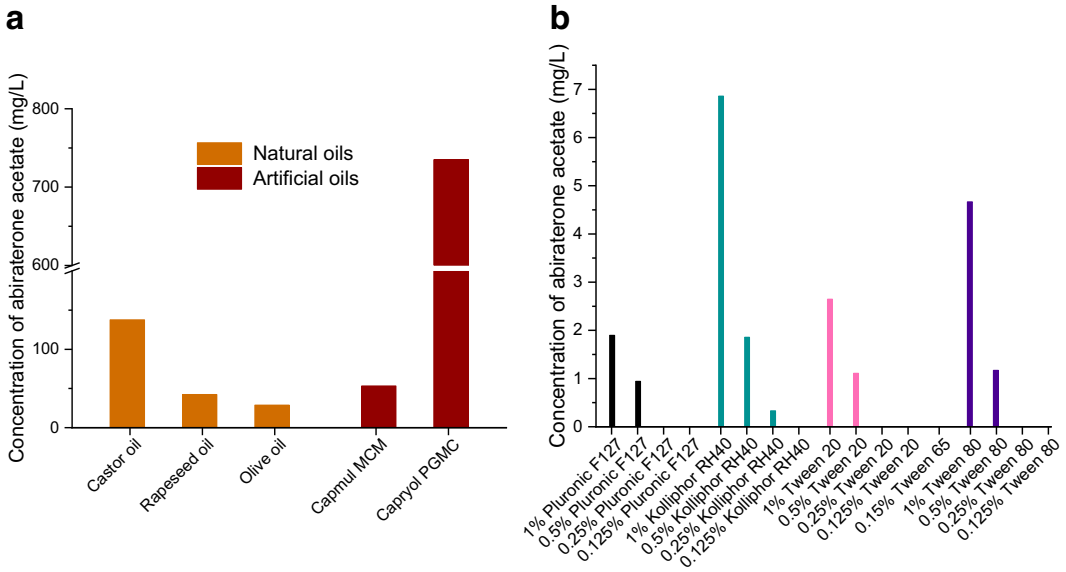

Fig. 1. **a** Solubility of abiraterone acetate in various natural and artificial oils. **b** The solubility enhancement of abiraterone acetate due to various surfactants in phosphate buffer pH 6.8

release since we believe that tuning the release of abiraterone acetate based on pH is crucial for food effect elimination; (ii) in our previous study (11), HPMCAS-LF was identified as a potent precipitation inhibitor—this might allow drug absorption even when supersaturated state is reached in a given environment (this phenomenon is usually referred to as parachute effect) (31). We were able to prepare marbles smaller than 2 mm in diameter that could be filled into capsules for rodents (capsule size 9el) as shown in Fig. 2. Larger size fractions were also prepared and used for studying the impact of OM size on the dissolution properties (see "*In Vitro* Dissolution Testing").

Figure 3 shows XRPD diffractograms of OM samples. Crystalline abiraterone acetate was not detected in any of the samples. It can be concluded that abiraterone acetate is probably molecularly dispersed in all four formulations. The detected diffraction peaks correspond to excipients, namely to triblock copolymers (Poloxamer 188, Pluronic F-127, Kolliphor) and solid co-surfactants (Span 65, Span 40). The XRPD diffractograms of these excipients are summarized in Supplementary Material, Fig. S1. The drug load as determined by methanol extraction corresponded with theoretical drug load in the melt. As anticipated, the actual drug load is decreased by addition of a thin layer of HPMCAS. The actual drug content determined for OM sample B (intended for the *in vivo* study) was found to be 6.2%.

In Vitro Dissolution Testing

As bioavailability of abiraterone acetate is reported to be limited in fasting conditions, special attention should be paid to dissolution in media closely mimicking these conditions. For this purpose, a pH shift experiment that represents a transfer of API from a fasting stomach to a fasting intestine was designed. The results for OM formulation B are shown in Fig. 4a. Less than 10% of abiraterone acetate was released under acidic condition—this is due to poor solubility of the coating material (HPMCAS-LF) in acidic pH. Coverage of the oil marbles by this polymeric excipient therefore seems to be very efficient. Interestingly, when OMs were administered to the dissolution test in the rodent capsules, there was a slight increase in the release rate in acidic pH (and a subsequent shift of dissolution curve in the FaSSIF stage). This is most probably due to mechanical damage of the covering powder layer of the marbles when they are placed into the capsules. Although the damage of the powder layer apparently translates into dissolution behavior, the overall effect on dissolution properties was considered negligible and hence all subsequent studies were performed without the capsules.

Having established that the HPMCAS-LF coating on the OMs effectively prevents dissolution under acidic conditions, all four OM formulations were then compared in a dissolu-

Table II. Oil Marbles—Different Samples and Their Composition (Weight Percent)

Sample	Abiraterone acetate (%)	Capmul oil MCM NF (%)	Capryol PGMC (%)	Castor oil (%)	Pluronics F-127 (%)	Kolliphor RH40 (%)	Tween 65 (%)	Span 40 (%)	Span 65 (%)	Poloxamer 188 (%)	BHA (%)
OM A	6.9	23.1	-	23.1	23.2	-	23.6	-	-	-	0.1
OM B	7.0	23.1	-	23.3	23.5	23.0	-	-	-	-	0.1
OM C	8.1	-	23.0	22.8	-	-	-	-	22.9	23.1	0.1
OM D	7.8	-	22.6	22.1	24.5	-	-	22.8	-	-	0.1

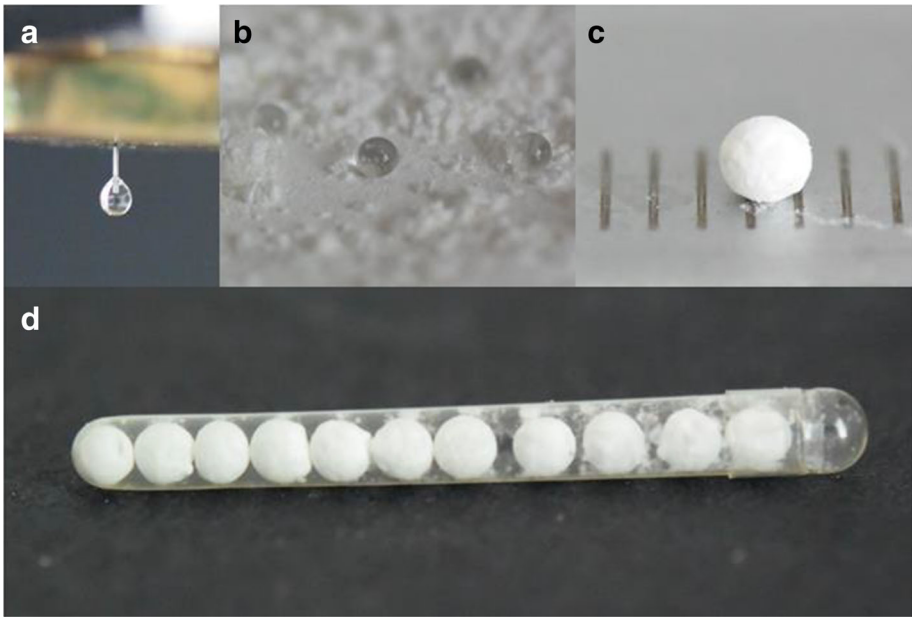

Fig. 2. Formation of oil marbles. **a** Initial droplet of the core material. **b** Droplets after deposition on a powder bed. **c** Finished oil marble coated by HPMCAS-LF. **d** Sub-2-mm OMs filled into rodent capsules size 9el

tion experiment in FaSSIF media (Fig. 4b). As a reference, the dissolution of a crushed Zytiga® tablet (original drug product containing abiraterone acetate) (2) under the same conditions is shown as reported in our previous study (11). The fraction dissolved for most OM formulations except formulation C is considerably higher. Also, no precipitation was observed throughout the experiment suggesting maintained supersaturation of abiraterone acetate when compared with crystalline API present in the original drug product.

OM formulation C contained only surfactants that did not show significant solubility enhancing properties (Span 65 and Poloxamer 188). On the other hand, significant improvement in dissolution rate was seen for both OM formulations A and D. Both of these formulations contained one surfactant that showed solubility enhancing properties (Pluronic F-127) and one that either showed only minor or no effect (Span 40 or Tween 65). Finally, the fastest dissolution rate was observed for OM formulation B; both surfactants used in this formulation increase the solubility of abiraterone acetate. As the release rate in FaSSIF buffer was the highest for OM formulation B and no precipitation was observed, this formulation was retained for further studies.

The effect of OM size on the release kinetics was assessed next. Although the size needed for *in vivo* study in the rat animal model was determined by the inner diameter of the rodent capsules, understanding the effect of OM is useful for further formulation development. The results of dissolution experiment plotted in Fig. 4c clearly show that marble size has a direct effect on the release rate from the oil marble. It is therefore possible to control the release rate from OMs just by changing their diameter. This might be especially useful when targeting certain dissolution profile. It is also a major distinguishing feature of OMs compared with liquid SMEDDS formulations.

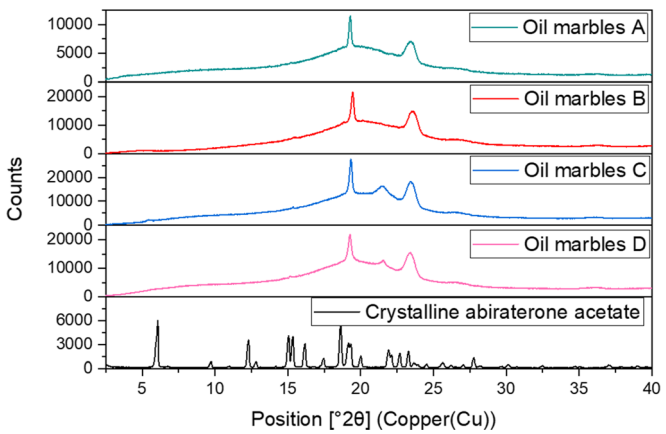

Fig. 3. XRPD diffractograms of OM formulations A–D compared with crystalline abiraterone acetate—the XRPD diffractograms of individual formulation components can be found in Supplementary Material, Fig. S1

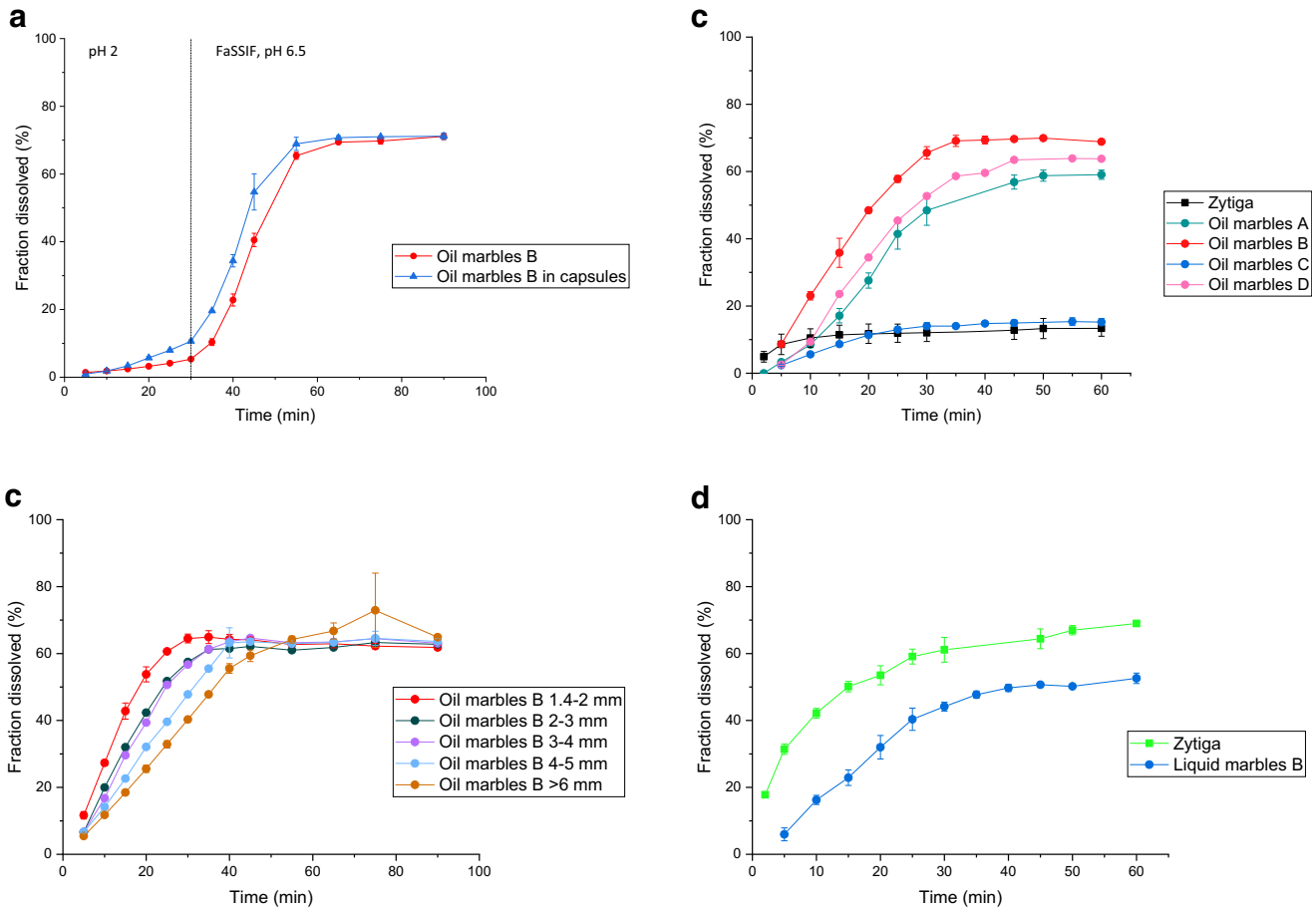

Fig. 4. Mean (± SD, $n = 3$) *in vitro* dissolution profiles of **a** OM formulation B in pH shift dissolution experiment. 0–30 min 10 mM HCl pH 2, 130 mL; 30–90 min FaSSIF pH 6.5, 195 mL; mini-paddles at 125RPM; **b** oil marbles A–D compared with Zytiga® in FaSSIF media, pH 6.5, 200 mL, mini-paddles at 125RPM; **c** different marble sizes of OM formulation B in FaSSIF media, pH 6.5, 200 mL, mini-paddles at 125RPM; **d** OM formulation B compared with Zytiga® in FeSSIF v2 media, pH 5.8, 200 mL, mini-paddles at 125RPM. Fraction dissolved corresponds to abiraterone acetate—abiraterone (product of hydrolysis of abiraterone acetate) was not detected in neither of the experiments. Fraction dissolved corresponds to abiraterone acetate—abiraterone (product of hydrolysis of abiraterone acetate) was not detected in neither of the experiments

As abiraterone acetate is prone to enzymatic hydrolysis upon oral administration (24,32), a dissolution experiment in biorelevant media supplemented with pancreatic enzymes was designed. Also, the effect of lipolysis is assessed when pancreatic enzymes are present in the dissolution media (17). The digestion of lipidic excipients present in the OM formulation might play an important role in the absorption of the drug even though the mixtures prepared in this study fall into group III according to LFCS—drugs can be reportedly absorbed from type III formulations even without digestion (13,14). Three different formulations were tested in the presence of pancreatic enzymes: (i) original drug product Zytiga®; (ii) amorphous solid dispersion with HPMCAS-LF as a carrier (11); (iii) formulation in oil marbles (OM B). The concentration of abiraterone acetate, its hydrolysis product abiraterone, and the total concentration of both compounds are plotted over time in Fig. 5. The area under the curve was calculated for total concentration as a measure of the overall quantity of the API theoretically available for absorption.

It is believed that both abiraterone acetate and abiraterone can permeate through the intestinal wall (32). These results therefore imply that highest bioavailability should be reached for the OM formulation. Moreover, the dissolution curves in pancreatin-enriched media provide an insight into the lipolysis of lipids. The release rate of the drug (when plotted as the combined concentration of abiraterone and abiraterone acetate) is slightly higher when compared with dissolution experiment in FaSSIF (see Fig. 4). This might be caused by the degradation of lipids thus releasing the drug. Also, last time point (90 min) indicates some precipitation of the drug. However, the time window in which the drug is solubilized should be wide enough to allow drug absorption before the precipitation starts.

Finally, since our goal is to suppress food effect reported for abiraterone acetate, also *in vitro* experiments simulating fed conditions were evaluated. For this purpose, dissolution in FeSSIF v2 was conducted. The results are plotted in Fig. 4d.

FeSSIF v2 media have pH 5.8, which is close to the borderline where HPMCAS-LF dissolves (pH 5.5–6). That explains why less API is released from the oil marbles in the fed state simulated fluid (approximately 53% of the administered dose) than in the fasted state simulated fluid (68% of the administered dose). For Zytiga®, only 13% of the

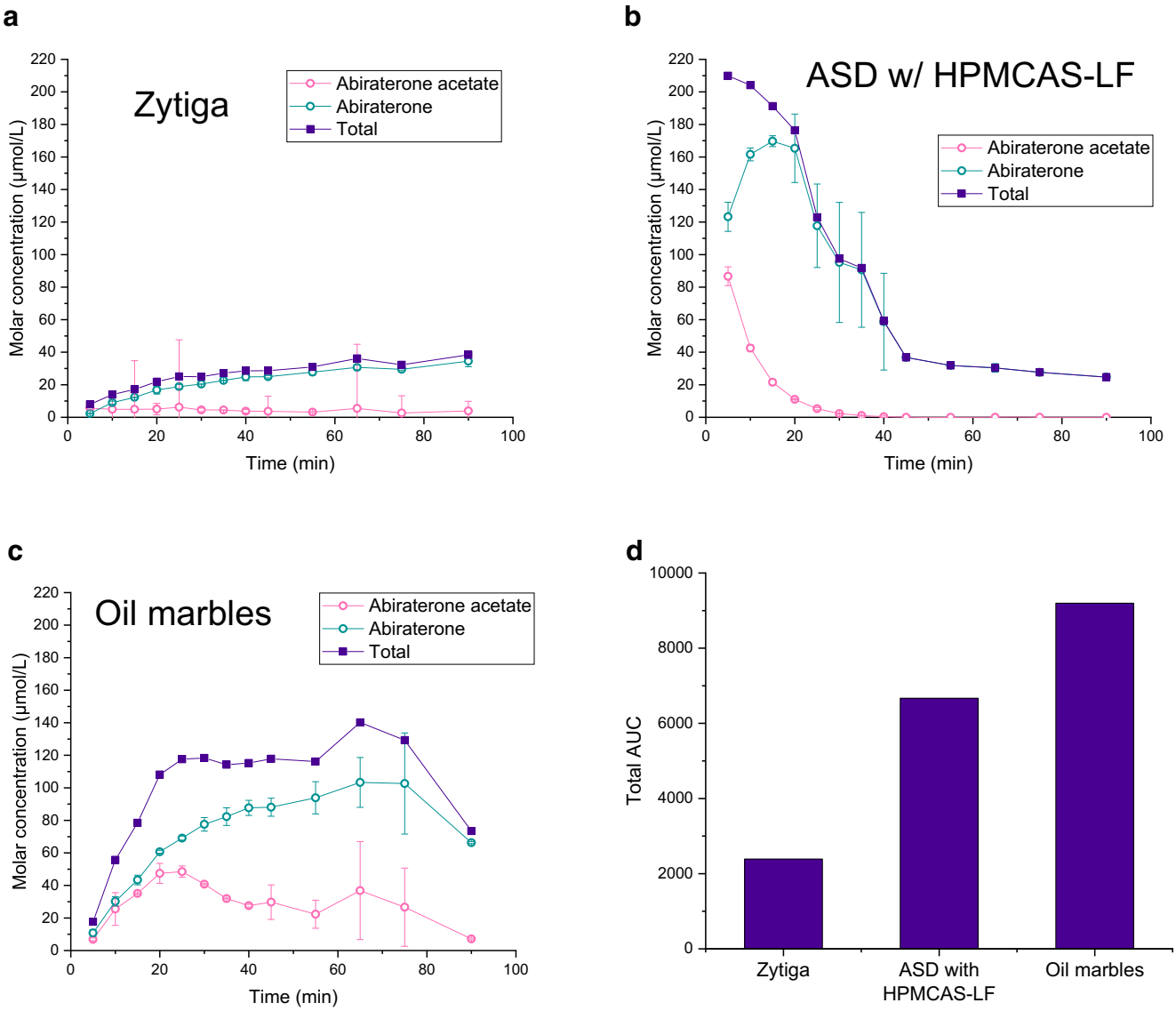

Fig. 5. *In vitro* dissolution in FaSSIF buffer supplemented with pancreatin. Abiraterone acetate (in pink), abiraterone (in green), and total concentration of both compounds (in blue) are plotted. **a** Original drug product Zytiga®. **b** Amorphous solid dispersion with HPMCAS-LF as carrier. **c** Oil marbles B. **d** Total API available for absorption plotted as area under the curve of all three formulations

administered dose is dissolved under simulated fasted conditions compared with 69% of the administered dose dissolved under simulated fed conditions. Moreover, Zytiga® apparently dissolves faster in the fed state simulated intestinal fluids than the OM formulation. If this behavior translates into *in vivo* scenario, the positive food effect reported for original drug product Zytiga® that can lead to toxic exposures of abiraterone acetate could be suppressed.

In Vivo Study

In crossover bioavailability study design, 8 rats completed both periods as planned. The weight of enrolled rats ranged between 309 and 428 g, while administered weigh-normalized doses ranged from 10.30 to 13.78 mg/kg.

Abiraterone pharmacokinetic parameters after administration of test (oil marbles B) and reference (Zytiga®) formulations to fasted rats are summarized in Table III. The rate of drug absorption was substantially higher after administration of test formulation in comparison to reference product as documented by approximately 4-fold C_{max} and shorter T_{max}, although the difference in T_{max} values between test and reference formulations did not reach statistical significance. The extent of abiraterone absorption was approximately 2.7-fold higher after the test formulation in comparison to the reference product. Figure 6a shows the mean abiraterone pharmacokinetic profiles after both products.

Concentrations of pre-dose blood samples were all below the limit of quantification (1 ng/mL) indicating that the wash-out period (48 h) was sufficient. However, the sampling interval, although derived from our previous experience (11), was rather short as the β elimination phase has not been covered in 3 and 2 pharmacokinetic profiles after administration of reference and test formulations, respectively. The AUC_{last}/AUC_{inf} ratio in the rest of animals ranged from 0.71

Table III. Abiraterone PK Parameters After Administration of Test (OM B) and Reference (Zytiga®) Formulations to Rats ($n = 8$) in the Fasted State. T_{max} Values Are Given as Median (interquartile range). C_{max}, AUC_{last}, and Test/Reference Ratios Are Given as Geometric Mean (90% Confidence Intervals)

Formulation	C_{max} (ng/mL g)	T/R C_{max} (%)	AUC_{last} (mg/mL min g)	T/R AUC_{last} (%)	T_{max} (min)
Reference	0.143 (0.073–0.281)	N/A	30.3 (14.3–64.2)	N/A	244 (228–420)
Test	0.569 (0.206–1.566)	397.8 (213.8–740.1)	81.0 (32.1–204.4)	267.4 (165.7–431.6)	168 (114–252)

to 0.99 for the reference formulation and 0.58 to 0.95 for the test formulation, which indicates that the difference in total exposure between formulations is underestimated and would be probably even higher, if the sampling interval covered the whole PK profile thoroughly.

A total of 12 rats were enrolled into the food effect study to get complete pharmacokinetic profiles from 11 subjects. One of the rats had to be excluded due to difficulties with sample collection. Thus, pharmacokinetic profiles under fasted and fed conditions were compared after administration of reference and test formulations in 5 and 6 subjects, respectively. The weight of rats ranged between 355 and 432 g. Weight-normalized doses of abiraterone ranged from 10.75 to 13.33 mg/kg. Table IV shows summarized pharmacokinetic parameters after administration of test (OM B) and reference (Zytiga®) products under fasted or fed state. The reference formulation resulted in approximately twice as high as AUC_{last} in the fed state compared with fasted rats, which corresponds to significantly increased exposure of abiraterone observed with food in humans (2).

There was, however, no food effect on abiraterone absorption from test formulation evidenced by similar C_{max} and AUC_{last} values under the fasted and fed states. For both formulations, absorption was prolonged in the fed state. The test formulation required less time to reach the maximum plasma concentration than the reference. Mean (SD) abiraterone pharmacokinetic profiles are showed in Fig. 6b and c.

Concentrations of pre-dose blood samples were all below the limit of quantification (1 ng/mL), suggesting that the wash-out period between dosing (48 h) was sufficient. Although this food effect study was not powered to compare differences between formulations in fasting conditions, the results correspond with observations from the first part of the study. Zytiga® is standardly administrated in the fasted state. When comparing abiraterone exposure of both formulations, administration of oil marbles led to twice as high AUC_{last} as Zytiga® in the same dose. If we consider the advantage of eliminated food effect, oil marbles seem to be a promising drug formulation for abiraterone acetate.

DISCUSSION

The main goal of this work was to prepare and test a new formulation concept for abiraterone acetate based on the so-called oil marbles (OMs). We have successfully prepared OMs from different mixtures of oils and surfactants that showed an ability to solubilize abiraterone acetate. Although the design space for the preparation of oil marbles was not covered exhaustively, we have shown several manufacturable OM formulations using surfactants of different chemical structures and physical properties.

All prepared samples of OMs exhibited an amorphous character which shows that abiraterone acetate remains molecularly dispersed in the oil-based matrix even after it cools down to room temperature. This implies that the dissolution rate from the OM formulation will depend only on the rate at which the matrix components are being dispersed in the dissolution media. The marble size hence turned out to be the crucial parameter for the *in vitro* performance of the oil marbles. While keeping in mind that the performance of lipid-based formulations does not rely solely on the dissolution profiles, the results showed that

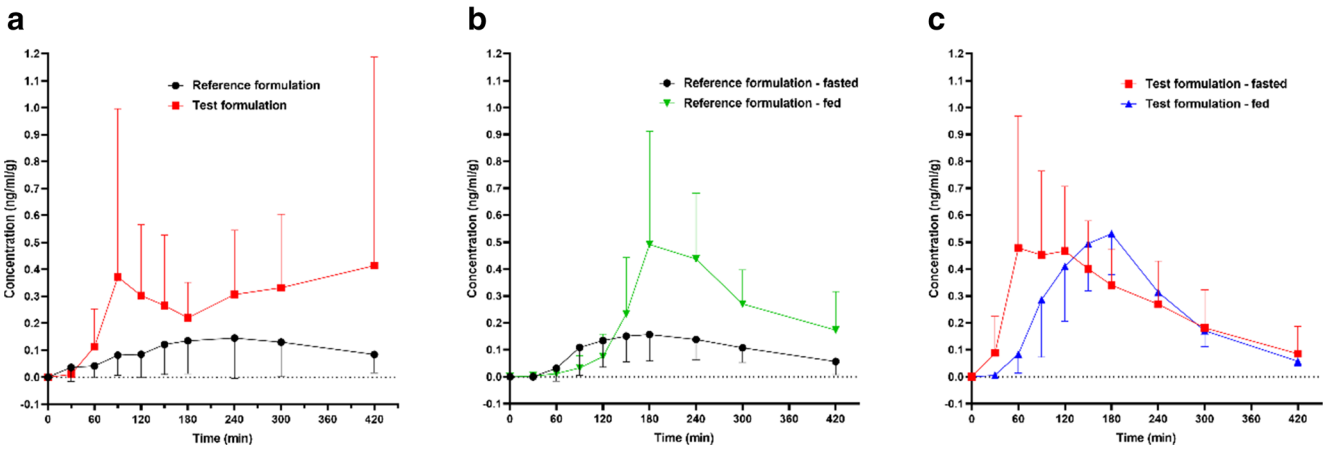

Fig. 6. Mean (± SD) abiraterone pharmacokinetic profiles in rats: **a** after administration of reference and test formulations in fasted condition; **b** after administration of reference formulation in fasted and fed conditions; **c** after administration of test formulation in fasted and fed conditions

Table IV. Abiraterone PK Parameters After Administration of Test and Reference Formulations to Rats ($n = 11$) in Fasted and Fed Conditions. T_{max} Values Are Given as Median (Interquartile Range). C_{max}, AUC_{last}, and Fed/Fasted Ratios Are Given as Geometric Mean (90% Confidence Intervals)

Formulation	C_{max} (ng/mL g)	Fed/fasted C_{max} (%)	AUC_{last} (mg/mL min g)	Fed/fasted AUC_{last} (%)	T_{max} (min)
Reference fasted	0.231 (0.176–0.302)	N/A	40.0 (31.3–51.1)	N/A	179 (157–226)
Reference fed	0.550 (0.318–0.950)	238.5 (131.1–433.9)	80.7 (40.6–160.4)	201.8 (86.7–469.4)	218 (185–288)
Test fasted	0.546 (0.199–1.480)	N/A	94.7 (43.2–207.4)	N/A	125 (68–178)
Test fed	0.530 (0.351–0.801)	103.8 (58.3–184.9)	93.6 (62.6–140.1)	105.1 (76.4–144.5)	152 (148–178)

release profiles can be controlled simply by adjusting the size of OMs. This can be crucial when targeting certain dissolution/absorption profile.

To further understand the behavior of OM formulation, *in vitro* experiment with pancreatic enzymes was designed. Overall, all conducted *in vitro* tests showed a tendency towards higher fraction dissolved under fasting conditions for OM formulation when compared with the original drug formulation Zytiga®. These results provided a solid base for subsequent *in vivo* testing, where a significantly higher relative bioavailability of OMs was indeed observed.

In order to address the effect of food on the bioavailability of different abiraterone acetate formulations, a fasted-fed *in vivo* study was designed and conducted. It had been shown before that a high fat content in meal has a significant impact on the bioavailability of abiraterone acetate (5). Limited bioavailability of the original drug product Zytiga® under fasting conditions resulted in a significant positive food effect in the rat animal model, which is consistent with previously conducted human studies.

A 1:1 mixture of olive oil and Nutridrink was dosed to rats to create the fed state. The use of this mixture was based not only on previous experience but also on conditions described in the literature. The administration of 1–2 mL of oil is a standard approach to introduce fed conditions in rat PK studies (33,34). However, since the formulation was dosed in hard gelatin capsules, we had to ensure that the rat stomach also contains some aqueous phase in which the capsules could dissolve.

The fasted state comparative bioavailability study has shown a rather unexpected double C_{max} pattern for abiraterone after OM (Fig. 6a). This finding was mainly driven by a single animal outlying with exceptionally high abiraterone serum concentrations at the sampling points between 240 and 420 min. In the food effect study, the C_{max} and AUC values demonstrated limited effect of food for OM formulation, but the T_{max} was substantially prolonged at the fed state, which could be a result of a non-formulation-dependent effect of the presence of food in the gastrointestinal tract that increased secretion, delayed gastric emptying, influenced intestinal peristaltic movement, or competed with drugs on absorption transporters (35). Furthermore, a large variability in the serum drug concentrations has been observed in the OM group at the fasted state. This observation was caused by the fact that always one of the animals achieved C_{max} was at 60, 90, and 120 min, while in the rest of the group, a "plateau" was seen between 90 and 300 min with no clear T_{max}. These findings point out to the main limitation of our studies, which is limited study population. Another limitation is that the pharmacokinetic performance of OM has been studied *in vivo* in a rat model, which is known to have different gastrointestinal physiologies and conditions that may make direct extrapolation of the findings to man difficult. However, the food effect, which is known from human studies, has been well captured in our food effect study, which suggests sufficient study sensitivity. Furthermore, we applied a crossover comparative study design, which allows to limit the study population as it is the most robust study design to limit intersubject variability for the comparison of performance of two (or more) formulations. The limitation of the small study sample is that we could not reliably describe the T_{max} and some other pharmacokinetic variables but the between-formulation comparison, which was the aim of the study, has been well demonstrated. The relatively higher bioavailability of oil marbles under fasting conditions resulted in a significantly suppressed food effect in rats.

CONCLUSION

Overall, it can be concluded that oil marbles represent a promising formulation approach that combines the advantages of liquid-state lipidic formulations such as SEDDS/SMEDDS, namely rapid dissolution, with advantages of solid dosage form such as handling, ability to be filled into hard gelatin capsules, and the possibility to adjust release rate by size. In the specific case of abiraterone acetate, the oil marble formulation made it possible to suppress differences in the oral bioavailability under fed and fasted conditions in rats, and therefore help to eliminate the strong positive food effect for which this molecule has been known. Due to natural differences in rat and human gastrointestinal physiology, these results should be confirmed in human studies as the next step.

AUTHOR CONTRIBUTIONS

The manuscript was written through contributions of all authors. All authors have given approval to the final version of the manuscript.

FUNDING

T.B. received support from the Specific University Research (project MŠMT no. 21-SVV/2019). F.Š. received support from the Czech Science Foundation (project GAČR no. 19-26127X). O.R. received support from the Technology Agency of the Czech Republic (project no. TJ02000143). T.K.

received support from Charles University Research Centre program no. UNCE/SCI/014. O.S. received support from the Charles University project PROGRES Q25/LF1. This work received support from Zentiva, k.s.

COMPLIANCE WITH ETHICAL STANDARDS

All experiments were performed in accordance with the Guiding Principles for the Use of Animals in Charles University, First Faculty of Medicine, and every effort was made to minimize animal suffering. The experimental animal project was approved by the Ministry of Education, Youth and Sports, Czech Republic (MSMT-9445/2018-8).

Conflict of Interest The authors declare that they have no competing interests.

REFERENCES

1. Boyd BJ, Bergstrom CAS, Vinarov Z, Kuentz M, Brouwers J, Augustijns P, et al. Successful oral delivery of poorly water-soluble drugs both depends on the intraluminal behavior of drugs and of appropriate advanced drug delivery systems. Eur J Pharm Sci. 2019;137:104967.
2. Zytiga, EMA/CHMP/542871 – Assessment report for Zytiga, EMA (European Medicines Agency). 2011.
3. Lubberman FJE, Benoist GE, Gerritsen W, Burger DM, Mehra N, Hamberg P, et al. A prospective phase I multicentre randomized cross-over pharmacokinetic study to determine the effect of food on abiraterone pharmacokinetics. Cancer Chemother Pharmacol. 2019;84(6):1179–85.
4. Chi KN, Spratlin J, Kollmannsberger C, North S, Pankras C, Gonzalez M, et al. Food effects on abiraterone pharmacokinetics in healthy subjects and patients with metastatic castration-resistant prostate cancer. J Clin Pharmacol. 2015;55(12):1406–14.
5. Chien C, Smith M, Porre P. Effect of food on abiraterone pharmacokinetics: a review. Int J Pharm. 2017;2.
6. Schultz HB, Meola TR, Thomas N, Prestidge CA. Oral formulation strategies to improve the bioavailability and mitigate the food effect of abiraterone acetate. Int J Pharm. 2020;577:119069.
7. Yonsa, Drug Approval Package: YONSA (abiraterone acetate), FDA (U.S. Food and Drug Administration). Food and Drug Admistration (FDA). 2018.
8. Goldwater R, Hussaini A, Bosch B, Nemeth P. Comparison of a novel formulation of abiraterone acetate vs. the originator formulation in healthy male subjects: two randomized, open-label, crossover studies. Clin Pharmacokinet. 2017;56(7):803–13.
9. Solymosi T, Ötvös Z, Angi R, Ordasi B, Jordán T, Molnár L, et al. Novel formulation of abiraterone acetate might allow significant dose reduction and eliminates substantial positive food effect. Cancer Chemother Pharmacol. 2017;80(4):723–8.
10. Solymosi T, Ötvös Z, Angi R, Ordasi B, Jordán T, Semsey S, et al. Development of an abiraterone acetate formulation with improved oral bioavailability guided by absorption modeling based on in vitro dissolution and permeability measurements. Int J Pharm. 2017;532(1):427–34.
11. Boleslavská T, Světlík S, Žvátora P, Bosák J, Dammer O, Beránek J, et al. Preclinical evaluation of new formulation concepts for abiraterone acetate bioavailability enhancement based on the inhibition of pH-induced precipitation. Eur J Pharm Biopharm. 2020;151:81–90.
12. Legen I, Peternel L, Novak Stagoj M, Homar M, Rozman Peterka T, Klancar U. Self-microemulsifying drug delivery system of abiraterone or abiraterone acetate, WO 2014/009434 A1 2014.
13. Pouton CW, Porter CJ. Formulation of lipid-based delivery systems for oral administration: materials, methods and strategies. Adv Drug Deliv Rev. 2008;60(6):625–37.
14. Mullertz A, Ogbonna A, Ren S, Rades T. New perspectives on lipid and surfactant based drug delivery systems for oral delivery of poorly soluble drugs. J Pharm Pharmacol. 2010;62(11):1622–36.
15. Mu H, Holm R, Müllertz A. Lipid-based formulations for oral administration of poorly water-soluble drugs. Int J Pharm. 2013;453(1):215–24.
16. Bernkop-Schnurch A, Jalil A. Do drug release studies from SEDDS make any sense? J Control Release. 2018;271:55–9.
17. Carriere F. Impact of gastrointestinal lipolysis on oral lipid-based formulations and bioavailability of lipophilic drugs. Biochimie. 2016;125:297–305.
18. Sonali BH, Sushmita SC, Sonali SK, Suchita LS, Sugave RV. A review on: soft gelatine capsule. Int J Innov Pharm Sci Res. 2018;6(6):59–71.
19. Joyce P, Dening TJ, Meola TR, Schultz HB, Holm R, Thomas N, et al. Solidification to improve the biopharmaceutical performance of SEDDS: opportunities and challenges. Adv Drug Deliv Rev. 2019;142:102–17.
20. Aussillous P, Quéré D. Liquid marbles. Nature. 2001;411(6840):924–7.
21. McHale G, Newton MI. Liquid marbles: principles and applications. Soft Matter. 2011;7(12):5473.
22. Hapgood KP, Khanmohammadi B. Granulation of hydrophobic powders. Powder Technol. 2009;189(2):253–62.
23. Janská P, Rychecký O, Zadražil A, Štěpánek F, Čejková J. Liquid oil marbles: increasing the bioavailability of poorly water-soluble drugs. J Pharm Sci. 2019;108(6):2136–42.
24. Geboers S, Stappaerts J, Mols R, Snoeys J, Tack J, Annaert P, et al. The effect of food on the intraluminal behavior of abiraterone acetate in man. J Pharm Sci. 2016;105(9):2974–81.
25. Rowe RC, Sheskey PJ, Quinn ME. Handbook of pharmaceutical excipients. 6th ed. USA: Pharmaceutical Press and American Pharmacists Association; 2009.
26. Kabanov AV, Batrakova EV, Alakhov VY. Pluronic® block copolymers as novel polymer therapeutics for drug and gene delivery. J Control Release. 2002;82(2):189–212.
27. Kolliphor RH40, BASF Technical information no. 03_111141e-01.
28. Tween 20, Sigma Alrdich Product information no. 1379.
29. Tween 80, Sigma Aldrich Product information no. 1754.
30. Kolliphor EL, BASF Technical information no. 03_111139e-02.
31. Brouwers J, Brewster ME, Augustijns P. Supersaturating drug delivery systems: the answer to solubility-limited oral bioavailability? J Pharm Sci. 2009;98(8):2549–72.
32. Stappaerts J, Geboers S, Snoeys J, Brouwers J, Tack J, Annaert P, et al. Rapid conversion of the ester prodrug abiraterone acetate results in intestinal supersaturation and enhanced absorption of abiraterone: in vitro, rat in situ and human in vivo studies. Eur J Pharm Biopharm. 2015;90:1–7.
33. Brocks DR, Wasan KM. The influence of lipids on stereoselective pharmacokinetics of halofantrine: important implications in food-effect studies involving drugs that bind to lipoproteins. J Pharm Sci. 2002;91(8):1817–26.
34. Shayeganpour A, Jun AS, Brocks DR. Pharmacokinetics of Amiodarone in hyperlipidemic and simulated high fat-meal rat models. Biopharm Drug Dispos. 2005;26(6):249–57.
35. Welling PG. Effects of food on drug absorption. Annu Rev Nutr. 1996;16:383–415.

Příloha 3

RYŠÁNEK, P., GRUS, T., LUKÁČ, P., KOZLÍK, P., KŘÍŽEK, T., POZNIAK, J., ROUŠAROVÁ, J., KRÁLOVIČOVÁ, J., KUTINOVÁ CANOVÁ, N., BOLESLAVSKÁ, T., BOSÁK, J., ŠTĚPÁNEK, F., ŠÍMA, M., SLANAŘ, O. Validity of cycloheximide chylomicron flow blocking method for the evaluation of lymphatic transport of drugs. *Br J Pharmacol*, 2021, 1-12.

Received: 28 May 2021 | Revised: 14 July 2021 | Accepted: 24 July 2021

DOI: 10.1111/bph.15644

RESEARCH ARTICLE

Validity of cycloheximide chylomicron flow blocking method for the evaluation of lymphatic transport of drugs

Pavel Ryšánek[1] | Tomáš Grus[2] | Peter Lukáč[2] | Petr Kozlík[3] | Tomáš Křížek[3] | Jiří Pozniak[4] | Jaroslava Roušarová[1] | Jana Královičová[1] | Nikolina Kutinová Canová[1] | Tereza Boleslavská[5,6] | Jan Bosák[5] | František Štěpánek[6] | Martin Šíma[1] | Ondřej Slanař[1]

[1]Institute of Pharmacology, First Faculty of Medicine, General University Hospital in Prague, Charles University, Prague, Czech Republic

[2]Department of Cardiovascular Surgery, First Faculty of Medicine, General University Hospital in Prague, Charles University, Prague, Czech Republic

[3]Department of Analytical Chemistry, Faculty of Science, Charles University, Prague, Czech Republic

[4]Third Department of Surgery, First Faculty of Medicine, Motol University Hospital, Charles University, Prague, Czech Republic

[5]Preformulation and Biopharmacy Department/Clinical Development Department, Zentiva, k.s, Prague, Czech Republic

[6]Department of Chemical Engineering, University of Chemistry and Technology, Prague, Czech Republic

Correspondence
Pavel Ryšánek, Institute of Pharmacology, Albertov 4, 128 00 Praha 2, Czech Republic.
Email: pavel.rysanek@lf1.cuni.cz

Martin Šíma, Institute of Pharmacology, Albertov 4, 128 00 Praha 2, Czech Republic.
Email: martin.sima@lf1.cuni.cz

Funding information
Charles University Research Centre, Grant/Award Number: UNCE/SCI/014; Univerzita Karlova v Praze, Grant/Award Number: SVV 260 523

Background and purpose: Lymphatic transport of drugs after oral administration is an important mechanism for absorption of highly lipophilic compounds. Direct measurement in lymph duct cannulated animals is the gold standard method, but non-invasive cycloheximide chylomicron flow blocking method has gained popularity recently. However, concerns about its reliability have been raised. The aim of this work was to investigate the validity of cycloheximide chylomicron flow blocking method for the evaluation of lymphatic transport using model compounds with high to very high lipophilicity, that is, abiraterone and cinacalcet.

Experimental approach: Series of pharmacokinetic studies were conducted with abiraterone acetate and cinacalcet hydrochloride after enteral/intravenous administration to intact, lymph duct cannulated and/or cycloheximide pre-treated rats.

Key results: Mean total absolute oral bioavailability of abiraterone and cinacalcet was 7.0% and 28.7%, respectively. There was a large and significant overestimation of the lymphatic transport extent by the cycloheximide method. Mean relative lymphatic bioavailability of abiraterone and cinacalcet in cycloheximide method was 28-fold and 3-fold higher than in cannulation method, respectively.

Conclusion and implications: Cycloheximide chylomicron flow blocking method did not provide reliable results on lymphatic absorption and substantially overestimated lymphatic transport for both molecules, that is, abiraterone and cinacalcet. This non-invasive method should not be used for the assessment of lymphatic transport and previously obtained data should be critically revised.

KEYWORDS
abiraterone, bioavailability, biodistribution, cinacalcet, lymph duct cannulation, pharmacokinetics

1 | INTRODUCTION

Lymphatic transport is a potential way of drug transfer into systemic circulation after oral dosing. Upon absorption into intestinal mucosa, highly lipophilic compounds are typically incorporated into chylomicrons and secreted into mesenteric lymph, which is drained into systemic circulation by a system of lymphatic vessels (Charman & Stella, 1986; Porter et al., 2007). Lymphatic transport has been

Abbreviations: IS, internal standard; SRM, selected reaction mode; LLOQ, lower limit of quantification; RSD, relative standard deviation; ULOQ, upper limit of quantification.

studied for several compounds in the last few decades. It has been shown as a potential way of increasing oral bioavailability, evading the liver first-pass effect and enhancing pharmacodynamic effects in compounds targeting immune cells physiologically present in the lymph (Han, Hu, Quach, Simpson, Edwards, et al., 2016a; Shackleford et al., 2003).

There are several animal models currently used for the investigation of lymphatic transport of drugs. The gold standard methodology relies on direct measurement of drug concentration in the lymph in various animal species, whereas rat is the most common one (Trevaskis et al., 2015). However, a non-invasive chylomicron flow blocking approach in rats has also been used gaining substantial popularity in recent years (Dahan & Hoffman, 2005). This method is based on the assumption that cycloheximide administered intraperitoneally shortly before oral dosing of the investigated compound blocks its lymphatic transport without affecting other ways of intestinal absorption.

Yet there are no robust validation data with only one direct comparative study for **cholecalciferol, vitamin D_3**, (Dahan & Hoffman, 2005) and one indirect comparison for **halofantrine** (Caliph et al., 2000; Lind et al., 2008). In a recently published systematic review, we observed a general trend towards higher relative bioavailability via lymph in **cycloheximide** studies (Rysanek et al., 2020). The median relative bioavailability via lymph was 47.3% and 25.7% in cycloheximide and lymph duct cannulation studies, respectively. Furthermore, a significant difference was reported for compounds with log P < 5, where the respective parameters were 47.3% and 2.26%. We therefore suspected a vast overestimation by the cycloheximide method especially for drugs with lower lipophilicity.

Abiraterone acetate is a highly lipophilic compound (log P ~ 4.5) used in the treatment of castration resistant prostate cancer. It has a pronounced food effect in men, with up to 17-fold increase in C_{max} and tenfold increase in AUC when administered with high-fat meal (Chi et al., 2015). For safety reasons, this led to posology restriction to fasted state only.

Cinacalcet hydrochloride is another highly lipophilic molecule (log P ~ 6.5) used in the treatment of hyperparathyroidism. Similarly to abiraterone, there is a significant food effect after oral administration in humans, albeit not that high. Its bioavailability increases by 50–70% depending on the fat content in the meal (Padhi et al., 2007).

As shown for other lipophilic compounds, significantly increased bioavailability after high-fat food intake may be caused by enhanced lymphatic transport (Khoo et al., 2001; Trevaskis et al., 2010). Therefore, we hypothesized that intestinal lymphatic transport could be involved in the processes of abiraterone and cinacalcet absorption after oral administration.

The aim of this study was to investigate the validity of the non-invasive cycloheximide chylomicron flow blocking method for the evaluation of lymphatic transport by a comparison with invasive lymph duct cannulation method using two model compounds with high to very high lipophilicity, that is, abiraterone and cinacalcet.

What is already known?

- Lymphatic transport of drugs plays an important role in intestinal absorption of many highly lipophilic compounds
- Cinacalcet and abiraterone are highly lipophilic drugs used to treat hyperparathyroidism and prostate cancer, respectively.

What does this study add?

- Non-invasive cycloheximide chylomicron flow blocking method is not reliable in estimating intestinal lymphatic transport of drugs.
- Oral cinacalcet is absorbed by a high proportion through the lymph, whereas abiraterone is not.

What is the clinical significance?

- Lymphatic transport may be involved in cinacalcet pronounced positive food effect.

2 | METHODS

2.1 | Abiraterone dosing forms preparation

Zytiga tablets were crushed and filled into mini gelatine capsules, size 9el (Harvard Apparatus, USA). Abiraterone acetate content in one capsule was 4.1 mg.

Abiraterone oil solution was prepared by abiraterone acetate powder dissolution in DMSO to achieve a concentration of 40 mg ml^{-1}. Abiraterone DMSO solution 100 μl was then added to 1 ml olive oil and vortexed (Vortex mixer, Labnet international, Inc.) for 1 min to produce a homogenous emulsion. The dosing form was prepared freshly not more than 30 min before dosing.

Abiraterone solution for intravenous administration (1 mg ml^{-1}) was prepared according to Kumar et al. (2013). Briefly, abiraterone was dissolved in solution containing 10% DMSO, 10% mixture of Kolliphor HS 15 and ethanol (1:1, V/V), 10% Cremophor EL and 70% Captisol (20% Captisol in water). The concentration of abiraterone was determined using HPLC analysis.

2.2 | Cinacalcet dosing forms preparation

Cinacalcet hydrochloride powder was dissolved in DMSO to achieve a concentration of 30 mg ml^{-1}. Cinacalcet DMSO solution 100 μl was then added to 1 ml olive oil and shaken to mix the DMSO and oil fractions. The dosing form was prepared freshly not more than 30 min before dosing.

Cinacalcet intravenous formulation was prepared by cinacalcet hydrochloride powder dissolution in DMSO in concentration 3 mg ml^{-1}. This solution was further diluted with distilled water to achieve a concentration of 0.3 mg ml^{-1}.

2.3 | Animals

All animal experiments were performed under approval from the Ministry of Education, Youth and Sports, Czech Republic (MSMT-9445/2018-8) and are reported in compliance with the ARRIVE guidelines (Percie du Sert et al., 2020) and with the recommendations made by the *British Journal of Pharmacology* (Lilley et al., 2020). All efforts were made to minimize animal suffering. Male Wistar rats (weight 300–450 g, age 3–5 months) were purchased from Velaz s. r. o., Prague, Czech Republic. They were housed under standard conditions (12-h light/dark cycle, 22°C temperature and 50% humidity) in cages with wood shavings bedding (two rats per cage during acclimation and one rat per cage during experiment) and fed on water and granulated diet ad libitum. The acclimation period took at least 1 week. The animals were randomly assigned to experimental arms.

2.4 | Lymphatic transport studies in cannulated rats

Mesenteric lymph duct cannulated anaesthetized rat model was used as previously described with slight modifications (Trevaskis et al., 2015). Rats were left on normal diet and given 1 ml olive oil 1 h prior to surgery to facilitate the mesenteric lymph duct visualization. They were anaesthetized with an i.m. combination of xylazine (5 mg kg^{-1}) and ketamine (100 mg kg^{-1}) after a rapid isoflurane induction maintaining spontaneous breathing throughout the whole experiment. Transverse laparotomy was performed. Mesenteric duct was identified cranially to superior mesenteric artery and cannulated with heparin prefilled 0.97 mm O.D., 0.58 mm I.D. polyethylene catheter (Instech Laboratories, Plymouth Meeting, USA). The catheter was fixed in place with two to three drops of tissue adhesive (Surgibond®, SMI AG, Belgium). A duodenal catheter was also placed (same parameters as for lymphatic catheter) via a small duodenotomy and fixed with a purse string suture or tissue adhesive. The abdominal wall was sutured in two layers with both catheters leaving the abdominal cavity on the right side of the animal. At the end of the procedure, right jugular vein was cannulated for blood sampling (3 Fr polyurethane catheter, Instech Laboratories, Plymouth Meeting, USA).

The rats were then placed on heated pads and covered with blanket to prevent heat loss. Cinacalcet (3 mg) oil solution and abiraterone (4 mg) oil solution were dosed slowly via duodenal catheter over 30 min. The mass of olive oil administered in each dosage form was 1 ml. Abiraterone (4 mg) capsule was dosed deeply intraduodenally via small incision during the surgery before the wound closure. Whole lymph was collected in regularly changed Eppendorf tubes from the time when oil solution dosing started, or capsule was inserted into duodenum. The rats were continuously hydrated with normal saline at a rate of 3 ml h^{-1} intraduodenally using infusion pump (Perfusor® compact^{plus}, B. Braun Melsungen AG, Germany). Anaesthesia was maintained throughout the rest of the experiment and additional ketamine i.m. boluses were given whenever necessary. Eppendorf tubes were changed hourly and systemic blood was drawn at the same time points. At the end of the experiment with abiraterone capsules, cranial part of the small intestine was exposed in all animals to verify complete capsule dissolution. The animals were killed by anaeshtetic overdose.

2.5 | Lymphatic transport studies with cycloheximide

Two separate two-period, one sequence, crossover studies were conducted to compare the bioavailability of either abiraterone capsule or cinacalcet oil solution after oral dosing with and without pre-treatment with chylomicron flow blocking agent cycloheximide. The crossover study design in rats was chosen and conducted as described previously (Boleslavská, Rychecký, et al., 2020). Both studies were conducted similarly. In both periods, rats were fasted for at least 4 h before and 4 h after the dosing. In the first period, the test drug (abiraterone 4 mg or cinacalcet 3 mg) was administered via oral gavage with no additional treatment. In the second period, the animals were pre-treated with 3 mg kg^{-1} of cycloheximide administered intraperitoneally 1 h before dosing. The cycloheximide DMSO solution was diluted in normal saline in a concentration of 3 mg ml^{-1} for this purpose. The wash-out period lasted 48 and 72 h in abiraterone and cinacalcet study, respectively. Systemic blood draws were taken at 1, 2, 3, 4, 5, 7 and 10 h after abiraterone administration and at 1, 2, 3, 4, 5, 6, 8, 12 and 24 h after cinacalcet administration. In the second period, a pre-dose blood sample was taken additionally (0 h) to verify lack of carry over effect.

2.6 | Lymphatic transport study with both cycloheximide and lymph duct cannulation

In order to directly assess the cycloheximide effect on lymphatically and non-lymphatically absorbed amount of drug, a study with cycloheximide pre-treated and lymph duct cannulated rats was conducted. Cycloheximide 3.0 mg kg^{-1} was administered i.p. immediately before the surgery. The lymph duct, duodenum and jugular vein were cannulated within 60 min as described for lymphatic transport studies in cannulated animals. After the surgery and exactly 60 min after the cycloheximide pre-treatment, cinacalcet oil solution was administered over 30 min via duodenal catheter. The lymph and blood were sampled hourly as described above.

2.7 | Bioavailability studies

Absolute oral bioavailability of cinacalcet oil solution was evaluated in a two-period, one sequence (i.v. - p.o.), cross-over bioavailability study and parallel comparison of two groups (i.v. - p.o.) was conducted for abiraterone capsule. Right jugular vein was cannulated in both studies. After overnight recovery, the rats were i.v. dosed with cinacalcet or abiraterone (both 1 mg kg^{-1}). Systemic blood was drawn at 10 and 30 min and at 1, 2, 3, 5, 8, 12 and 24 h after cinacalcet administration or at 5 and 15 min and at 0.5, 1, 1.5, 2, 2.5, 3, 4, 5 and 7 h after abiraterone administration. The p.o. dosing and sampling were performed as described for the cycloheximide lymphatic transport studies (see above).

2.8 | Cinacalcet biodistribution study

Cinacalcet biodistribution was compared between cycloheximide pre-treated and control rats. The rats were fasted for 12 h before and 4 h after dosing. Six rats were dosed with cinacalcet via oral gavage (3 mg) with no further treatment. Nine other rats were pre-treated with cycloheximide before the cinacalcet administration. The animals were killed at 8 and 24 h (both groups) and at 48 h (cycloheximide group) by cervical dislocation under deep isoflurane anaesthesia. Systemic blood sample was taken and the abdominal cavity was exposed. Small intestine, liver, right kidney and spleen were harvested. The kidney and the spleen were homogenized (IKA® T10 basic Ultra-Turrax®) in 100% DMSO solution. A 1 to 2 mg sample was taken from the liver and homogenized. The small intestine was longitudinally cut and washed thoroughly to remove all intraluminal contents. The organ was then homogenized as a whole.

Moreover, a single group extended cinacalcet pharmacokinetic study with cycloheximide pre-treatment was conducted. The blood draws were taken at 4, 8, 18, 21, 24, 28, 32, 42 and 48 h to cover the late pharmacokinetic profile.

2.9 | Sample processing

Blood samples were centrifuged (1811x g for 10 min) and serum was extracted. Lymph volume was measured gravimetrically and the samples were further processed without additional adjustment. Organ homogenates were centrifuged (1431x g for 10 min) and the DMSO supernatant was extracted. All samples were stored in −80°C until analysis. Laboratory was unaware of animal assignment to particular experimental group (laboratory blinding).

2.10 | Analytical methods

Determination of cinacalcet in studied samples was performed using the Shimadzu UHPLC Nexera X3 coupled with a Triple Quad 8045 tandem mass spectrometer (Shimadzu, Kyoto, Japan). Poroshell 12 SB AQ column (100 mm × 2.1 mm, 2.6 μm particle size) from Agilent Technologies (Waldbronn, Germany) was used for the analysis. The mobile phase consisted of 0.1% formic acid in deionized water (Solvent A) and acetonitrile (Solvent B). The flow rate of the mobile phase was maintained at 0.45 ml min^{-1} and the injection volume was 1 μl. The temperature of the column was kept at 40°C and samples were thermostated at 5°C. The optimized gradient program (min/% B) was 0/30, 1.0/30, 3.0/80, 4.0/80, 4.5/30 and 6.5/30. The MS/MS measurements (operated in positive mode) were performed in the selected reaction mode (SRM). Two SRM transitions were monitored for cinacalcet: Quantifier transition was 358.2 > 155.2 (Q1 pre-bias −18 V, Q3 pre-bias −29 V and collision energy −20 V), and qualifier transition was 358.2 > 208.2 (Q1 pre-bias −16 V, Q3 pre-bias −25 V and collision energy −15 V). The transition 362.2 > 155.2 (Q1 pre-bias −18 V, Q3 pre-bias −28 V and collision energy −18 V) was monitored for cinacalcet-d_4 (internal standard, IS). The ion source was set as follows: interface temperature: 300°C, desolvation line temperature: 250°C, heat block temperature: 400°C, nebulizing gas flow: 3 L min^{-1}, heating gas flow: 10 L min^{-1} and drying gas flow: 10 L min^{-1}.

The concentration of cinacalcet was determined in serum, lymph and different tissues (dimethyl sulfoxide extracts). Before the LC–MS/MS analysis, 20 μl of sample (serum, lymph or tissue extracts) was deproteinized with 60 μl of 100% acetonitrile containing IS (cinacalcet-d_4, $c = 30$ ng ml^{-1}) in an Eppendorf tube by vortexing for 15 s. Then, samples were centrifuged at 16,500×g for 8 min and 50 μl of supernatant was transferred into LC vials. The method was validated in terms of linearity, lower limit of quantification (LLOQ), upper limit of quantification (ULOQ), accuracy, precision, selectivity, recovery and matrix effects. Selectivity was monitored by injecting six samples of each matrix (serum, lymph and all studied tissue extract samples) with mass spectrometer set in scan mode. The obtained chromatograms showed no interfering compound within the retention time window of cinacalcet. Moreover, the developed method uses a tandem mass spectrometer in specific SRM mode, which ensures high selectivity. The calibration curves were constructed in each blank matrix (serum, lymph and pooled tissue extracts) with seven concentrations by plotting the ratio of the peak area of cinacalcet to that of IS against cinacalcet concentration. The weighted least-squares linear regression method was used with weighting factor of 1 x^{-2}, which improved the accuracy in low concentrations. Due to the use of cinacalcet-d_4 as the IS, no significant difference in calibration curves in different matrices was observed. The method was linear (coefficients of determination [R^2] higher than 0.9997) in the concentration range of 0.5–1,600 ng ml^{-1}. LLOQ, which was the lowest calibration standard, was 0.5 ng ml^{-1} with precision and accuracy up to 10% (back calculated). ULOQ, which was the highest calibration standard, was 1,600 ng ml^{-1} with precision and accuracy up to 4% (back calculated). The accuracy and precision of back-calculated concentrations of other calibration points were within 5% of the nominal concentration. Method accuracy and precision were evaluated by measuring five replicates at three different concentrations of 1, 50 and 1,000 ng ml^{-1} in each

matrix on two different days. The accuracy was expressed as the relative error, RE (%) = (measured concentration − expected concentration)/expected concentration × 100 and the precision expressed by repeatability as the relative standard deviation (RSD). The inter-day and intra-day precisions (RSD %) ranged from 0.9% to 6.5%, and the relative accuracy (RE%) was within ±6.1%. The same samples were also used as quality control samples. Quality control samples were injected after each sixth sample to assess the validity of the analytical method. Recovery was evaluated by comparing the area of the cinacalcet standard peak of the pre-protein-precipitation spiked sample with that of the corresponding post-protein-precipitation spiked sample at three concentrations (1, 50 and 1,000 ng ml^{-1}). The recovery ranged in each matrix from 98.9% to 101.1%. Matrix effect was determined by comparing the area of the cinacalcet standard peak of the post-protein-precipitation spiked sample with that of the 80% acetonitrile (without matrix effect). It was evaluated at three concentration levels (1, 50 and 1,000 ng ml^{-1}) using six different samples of each matrix. The matrix effect ranged from 74% to 102%. In our method, the matrix effect is eliminated by the use of an isotopically labelled standard because the analyte/IS response ratio remains unaffected, even when the absolute responses of the analyte and IS are affected significantly. The LC–MS/MS validation proved the suitability of our analytical method for the determination of cinacalcet in different matrices.

Abiraterone concentrations in serum and lymph were analysed using LC–MS as described previously (Boleslavská, Světlík, et al., 2020). The method was validated for the same validation parameters and using the same procedure as for cinacalcet for both studied matrices, that is, serum and lymph. The LC–MS/MS was selective since no interfering endogenous components were observed at the retention time of abiraterone. A 7-point calibration curve was constructed using the analyte-to-internal standard peak area ratio in each matrix. Weighted least-squares linear regression (1 x^{-2} weighting factor) was used. The developed method was linear in the range of 0.5–600 ng ml^{-1} (R^2 > 0.9996). The accuracy and precision of back-calculated concentrations of all calibration points deviated within 8% of the nominal concentration, except for LLOQ (0.5 ng ml^{-1}), which deviated by ±15%. The accuracy and precision (five replicates at concentrations of 1, 50 and 500 ng ml^{-1} in each matrix on two different days) were between 1.2% to 7.8% and 0.8% to 4.9%, respectively. The recovery of abiraterone and matrix effect (1, 50 and 500 ng ml^{-1}) ranged from 97% to 102% and 85% to 105%, respectively. The mentioned validation performance parameters confirmed that LC–MS/MS method is suitable for quantification of abiraterone in serum and lymph samples.

2.11 | Data analysis and statistics

Serum concentrations in all pharmacokinetic studies were dose normalized to 1 mg kg^{-1} prior to further calculations. AUC values were determined using linear trapezoidal rule. Exact actual sampling times were used for this purpose. Scheduled sampling times were used for mean concentration plotting in the graphs. In the cinacalcet biodistribution study, dose normalized (1 mg kg^{-1}) absolute amount of drug in DMSO supernatant was determined and further normalized to weight of the homogenized organ sample (1 g^{-1}). Lymph drug concentrations were dose normalized to 1 mg kg^{-1} as well. Lymph pharmacokinetic profiles were plotted in the graphs using drug concentrations measured in the sampled lymph as actual concentrations in the middle of each collection period, that is, assuming linear absorption. GraphPad Prism version 9.1.0 (GraphPad Software, San Diego, CA, USA) was used for all statistical analyses. Unpaired Student's *t*-test was used to compare pharmacokinetic and lymphatic transport parameters. Level of significance was set to $p < 0.05$.

2.12 | Bioavailability and lymphatic transport calculations

Absolute bioavailability via lymph (F_{AL}) was defined as percentage of administered drug dose absorbed into the lymph. It was determined directly from lymph volume and drug concentration in lymph duct cannulated rats. Absolute bioavailability via portal vein (F_{AP}) was analogically defined as percentage of administered drug dose reaching the systemic circulation after direct absorption into blood. It was calculated using the following equation:

$$F_{AP} = AUC_{ent} \times AUC_{iv}^{-1}, \quad (1)$$

where AUC_{ent} is the area under the dose normalized blood concentration-time curve after enteral dosing in lymph duct cannulated (i.e. lymph deprived) rats and AUC_{iv} is the respective parameter in a separate intravenously dosed group. Total absolute bioavailability (F) in lymph duct cannulated rats was calculated as a sum of F_{AL} and F_{AP}. In intact, non-cannulated animals, F was calculated using standard formula for oral bioavailability:

$$F = AUC_{po} \times AUC_{iv}^{-1} \quad (2)$$

Relative bioavailability via lymph (F_{RL}) was defined as percentage of systemically available drug that was absorbed via lymph. It was calculated using the following equation:

$$F_{RL} = F_{AL} \times F^{-1}. \quad (3)$$

F_{RL} in the cycloheximide studies was calculated directly by comparing dose normalized AUC with and without cycloheximide pretreatment:

$$F_{RL} = \left(AUC_{po} - AUC_{cycloheximide}\right) \times AUC_{po}^{-1}. \quad (4)$$

2.13 | Materials

Abiraterone acetate commercial tablets (Zytiga®) and abiraterone acetate powder were kindly donated by Zentiva, k.s. (Prague, Czech Republic), Cinacalcet hydrochloride powder and its internal standard, cycloheximide solution 100 mg ml^{-1} in 100% DMSO, Kolliphor HS 15 and Cremophor EL were purchased from Sigma-Aldrich, Prague, Czech Republic. All solvents used were at least of HPLC grade. Xylazine 20 mg ml^{-1} solution (Rometar®, Bioveta a.s., Czech Republic), Ketamine 100 mg ml^{-1} solution (Narkamon®, Bioveta a.s., Czech Republic) and isoflurane (IsoFlo®, Zoetis/Pfizer, Czech Republic) were used for animal anaesthesia. Ketoprofen 100 mg ml^{-1} (Ketodolor®, Le Vet Beheer B.V., Netherlands) was used as analgesic. Heparin solution 5,000 IU ml^{-1} (Zentiva k.s., Czech Republic) was used for catheter patency maintenance. T61® (Intervet International B.V., Netherlands) was used for killing the animals at the end of experiments.

2.14 | Nomenclature of targets and ligands

Key protein targets and ligands in this article are hyperlinked to corresponding entries in the IUPHAR/BPS Guide to PHARMACOLOGY http://www.guidetopharmacology.org and are permanently archived in the Concise Guide to PHARMACOLOGY 2019/20 (Alexander et al., 2019).

3 | RESULTS

Basic pharmacokinetic parameters for abiraterone and cinacalcet after oral and intravenous dosing to rats as well as pharmacokinetic parameters after cycloheximide pre-treatment are summarized in Tables 1 and 2. The corresponding pharmacokinetic profiles are shown in Figures 1 and 2.

Absolute oral bioavailability of abiraterone after administration of capsules was 7.0%. Cycloheximide pre-treatment significantly decreased both the rate and extent of absorption of abiraterone as indicated by threefold C_{max} decrease and a twofold AUC decrease. Although the mean half-life was approximately 2 h after both oral and intravenous administrations, it was apparently prolonged to 18 h in the cycloheximide pre-treated group.

Absolute oral bioavailability of cinacalcet was 28.7% (pharmacokinetic profile from the p.o. period of the bioavailability study not shown). Cinacalcet pharmacokinetic profile up to 12 h was substantially flattened by cycloheximide pre-treatment. From 12 h onwards, the mean serum concentration rose surprisingly to its maximum at the last sampling point at 24 h. This pattern was seen consistently in all animals after pre-treatment with cycloheximide. The mean C_{max} values were similar between the periods; however, T_{max} was significantly delayed after cycloheximide pre-treatment.

Tissue cinacalcet concentrations after oral dosing with and without cycloheximide pre-treatment are shown in Supporting Information S1. Particularly high concentrations were observed in the

TABLE 1 Mean ± SD pharmacokinetic parameters of abiraterone after oral administration of capsule (4 mg) to rats with or without cycloheximide (CHX) pre-treatment and mean ± SD pharmacokinetic parameters of abiraterone after intravenous administration (1 mg kg^{-1})

	p.o. ($n = 8$)	p.o. + CHX ($n = 6$)	i.v. ($n = 5$)
C_{max} (ng ml^{-1})	4.2 ± 2.4	1.4 ± 1.0*	N/A
T_{max} (h)	2.9 ± 0.8	3.5 ± 1.1	N/A
$T_{1/2}$ (h)	1.9 ± 0.7	17.9 ± 12.6*	2.1 ± 1.0
AUC_{0-7} (ng h ml^{-1})	12.3 ± 5.5	5.5 ± 4.3*	197.8 ± 24.4
V_{ss} (L kg^{-1})	N/A	N/A	3.7 ± 0.5

Note: All concentration and AUC values are dose normalized (1 mg kg^{-1}).
*P< 0.05 versus p.o. dosing.

TABLE 2 Mean ± SD pharmacokinetic parameters of cinacalcet after oral administration of oil solution (3 mg) to rats with or without cycloheximide (CHX) pre-treatment and mean ± SD pharmacokinetic parameters of cinacalcet after intravenous administration (1 mg kg^{-1})

	Cycloheximide study ($n = 8$)		Bioavailability study ($n = 6$)	
	p.o.	p.o. + CHX	p.o.	i.v.
C_{max} (ng ml^{-1})	5.2 ± 1.2	4.6 ± 1.8	21.7 ± 5.6	N/A
T_{max} (h)	10.0 ± 2.6	24.2 ± 0.1*	6.8 ± 2.7	N/A
$T_{1/2}$ (h)	4.8 ± 0.3	N/A	2.7 ± 0.3	6.8 ± 3.3
AUC_{0-12} (ng h ml^{-1})	36.3 ± 6.7	10.9 ± 4.5*	137.3 ± 38.1	514 ± 117
AUC_{0-24} (ng h ml^{-1})	66.6 ± 12.3	46.2 ± 14.4*	196.9 ± 62.8	633 ± 200
V_{ss} (L kg^{-1})	N/A	N/A	N/A	11.6 ± 5.1

Note: All concentration and AUC values are dose normalized (1 mg kg^{-1}). $T_{1/2}$ was not estimated in the cycloheximide profile due to increasing concentrations towards the last sampling in all subjects.
*P < 0.05 versus p.o. dosing.

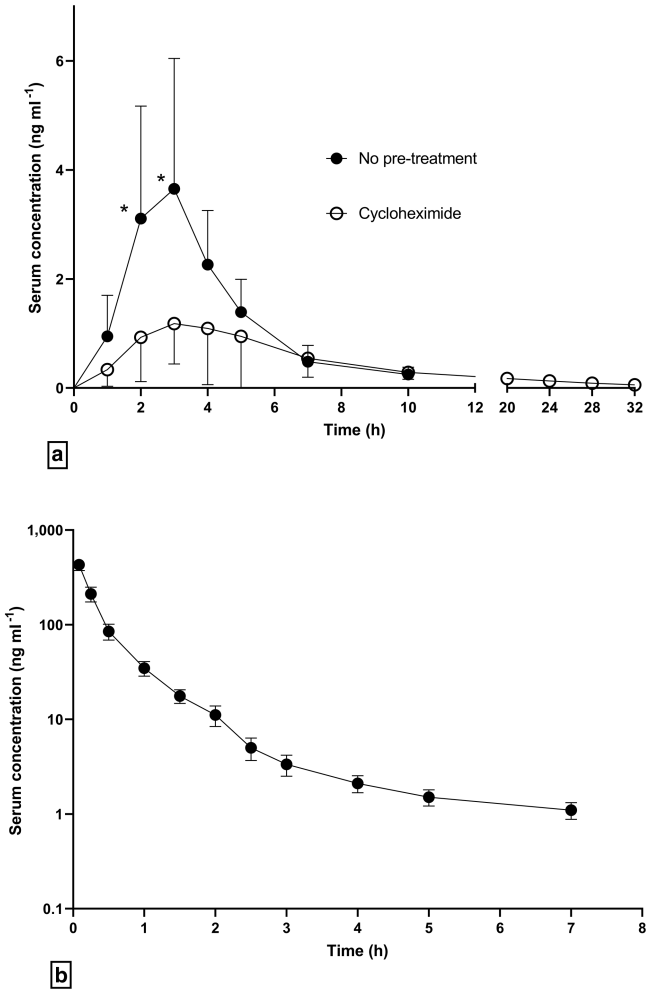

FIGURE 1 Dose normalized abiraterone serum pharmacokinetic profiles. (a) Mean ± SD pharmacokinetic profiles of abiraterone administered orally to rats as capsule (4 mg) with or without cycloheximide pre-treatment. Profiles are derived from one group of animals (two-period, crossover study design, cycloheximide given in the second period), $n = 8$. $^{*}P < 0.05$ versus cycloheximide. (b) Mean ± SD abiraterone pharmacokinetic profile after intravenous dosing (1 mg kg^{-1}), $n = 5$

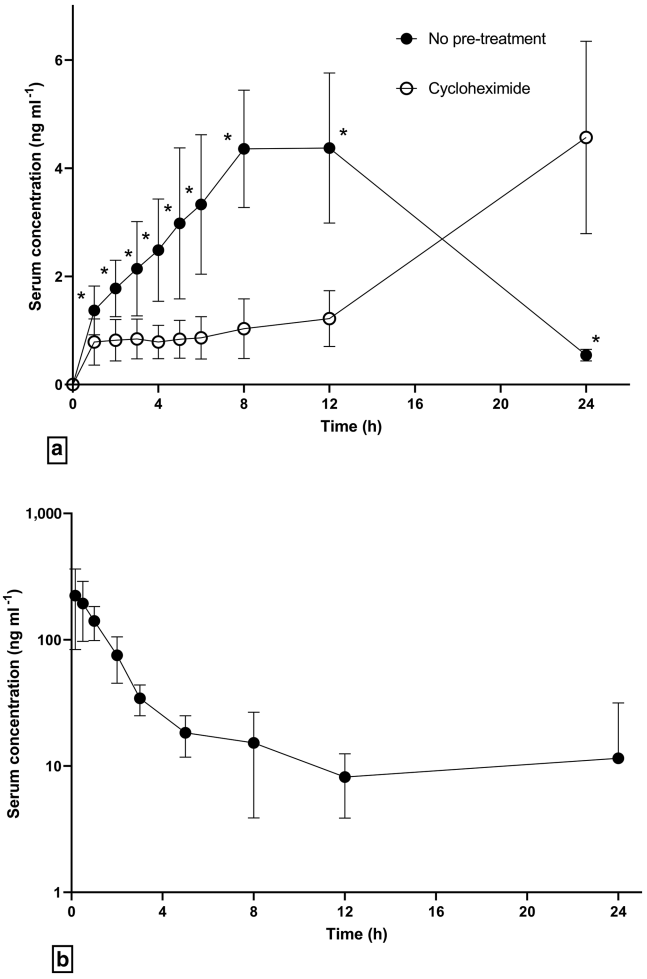

FIGURE 2 Dose normalized cinacalcet pharmacokinetic profiles. (a) Mean ± SD pharmacokinetic profiles of cinacalcet administered orally to rats as oil solution (3 mg) with or without cycloheximide pre-treatment. Profiles are derived from one group of animals (two-period, crossover study design, cycloheximide given in the second period), $n = 8$. $^{*}P < 0.05$ versus cycloheximide. (b) Mean ± SD cinacalcet pharmacokinetic profile after intravenous dosing (1 mg kg^{-1}), $n = 6$

intestinal wall and in the spleen. In animals without cycloheximide pre-treatment, the mean tissue drug concentrations in all organs dropped, following a maximum noted at 8 h sampling time. In the cycloheximide pre-treated rats, cinacalcet tissue level remained low in the first 24 h. It rose then and the peak concentration was achieved at 48 h in all investigated organs. There was no cinacalcet depot found responsible for the late serum concentration increase.

The rising concentrations pattern was confirmed in the extended pharmacokinetic study in a separate group of cycloheximide pre-treated rats (Supporting Information S1), where the late increase of serum cinacalcet concentrations started 20 h post-dose and the concentrations oscillated around maximum between approximately 24 and 48 h. Mean C_{max} and T_{max} were 9.1 ng ml^{-1} and 37.7 h, respectively. Thus, the plateau phase was comparably high to cinacalcet C_{max} value observed in animals with no pre-treatment. Mean AUC at 12, 24 and 48 h was 16.5, 43.8 and 179.5 ng h ml^{-1}, respectively.

Lymphatic concentration profiles and cumulative lymphatic transport of abiraterone and cinacalcet in lymph duct cannulated rats are displayed in Figures 3 and 4. Drug concentrations achieved in the lymph were considerably higher (two orders) compared to serum concentrations after oral dosing for both drugs. Mean dose normalized lymphatic C_{max} was 434 ng ml^{-1} for abiraterone and 1,180 ng ml^{-1} for cinacalcet. The cumulative lymphatic transport curve had a sigmoidal shape in both drugs with slower absorption onset and faster intermediate transport which later decelerated. Cycloheximide pre-treatment in the lymph duct cannulated rats severely inhibited both lymphatic transport and portal absorption of cinacalcet (Figure 4).

Table 3 presents parameters of lymphatic transport for abiraterone and cinacalcet obtained via cannulation and cycloheximide chylomicron flow blocking methods. Absolute and relative bioavailability via lymph assessed using cannulation method was lower for abiraterone than for cinacalcet. Absorption of abiraterone did not increase after administration of abiraterone acetate in the form of oil solution in a separate experiment (Supporting Information S2). The absorption from abiraterone oil solution resulted in mean total absolute bioavailability of 1.7%, absolute bioavailability via lymph of 0.1% and relative bioavailability via lymph of 4.0% (at 7 h).

Cycloheximide chylomicron flow blocking method significantly overestimated the parameters of lymphatic transport for both drugs except for cinacalcet absolute bioavailability via lymph, for which the twofold higher mean value versus cannulation method did not reach statistical significance. The difference between the methods was particularly high in the estimation of relative bioavailability via lymph

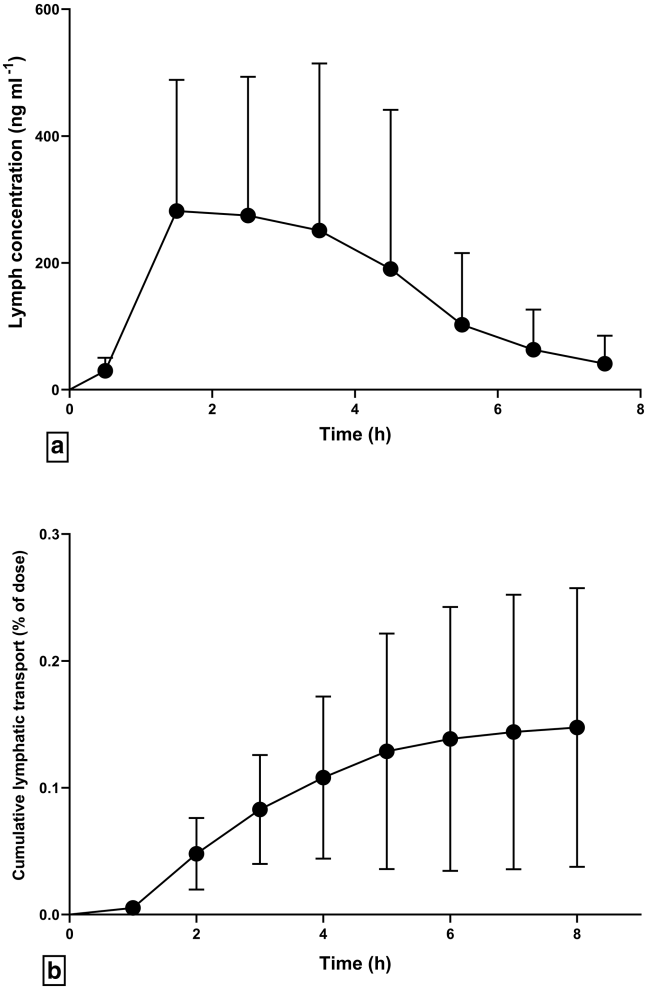

FIGURE 3 Lymphatic transport of abiraterone after enteral administration of abiraterone capsule (4 mg) to lymph duct cannulated anaesthetised rats, $n = 6$. (a) Mean ± SD dose normalized lymph concentration profile; (b) mean ± SD cumulative lymphatic transport

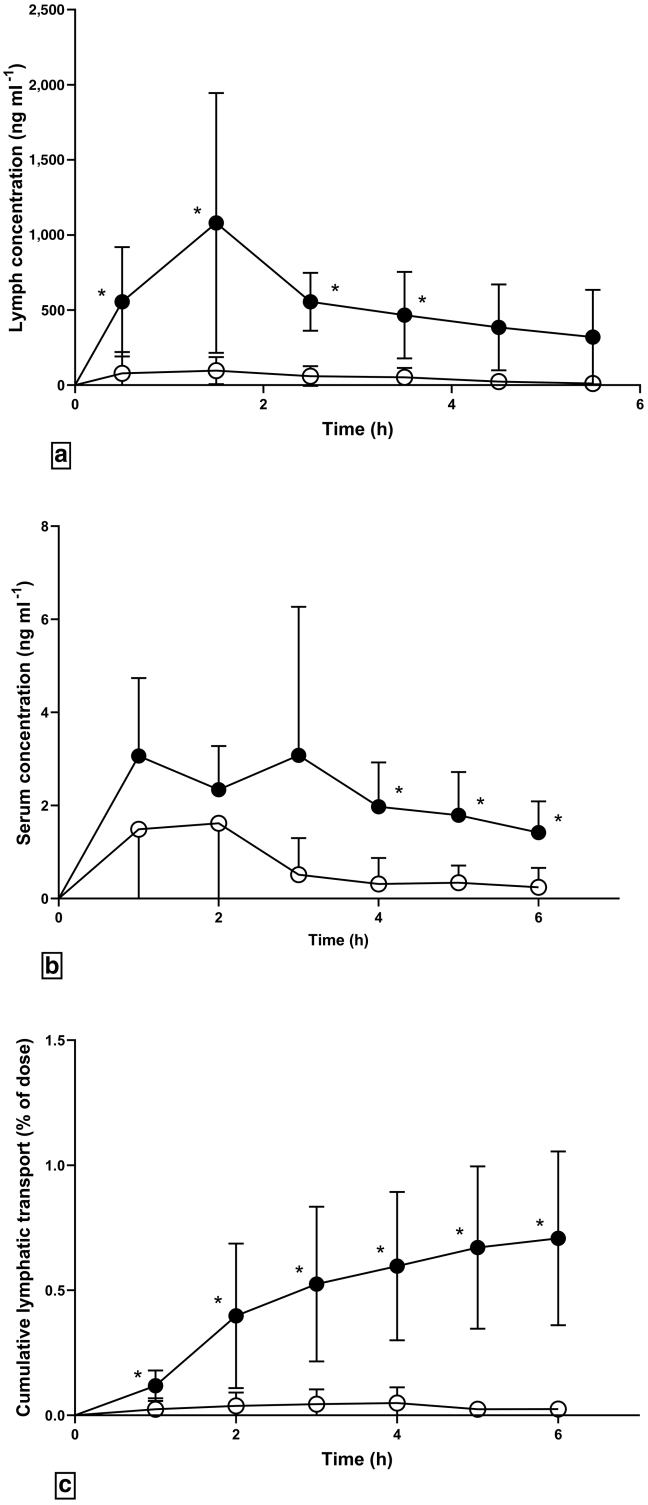

FIGURE 4 Lymphatic transport and portal absorption of cinacalcet after enteral administration of cinacalcet (3 mg) oil solution to lymph duct cannulated anaesthetised rats (closed circles, $n = 6$) and to lymph duct cannulated anaesthetised and cycloheximide pretreated rats (open circles, $n = 5$). (a) Mean ± SD dose normalized lymph concentration profiles; (b) mean ± SD dose normalized serum concentration profiles; (c) mean ± SD cumulative lymphatic transport. *$P < 0.05$ versus cycloheximide group

TABLE 3 Mean ± SD lymphatic transport parameters of abiraterone and cinacalcet after oral and duodenal administration of abiraterone capsule and cinacalcet oil solution assessed by lymph duct cannulation in anaesthetised rats and by cycloheximide chylomicron flow blocking method

	Method	n	Time (h)	F (%)	F_{AL} (%)	F_{RL} (%)
Abiraterone capsules	Cannulation	5	7.0	21.1 ± 22.0	0.15 ± 0.11	2.0 ± 2.1
	Cycloheximide	6	7.0	6.8 ± 3.0	4.1 ± 3.0*	56.4 ± 28.6*
Cinacalcet oil solution	Cannulation	6	6.0	3.7 ± 1.6	0.71 ± 0.35	21.0 ± 8.4
	Cycloheximide	8	6.0	2.3 ± 0.8*	1.4 ± 0.9	57.5 ± 21.8*

Abbreviations: F, total absolute bioavailability; F_{AL}, absolute bioavailability via lymph; F_{RL}, relative bioavailability via lymph.
*$P < 0.05$ versus cannulation method.

where cycloheximide method showed 28-fold higher value for abiraterone and 2.7-fold higher value for cinacalcet compared with cannulation method.

4 | DISCUSSION

Abiraterone serum pharmacokinetic parameters after oral and intravenous administration obtained in the current study correspond with previously published data (Gurav et al., 2012). Its low oral bioavailability (<10%) has been confirmed in intact animals and the value is very similar to the previously reported absolute bioavailability of 4.1% (Gurav et al., 2012). In lymph duct cannulated animals, the total absolute bioavailability was higher which could correspond with olive oil premedication as opposed to fasted state in the bioavailability study.

Absolute bioavailability of cinacalcet after oral administration in rats has not been previously reported. Although the oral bioavailability of 29% observed in our study is less compared to the 80% bioavailability reported in man, it corresponds to the range of 35–69% seen in animal mass balance studies in other species (G. N. Kumar et al., 2004). Oil solution administered in our study resulted in approximately two times longer T_{max} compared with previous study in rats receiving cinacalcet in aqueous drug dosing forms (Kuijpers, 2004).

Lymphatic transport of abiraterone administered as capsules was low in lymph duct cannulated rats despite achieving approximately 100 times higher lymphatic concentrations compared with serum. Long chain triglycerides present in the drug formulation or in the food ingested concurrently with the drug administration are inevitable for a significant extent of lymphatic transport (Han, Hu, Quach, Simpson, Trevaskis, & Porter, 2016b; Khoo et al., 2003). Therefore, abiraterone oil solution was tested in a separate study, but its oral bioavailability decreased compared to capsules, although the relative bioavailability via lymph was approximately twice as high. We assume that the main factor limiting lymphatic transport of abiraterone is its insufficient lipophilicity. There is strong evidence that lymphatic transport contributes significantly (F_{RL} > 10%) to the drug absorption only in compounds with log P > 5 (Charman & Stella, 1986). Log P value of abiraterone predicted by multiple calculation algorithms (ChemAxon, ALOGPS, PubChem) is approximately 4.5. Hence, it is relatively close under the cut point, which also corresponds to the 'borderline' lymphatic transport (F_{RL} of several %). Other molecules with similar log P and known extent of lymphatic transport are **seocalcitol** (log P 4.8, F_{RL} 7.4%) and ontazolast (log P 4.0, F_{RL} 6.8%) with comparable results (Grove et al., 2006; Hauss et al., 1998).

Both absolute and relative bioavailability via lymph increase with increasing bodyweight of animal species tested (dog > rat > mouse; Trevaskis et al., 2013). Using recently published allometric scaling formulas (Trevaskis et al., 2020), abiraterone F_{AL} in humans could be expected approximately fourfold higher than in rats, meaning 0.60% for the capsule formulation. Given the low absolute bioavailability, this could result in F_{RL} of 10–15% in men. Therefore, other factors than lymphatic transport seem to be more important for the extremely pronounced positive food effect on intestinal absorption of abiraterone, such as intraluminal solubilization in the presence of lipids and bile after food intake (Schultz et al., 2020) or enhanced supersaturation in the gastrointestinal fluids, which seems to be the driving factor for the drug absorption as reported *in vitro* (Stappaerts et al., 2015).

Cinacalcet lymphatic transport was shown to play a significant role in the intestinal drug absorption in our cannulation study. The results fit into the range of reported lymphatic transport parameters for compounds with similar lipophilicity while being close to those of venetoclax (log P 6.9, F_{RL} 18.8%; Choo et al., 2014). Predicted human F_{AL} of 2.8% and F_{RL} of ~50% calculated according to the allometric scaling formulas mentioned above suggest that lymphatic transport is highly relevant for cinacalcet absorption and it also likely contributes to the known food effect in humans.

Cycloheximide chylomicron flow blocking method has been used extensively in the last few years in the development of new drug formulations and investigation of their lymphatic transport. During the last 5 years, 46% of studies focusing on lymphatic drug transport applied the cycloheximide method (Rysanek et al., 2020). The main reason for its popularity is that the method does not require advanced surgical skills compared with the delicate lymph duct cannulation. Furthermore, it is inexpensive and overall easy to conduct. However, as the results of our current comparability studies demonstrate, cycloheximide method substantially overestimates lymphatic transport. It provided significantly higher F_{RL} values for both tested drugs when

compared to cannulation method. The overestimation was more pronounced in the less lipophilic abiraterone than in cinacalcet.

The lipophilicity dependent extent of overestimation seems to well correspond with the results published so far, where cycloheximide method yielded comparable lymphatic transport parameters to cannulation in highly lipophilic cholecalciferol (log P 7.5; Dahan & Hoffman, 2005) and halofantrine (log P 8.9; Lind et al., 2008). On the other hand, there are suspicious data for drugs with low lipophilicity that are not likely to be significantly transported through intestinal lymph vessels. Exorbitantly high lymphatic transport parameters have been reported for **topotecan** (log P 0.8, F_{RL} 53% for aqueous dosing solution; Wang et al., 2017), **docetaxel** (log P 2.4, F_{RL} 91%; Valicherla et al., 2016) and **paclitaxel** (log P 3, F_{RL} 60%; Zhang et al., 2016). Some of these unusually high lymphatic transport results have been attributed by the authors to the properties of the advanced drug formulations that should target and enhance lymphatic transport. However, the reliability of these data is questioned by the comparability evidence provided in our study and the performance of the advanced drug formulations supported solely by the cycloheximide chylomicron flow blocking method is uncertain.

Analysis of the limited amount of comparability data between cycloheximide and cannulation methods provided relationship between lipophilicity and the extent of F_{RL} overestimation in the cycloheximide method (Supporting Information S3). The reason why the lymphatic transport of less lipophilic drugs seems to be more overestimated by the cycloheximide method may lie in the proportion of inhibition of different ways involved in the drug absorption. In the combined cycloheximide/cannulation study, cycloheximide was shown to have deleterious effect both on lymphatic and non-lymphatic ways of cinacalcet absorption.

Another fact is that mean AUC decrease of abiraterone and cinacalcet after cycloheximide administration was 56% and 57%, respectively, that is, absorption and total bioavailability of both drugs were impaired similarly. Hence, the degree of F_{RL} overestimation was derived from the real extent of lymphatic transport assessed by lymph exposure measurement which was minimal in abiraterone but considerable in cinacalcet. These results correspond to data from cycloheximide studies published so far where there is no significant difference between cycloheximide induced AUC decrease ($\approx F_{RL}$) in compounds with log P < 5 and log P > 5 (median AUC decrease of 47.3% vs. 70.7%, $P > 0.05$; Rysanek et al., 2020). In this regard, the overestimation effect of cycloheximide method is inversely related to the real extent of lymphatic transport assessed in lymph duct cannulated animals, which is generally low in compounds with log P < 5 but can play a significant role in more lipophilic drugs.

It is evident that the effects of cycloheximide are complex. We observed rather unusual pattern of cinacalcet serum/tissue concentration increase in cycloheximide pre-treated animals that started approximately 20 h after the drug dosing. This pattern was consistent across all three experiments and was also apparent in all animals studied. Scanning the literature, such an increase was also seen in halofantrine, where the authors assumed there would be a depot from which the drug would later be released (Lind et al., 2008). Respecting the proposed cycloheximide mechanism of action (inhibition of intestinal chylomicron assembly), we hypothesized that this depot could be formed in the intestinal wall. However, this hypothesis was not supported by our biodistribution study results. Cinacalcet levels in the intestinal wall followed similar pattern to other organs or serum with no signs of early drug accumulation and subsequent release. We assume therefore that the late increase in cinacalcet concentrations was primarily due to delayed absorption from gastrointestinal lumen that was caused by severely reduced gastrointestinal motility, although possible contribution of impaired elimination by cycloheximide cannot be ruled out based on our data.

Previous *in vivo* cycloheximide studies have indeed shown multiple negative effects on gastrointestinal tract including delayed gastric emptying, reduced gastric secretion, reduced intestinal motility and various histopathologic changes (Plattner et al., 2001; Verbin et al., 1971; Yeh & Shils, 1969a, 1969b). These reports are not in concordance with the report by Dahan and Hoffman (2005) on good cycloheximide tolerability. In our study, the health status of the animals in the cycloheximide arms was frequently deteriorating. Within 4 to 5 h after cycloheximide treatment, about half of the rats were apathic and had bristled fur or diarrhoea-like exudate. This is linked to the fact that the administered cycloheximide dose in the standard protocol for chylomicron flow blocking method is close to its known LD_{50} (3.7 mg kg^{-1}; Cycloheximide Safety Datasheet, 2019).

Moreover, for the molecules like cinacalcet (and halofantrine), in which cycloheximide causes delayed and long-lasting increase of serum concentrations, the estimates of AUC and thus bioavailability strongly depend on the timeframe over which the study is conducted. The absorption was not only delayed but also significantly enhanced by cycloheximide if the pharmacokinetic profiles were measured well beyond the usual timeframe. Even 48 h after a single cinacalcet dose, the absorption phase was not completed, which indicates that the model lacks physiological relevance for absorption studies.

5 | CONCLUSION

Non-invasive cycloheximide chylomicron flow blocking method does not provide correct and reliable estimate on lymphatic transport of drugs and therefore should not be used to address this process of drug absorption anymore. The cycloheximide method largely overestimates the true lymphatic absorption measured directly as drug exposure in lymph collection.

Comparison of lymphatic transport data generated by direct drug concentration measurements in lymph collection and cycloheximide chylomicron flow method in rats has been conducted for two modern highly lipophilic compounds, that is, abiraterone acetate and cinacalcet hydrochloride. Whereas the lymphatic transport in direct measurement was shown to play a significant role in the intestinal absorption of cinacalcet, lymphatic transport of abiraterone was low. Absolute bioavailability following oral dosing of both drugs has also been described.

ACKNOWLEDGEMENTS

This work was supported by the Charles University (Univerzita Karlova v Praze) Project Progres Q25, grant No. SVV 260 523 and Charles University Research Centre program no. UNCE/SCI/014. PR, JR, JK and TB wish to acknowledge the support provided by Pharmaceutical Applied Research Centre (The Parc) for their scientific work.

AUTHOR CONTRIBUTIONS

PR, MŠ and OS were responsible for study design, study conduct, data analysis and manuscript writing. TB, JB and FŠ prepared the drug dosing forms. TG, PL and JP performed the animal surgery. JR, JK and NKC conducted the study. PK and TK were responsible for bioanalysis.

CONFLICT OF INTEREST

The authors declare no conflict of interest.

DECLARATION OF TRANSPARENCY AND SCIENTIFIC RIGOUR

This declaration acknowledges that this paper adheres to the principles for transparent reporting and scientific rigour of preclinical research as stated in the BJP guidelines for Design and Analysis and Animal Experimentation, and as recommended by funding agencies, publishers and other organizations engaged with supporting research.

DATA AVAILABILITY STATEMENT

All data generated during the study are available from the corresponding author upon reasonable request.

ORCID

Pavel Ryšánek https://orcid.org/0000-0001-6727-1663
Martin Šíma https://orcid.org/0000-0002-6541-738X

REFERENCES

Alexander, S. P. H., Kelly, E., Mathie, A., Peters, J. A., Veale, E. L., Armstrong, J. F., Faccenda, E., Harding, S. D., Pawson, A. J., Sharman, J. L., Southan, C., Buneman, O. P., Cidlowski, J. A., Christopoulos, A., Davenport, A. P., Fabbro, D., Spedding, M., Striessnig, J., Davies, J. A., … Wong, S. S. (2019). The concise guide to pharmacology 2019/20: Introduction and other protein targets. *British Journal of Pharmacology*, *176*, S1–S20. https://doi.org/10.1111/bph.14747

Boleslavská, T., Rychecký, O., Krov, M., Žvátora, P., Dammer, O., Beránek, J., Kozlík, P., Křížek, T., Hořínková, J., Ryšánek, P., Roušarová, J., Canová, N. K., Šíma, M., Slanař, O., & Štěpánek, F. (2020). Bioavailability enhancement and food effect elimination of abiraterone acetate by encapsulation in surfactant-enriched oil marbles. *The AAPS Journal*, *22*(6), 122. https://doi.org/10.1208/s12248-020-00505-5

Boleslavská, T., Světlík, S., Žvátora, P., Bosák, J., Dammer, O., Beránek, J., Kozlík, P., Křížek, T., Kutinová Canová, N., Šíma, M., Slanař, O., & Štěpánek, F. (2020). Preclinical evaluation of new formulation concepts for abiraterone acetate bioavailability enhancement based on the inhibition of pH-induced precipitation. *European Journal of Pharmaceutics and Biopharmaceutics*, *151*, 81–90. https://doi.org/10.1016/j.ejpb.2020.04.005

Caliph, S. M., Charman, W. N., & Porter, C. J. (2000). Effect of short-, medium-, and long-chain fatty acid-based vehicles on the absolute oral bioavailability and intestinal lymphatic transport of halofantrine and assessment of mass balance in lymph-cannulated and non-cannulated rats. *Journal of Pharmaceutical Sciences*, *89*(8), 1073–1084. https://doi.org/10.1002/1520-6017(200008)89:8<1073::aid-jps12>3.0.co;2-v

Charman, W. N. A., & Stella, V. J. (1986). Estimating the maximal potential for intestinal lymphatic transport of lipophilic drug molecules. *International Journal of Pharmaceutics*, *34*(1–2), 175–178. https://doi.org/10.1016/0378-5173(86)90027-X

Chi, K. N., Spratlin, J., Kollmannsberger, C., North, S., Pankras, C., Gonzalez, M., Bernard, A., Stieltjes, H., Peng, L., Jiao, J., Acharya, M., Kheoh, T., Griffin, T. W., Yu, M. K., Chien, C., & Tran, N. P. (2015). Food effects on abiraterone pharmacokinetics in healthy subjects and patients with metastatic castration-resistant prostate cancer. *Journal of Clinical Pharmacology*, *55*(12), 1406–1414. https://doi.org/10.1002/jcph.564

Choo, E. F., Boggs, J., Zhu, C., Lubach, J. W., Catron, N. D., Jenkins, G., Souers, A. J., & Voorman, R. (2014). The role of lymphatic transport on the systemic bioavailability of the Bcl-2 protein family inhibitors navitoclax (ABT-263) and ABT-199. *Drug Metabolism and Disposition*, *42*(2), 207–212. https://doi.org/10.1124/dmd.113.055053

Cycloheximide Safety Datasheet. (2019). Retrieved from https://www.caymanchem.com/msdss/14126m.pdf

Dahan, A., & Hoffman, A. (2005). Evaluation of a chylomicron flow blocking approach to investigate the intestinal lymphatic transport of lipophilic drugs. *European Journal of Pharmaceutical Sciences*, *24*(4), 381–388. https://doi.org/10.1016/j.ejps.2004.12.006

Grove, M., Nielsen, J. L., Pedersen, G. P., & Mullertz, A. (2006). Bioavailability of seocalcitol IV: Evaluation of lymphatic transport in conscious rats. *Pharmaceutical Research*, *23*(11), 2681–2688. https://doi.org/10.1007/s11095-006-9109-z

Gurav, S., Punde, R., Farooqui, J., Zainuddin, M., Rajagopal, S., & Mullangi, R. (2012). Development and validation of a highly sensitive method for the determination of abiraterone in rat and human plasma by LC-MS/MS-ESI: Application to a pharmacokinetic study. *Biomedical Chromatography*, *26*(6), 761–768. https://doi.org/10.1002/bmc.1726

Han, S., Hu, L., Quach, T., Simpson, J. S., Edwards, G. A., Trevaskis, N. L., & Porter, C. J. (2016a). Lymphatic transport and lymphocyte targeting of a triglyceride mimetic prodrug is enhanced in a large animal model: Studies in greyhound dogs. *Molecular Pharmaceutics*, *13*(10), 3351–3361. https://doi.org/10.1021/acs.molpharmaceut.6b00195

Han, S., Hu, L., Quach, T., Simpson, J. S., Trevaskis, N. L., & Porter, C. J. H. (2016b). Constitutive triglyceride turnover into the mesenteric lymph is unable to support efficient lymphatic transport of a biomimetic triglyceride prodrug. *Journal of Pharmaceutical Sciences*, *105*(2), 786–796. https://doi.org/10.1002/jps.24670

Hauss, D. J., Fogal, S. E., Ficorilli, J. V., Price, C. A., Roy, T., Jayaraj, A. A., & Keirns, J. J. (1998). Lipid-based delivery systems for improving the bioavailability and lymphatic transport of a poorly water-soluble LTB4 inhibitor. *Journal of Pharmaceutical Sciences*, *87*(2), 164–169. https://doi.org/10.1021/js970300n

Holm, R., Porter, C. J., Mullertz, A., Kristensen, H. G., & Charman, W. N. (2002). Structured triglyceride vehicles for oral delivery of halofantrine: Examination of intestinal lymphatic transport and bioavailability in conscious rats. *Pharmaceutical Research*, *19*(9), 1354–1361. https://doi.org/10.1023/a:1020311127328

Khoo, S. M., Edwards, G. A., Porter, C. J. H., & Charman, W. N. (2001). A conscious dog model for assessing the absorption, enterocyte-based metabolism, and intestinal lymphatic transport of halofantrine. *Journal of Pharmaceutical Sciences*, *90*, 1599–1607. https://doi.org/10.1002/jps.1110

Khoo, S. M., Shackleford, D. M., Porter, C. J., Edwards, G. A., & Charman, W. N. (2003). Intestinal lymphatic transport of halofantrine

occurs after oral administration of a unit-dose lipid-based formulation to fasted dogs. *Pharmaceutical Research*, *20*(9), 1460–1465. https://doi.org/10.1023/a:1025718513246

Kuijpers, G. (2004). Pharmacology and toxicology review of NDA (Application number 21–688).

Kumar, G. N., Sproul, C., Poppe, L., Turner, S., Gohdes, M., Ghoborah, H., Padhi, D., & Roskos, L. (2004). Metabolism and disposition of calcimimetic agent cinacalcet HCl in humans and animal models. *Drug Metabolism and Disposition*, *32*(12), 1491–1500. https://doi.org/10.1124/dmd.104.000604

Kumar, S. V., Rudresha, G., Gurav, S., Zainuddin, M., Dewang, P., Kethiri, R. R., Rajagopal, S., & Mullangi, R. (2013). Validated RP-HPLC/UV method for the quantitation of abiraterone in rat plasma and its application to a pharmacokinetic study in rats. *Biomedical Chromatography*, *27*(2), 203–207. https://doi.org/10.1002/bmc.2776

Lilley, E., Stanford, S. C., Kendall, D. E., Alexander, S. P., Cirino, G., Docherty, J. R., George, C. H., Insel, P. A., Izzo, A. A., Ji, Y., Panettieri, R. A., Sobey, C. G., Stefanska, B., Stephens, G., Teixeira, M., & Ahluwalia, A. (2020). ARRIVE 2.0 and the *British Journal of Pharmacology*: Updated guidance for 2020. *British Journal of Pharmacology*, *177*, 3611–3616. https://doi.org/10.1111/bph.15178

Lind, M. L., Jacobsen, J., Holm, R., & Mullertz, A. (2008). Intestinal lymphatic transport of halofantrine in rats assessed using a chylomicron flow blocking approach: The influence of polysorbate 60 and 80. *European Journal of Pharmaceutical Sciences*, *35*(3), 211–218. https://doi.org/10.1016/j.ejps.2008.07.003

Padhi, D., Salfi, M., & Harris, R. Z. (2007). The pharmacokinetics of cinacalcet are unaffected following consumption of high- and low-fat meals. *American Journal of Therapeutics*, *14*(3), 235–240. https://doi.org/10.1097/01.mjt.0000212703.71625.26

Percie du Sert, N., Hurst, V., Ahluwalia, A., Alam, S., Avey, M. T., Baker, M., Browne, W. J., Clark, A., Cuthill, I. C., Dirnagl, U., Emerson, M., Garner, P., Holgate, S. T., Howells, D. W., Karp, N. A., Lazic, S. E., Lidster, K., MacCallum, C. J., Macleod, M., … Würbel, H. (2020). The ARRIVE guidelines 2.0: Updated guidelines for reporting animal research. *British Journal of Pharmacology*, *177*(16), 3617–3624. https://doi.org/10.1111/bph.15193

Plattner, V., Leray, V., Leclair, M. D., Aube, A. C., Cherbut, C., & Galmiche, J. P. (2001). Interleukin-8 increases acetylcholine response of rat intestinal segments. *Alimentary Pharmacology & Therapeutics*, *15*(8), 1227–1232. https://doi.org/10.1046/j.1365-2036.2001.01009.x

Porter, C. J., Trevaskis, N. L., & Charman, W. N. (2007). Lipids and lipid-based formulations: Optimizing the oral delivery of lipophilic drugs. *Nature Reviews. Drug Discovery*, *6*(3), 231–248. https://doi.org/10.1038/nrd2197

Rysanek, P., Grus, T., Sima, M., & Slanar, O. (2020). Lymphatic transport of drugs after intestinal absorption: Impact of drug formulation and physicochemical properties. *Pharmaceutical Research*, *37*(9), 166. https://doi.org/10.1007/s11095-020-02858-0

Schultz, H. B., Meola, T. R., Thomas, N., & Prestidge, C. A. (2020). Oral formulation strategies to improve the bioavailability and mitigate the food effect of abiraterone acetate. *International Journal of Pharmaceutics*, *577*, 119069. https://doi.org/10.1016/j.ijpharm.2020.119069

Shackleford, D. M., Faassen, W. A., Houwing, N., Lass, H., Edwards, G. A., Porter, C. J., & Charman, W. N. (2003). Contribution of lymphatically transported testosterone undecanoate to the systemic exposure of testosterone after oral administration of two andriol formulations in conscious lymph duct-cannulated dogs. *The Journal of Pharmacology and Experimental Therapeutics*, *306*(3), 925–933. https://doi.org/10.1124/jpet.103.052522

Stappaerts, J., Geboers, S., Snoeys, J., Brouwers, J., Tack, J., Annaert, P., & Augustijns, P. (2015). Rapid conversion of the ester prodrug abiraterone acetate results in intestinal supersaturation and enhanced absorption of abiraterone: In vitro, rat in situ and human in vivo studies. *European Journal of Pharmaceutics and Biopharmaceutics*, *90*, 1–7. https://doi.org/10.1016/j.ejpb.2015.01.001

Trevaskis, N. L., Caliph, S. M., Nguyen, G., Tso, P., Charman, W. N., & Porter, C. J. (2013). A mouse model to evaluate the impact of species, sex, and lipid load on lymphatic drug transport. *Pharmaceutical Research*, *30*(12), 3254–3270. https://doi.org/10.1007/s11095-013-1000-0

Trevaskis, N. L., Hu, L., Caliph, S. M., Han, S., & Porter, C. J. (2015). The mesenteric lymph duct cannulated rat model: Application to the assessment of intestinal lymphatic drug transport. *Journal of Visualized Experiments*, *97*, e52389. https://doi.org/10.3791/52389

Trevaskis, N. L., Lee, G., Escott, A., Phang, K. L., Hong, J., Cao, E., Katneni, K., Charman, S. A., Han, S., Charman, W. N., Phillips, A. R. J., Windsor, J. A., & Porter, C. J. H. (2020). Intestinal lymph flow, and lipid and drug transport scale allometrically from pre-clinical species to humans. *Frontiers in Physiology*, *11*, 458. https://doi.org/10.3389/fphys.2020.00458

Trevaskis, N. L., McEvoy, C. L., McIntosh, M. P., Edwards, G. A., Shanker, R. M., Charman, W. N., & Porter, C. J. (2010). The role of the intestinal lymphatics in the absorption of two highly lipophilic cholesterol ester transfer protein inhibitors (CP524,515 and CP532,623). *Pharmaceutical Research*, *27*(5), 878–893. https://doi.org/10.1007/s11095-010-0083-0

Valicherla, G. R., Dave, K. M., Syed, A. A., Riyazuddin, M., Gupta, A. P., Singh, A., Wahajuddin, Mitra, K., Datta, D., & Gayen, J. R. (2016). Formulation optimization of Docetaxel loaded self-emulsifying drug delivery system to enhance bioavailability and anti-tumor activity. *Scientific Reports*, *6*, 26895. https://doi.org/10.1038/srep26895

Verbin, R. S., Longnecker, D. S., Liang, H., & Farber, E. (1971). Some observations on the acute histopathologic effects of cycloheximide in vivo. *The American Journal of Pathology*, *62*(1), 111–125.

Wang, T., Shen, L., Zhang, Z., Li, H., Huang, R., Zhang, Y., & Quan, D. (2017). A novel core-shell lipid nanoparticle for improving oral administration of water soluble chemotherapeutic agents: Inhibited intestinal hydrolysis and enhanced lymphatic absorption. *Drug Delivery*, *24*(1), 1565–1573. https://doi.org/10.1080/10717544.2017.1386730

Yeh, S. D. J., & Shils, M. E. (1969a). Cycloheximide effect on vitamin B12 absorption and intrinsic factor production in the rat. *Proceedings of the Society for Experimental Biology and Medicine*, *130*(4), 1260–1264. https://doi.org/10.3181/00379727-130-33768

Yeh, S. D. J., & Shils, M. E. (1969b). Cycloheximide inhibition of gastric secretion in the rat. *Proceedings of the Society for Experimental Biology and Medicine*, *130*(3), 807–810. https://doi.org/10.3181/00379727-130-33660

Zhang, B., Xue, A., Zhang, C., Yu, J., Chen, W., & Sun, D. (2016). Bile salt liposomes for enhanced lymphatic transport and oral bioavailability of paclitaxel. *Pharmazie*, *71*(6), 320–326. Retrieved from https://www.ncbi.nlm.nih.gov/pubmed/27455550

SUPPORTING INFORMATION

Additional supporting information may be found in the online version of the article at the publisher's website.

How to cite this article: Ryšánek, P., Grus, T., Lukáč, P., Kozlík, P., Křížek, T., Pozniak, J., Roušarová, J., Královičová, J., Kutinová Canová, N., Boleslavská, T., Bosák, J., Štěpánek, F., Šíma, M., & Slanař, O. (2021). Validity of cycloheximide chylomicron flow blocking method for the evaluation of lymphatic transport of drugs. *British Journal of Pharmacology*, *178*(23), 4663–4674. https://doi.org/10.1111/bph.15644

Příloha 4

ŠÍMA, M., KUTINOVÁ-CANOVÁ, N., RYŠÁNEK, P., HOŘÍNKOVÁ, J., MOŠKOŘOVÁ, D., SLANAŘ, O. Gastric pH in rats: Key determinant for preclinical evaluation of pH-dependent oral drug absorption. *Prague Med. Rep.,* 2019, 120, 1, 5-9.

Gastric pH in Rats: Key Determinant for Preclinical Evaluation of pH-dependent Oral Drug Absorption

Martin Šíma, Nikolina Kutinová-Canová, Pavel Ryšánek, Jana Hořínková, Denisa Moškořová, Ondřej Slanař
Institute of Pharmacology, First Faculty of Medicine, Charles University and General University Hospital in Prague, Prague, Czech Republic

Received November 14, 2018; Accepted May 2, 2019.

Key words: Gastric pH – Rats – Oral drug absorption – Omeprazole – Pentagastrin

Abstract: Data on gastric pH in rats to be used in preclinical models for pH-dependent drug absorption are still limited or contradictory. The aim of this study was to describe gastric pH in rats at fasted state and to evaluate its changes induced by pentagastrin or omeprazole in order to mimic gastric pH at fasted and fed human subjects. Twenty Wistar rats, fasting for 12 h, were randomly assigned into four treatment groups (n=5): control, pre-treated with omeprazole 2 h before pH measurement, pre-treated with omeprazole 12 h before pH measurement, and pre-treated with pentagastrin 20 min before pH measurement. An incision on the stomach wall was made in anesthetized animals, and pH of gastric juice was measured. The observed pH values were significantly different among groups (p=0.0341), with the median (IQR) values of gastric pH of 3.5 (2.7–4.2), 6.7 (4.7–7.0), 5.6 (3.5–6.4) and 2.2 (1.6–3.1) in control, omeprazole 2 h, omeprazole 12 h and pentagastin group, respectively. We recommend using short interval pentagastrin and 2 h omeprazole pre-treatment in fasting animals to model similar gastric pH as is expected in human fasted and fed state pharmacokinetic studies, respectively.

This study was supported by the Charles University Project Progres Q25 and a grant no. SVV 260373.

Mailing Address: Martin Šíma, PharmDr., PhD., Institute of Pharmacology, First Faculty of Medicine, Charles University and General University Hospital in Prague, Albertov 4, 128 00 Prague 2, Czech Republic; Phone: +420 224 964 135; Fax: +420 224 968 149; e-mail: martin.sima@lf1.cuni.cz

https://doi.org/10.14712/23362936.2019.5

Introduction

Although animal models are extensively used in the preclinical testing of drugs, sparse work has been reported on evaluating rats as a preclinical model for pH-dependent absorption studies (McConnell et al., 2008; Lubach et al., 2013). Gastric pH in fasted state is generally reported higher (3.9) in rats as compared with men (1.7) (Dressman et al., 1990; McConnell et al., 2008). Previous animal studies also provided conflicting results with respect of impact of food and other factors (Eastman and Miller, 1935; Ward and Coates, 1987; McConnell et al., 2008; Lubach et al., 2013). Moreover, previously published studies report wide inter-individual and intra-individual variability of gastric pH in rats (Fleisher et al., 1999).

Many drugs possess pH-dependent dissolution, solubility, or penetration through biological membranes (Lubach et al., 2013; Yasumuro et al., 2018) that is likely to affect the drug absorption after oral administration. Therefore, preclinical assessment of drug pharmacokinetics may be challenging.

The pentapeptide pentagastrin is well-known to stimulate gastric acid secretion in mammals and is widely used to increase acidity and reduce inter-individual variability in animal pharmacokinetic studies (Lubach et al., 2013), while omeprazole is a proton-pump inhibitor widely used for its potent inhibitory effect on gastric acid secretion (Larsson et al., 1983).

The aim of this study was to describe gastric pH in rats at fasted state and to evaluate its changes by pentagastrin or omeprazole to more closely mimic gastric pH at fasted and fed human subjects.

Material and Methods

Chemicals

Pentagastrin was purchased from Sigma-Aldrich (Prague, Czech Republic) and omeprazole was used as Helicid 40 Inf (Zentiva, Prague, Czech Republic). Ketamine and xylazine were used as Narkamon 100 mg/ml inj sol and Rometar 20 mg/ml inj sol (Bioveta, Ivanovice na Hané, Czech Republic), respectively.

Animals

Male Wistar rats (Velaz, Prague, Czech Republic) were used throughout the study. They were maintained under standard conditions (12-h light-dark cycle, 22 ± 2 °C temperature and 50 ± 10% relative humidity) and fed on water and standard granulated diet *ad libitum*. Twelve hours before gastric pH measurement animals were fasted, with free access to water, and were housed on a grid. All experiments were performed in accordance with the Guiding Principles in the Use of Animals in Charles University, First Faculty of Medicine, and every effort was made to minimize animal suffering. The experimental animal project was approved by the Ministry of Education, Youth and Sports of the Czech Republic under the negotiation number MSMT-9445/2018-8.

Table 1 – Pretreatment schedule in the study groups

Group	Treatment
Control	no treatment
Omeprazole 2 h	omeprazole 20 mg/kg i.p. 2 h before pH measurement
Omeprazole 12 h	omeprazole 20 mg/kg i.p. 12 h before pH measurement
Pentagastrin	pentagastrin 0.25 mg/kg s.c. 20 min before pH measurement

Experimental design

The rats were randomly assigned into four treatment groups (Table 1). The control group were fasted overnight without treatment. The other groups were treated with intraperitoneal omeprazole 20 mg/kg two hours before pH measurement, twelve hours before pH measurement, and subcutaneous pentagastin 0.25 mg/kg twenty minutes before pH measurement, respectively.

Dissection procedure and gastric pH measurement

The anesthetized rat (ketamine 100 mg/kg i.m. and xylazine 5 mg/kg i.m.) was placed on its back with its tail toward the investigator. The abdominal cavity was opened with a V-cut made through the abdominal wall starting at the base of the abdomen and proceeding diagonally across each side to the dorsolateral edge of the thorax. The skin flap was moved onto the chest and the stomach was located. The antrum cardiacum and pylorus of the stomach were ligated. An incision to the stomach wall was made, and gastric juice pH was measured with a pH meter S2K712 (Isfetcom Co., Ltd., Shimokayama, Japan). The pH meter was previously calibrated at two points using standards solutions of pH 4.0 and pH 7.0.

Statistical analysis

Median and interquartile range (IQR) values were calculated using MS Excel 2010 (Microsoft Corporation, Redmond, USA). Significance of differences in gastric pH between the groups was determined by the Kruskal-Wallis test using GraphPad Prism 3.02 (GraphPad Software, Inc., La Jolla, USA). Statistical significance was accepted at $p<0.05$.

Results

Twenty rats weighting 275–379 g were enrolled in this study; five rats per group. Measured gastric pH values in each group are presented in Figure 1. The observed pH values were significantly different among groups ($p=0.0341$), with the median (IQR) values of gastric pH of 3.5 (2.7–4.2), 6.7 (4.7–7.0), 5.6 (3.5–6.4) and 2.2 (1.6–3.1) in control, omeprazole 2 h, omeprazole 12 h and pentagastin group, respectively.

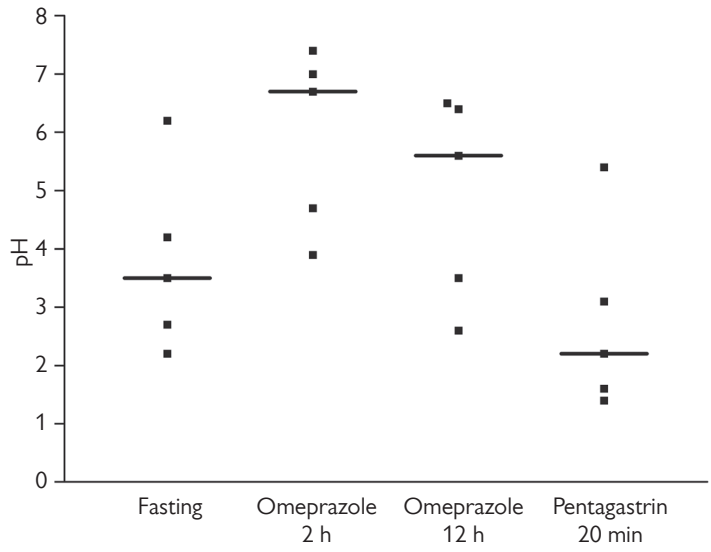

Figure 1 – Individual gastric pH values in fasted rats and rats treated with omeprazole and pentagastrin.

Discussion

We conducted this study to propose experimental conditions for subsequent preclinical pharmacokinetic studies with respect to gastric pH similarity to man.

Despite high inter-individual variability, median as well as minimum and maximum pH values increased in the following order: pentagastrin group, control group, omeprazole 12 h group, omeprazole 2 h group.

The pentagastrin group had similar median gastric pH to that reported in humans at fasting state (Dressman et al., 1990). Although the pH decreasing effect of pentagastrin was expected based on its known mechanism of action, previously published study by Lubach et al. (2013) did not show relevant impact of pentagastrin pretreatment on gastric pH that might be caused by unusually low control fasted state pH. Since pentagastrin is a compound with fast onset of action and short elimination half-life, the longer time interval between pentagastrin administration and pH measurement as compared with our study could also contribute to previously reported lack of pentagastrin effect.

Omeprazole pretreatment 2 hours before pH measurement increased the gastric pH to the range that is comparable to pH seen in man in fed state (Dressman et al., 1990) and similar omeprazole effect on pH in rats has been published recently by Yasumuro et al. (2018). However, although omeprazole is an irreversible proton pump inhibitor that maintains more than 50% of the effect at 24 h after dosing, the 12 h interval already lead to observable diminished omeprazole activity.

Numerous preclinical studies reported administration of drugs at fasting conditions based only on the fact that animals were food-deprived for specified time. It should be noted that we observed undigested wood shavings, fur, or excrements in the stomach of approximately half of the animals even when housed on a grid for the

whole 12 h fasting period before pH measurement. Thus, the animal model may mirror gastric pH with the standard human conditions at pharmacokinetic studies, however, the fasted state in cooperating human subjects might not be fully modelled in large proportion of animals with respect to potential effect of gastric content on gastric motility, its buffering and adsorption effects etc.

Conclusion

Based on our results, we recommend using short interval pentagastrin and 2 h omeprazole pretreatment in fasting animals to model similar gastric pH as is expected in human fasted and fed state pharmacokinetic studies, respectively.

References

Dressman, J. B., Berardi, R. R., Dermentzoglou, L. C., Russell, T. L., Schmaltz, S. P., Barnett, J. L., Jarvenpaa, K. M. (1990) Upper gastrointestinal (GI) pH in young, healthy men and women. *Pharm. Res.* **7**, 756–761.

Eastman, I. M., Miller, E. G. Jr. (1935) Gastrointestinal pH in rats as determined by the glass electrode. *J. Biol. Chem.* **110**, 255–262.

Fleisher, D., Li, C., Zhou, Z., Pao, L. H., Karim, A. (1999) Drug, meal and formulation interactions influencing drug absorption after oral administration. Clinical implications. *Clin. Pharmacokinet.* **36**, 233–254.

Larsson, H., Carlsson, E., Junggren, U., Olbe, L., Sjostrand, S. E., Skanberg, I., Sundell, G. (1983) Inhibition of gastric acid secretion by omeprazole in the dog and rat. *Gastroenterology* **85**, 900–907.

Lubach, J. W., Chen, J. Z., Hau, J., Imperio, J., Coraggio, M., Liu, L., Wong, H. (2013) Investigation of the rat model for preclinical evaluation of pH-dependent oral absorption in humans. *Mol. Pharmacol.* **10**, 3997–4004.

McConnell, E. L., Basit, A. W., Murdan, S. (2008) Measurements of rat and mouse gastrointestinal pH, fluid and lymphoid tissue, and implications for *in-vivo* experiments. *J. Pharm. Pharmacol.* **60**, 63–70.

Ward, F. W., Coates, M. E. (1987) Gastrointestinal pH measurement in rats: influence of the microbial flora, diet and fasting. *Lab. Anim.* **21**, 216–222.

Yasumuro, O., Uchida, S., Kashiwagura, Y., Suzuki, A., Tanaka, S., Inui, N., Watanabe, H., Namiki, N. (2018) Changes in gefitinib, erlotinib and osimertinib pharmacokinetics under various gastric pH levels following oral administration of omeprazole and vonoprazan in rats. *Xenobiotica* **48**, 1106–1112.

Příloha 5

HOŘÍNKOVÁ, J., KOZLÍK, P., KŘÍŽEK, T., MICHALIČKOVÁ, D., ŠÍMA, M., SLANAŘ, O. Post-mortem redistribution of alprazolam in rats. *Prague Med. Rep.*, 2020, 121, 4, 244-253.

 Prague Medical Report / Vol. 121 (2020) No. 4, p. 244–253

Post-mortem Redistribution of Alprazolam in Rats

Jana Hořínková[1], Petr Kozlík[2], Tomáš Křížek[2], Danica Michaličková[1], Martin Šíma[1], Ondřej Slanař[1]

[1]Institute of Pharmacology, First Faculty of Medicine, Charles University and General University Hospital in Prague, Prague, Czech Republic; [2]Department of Analytical Chemistry, Faculty of Science, Charles University, Prague, Czech Republic

Received March 7, 2020; Accepted November 2, 2020.

Key words: Alprazolam – Benzodiazepines – Overdose – Post-mortem redistribution – Animal model – Forensic toxicology

Abstract: The post-mortem toxicological findings may be misinterpreted, if the drug undergoes substantial post-mortem redistribution. As alprazolam is one of the most frequently evaluated drug for legal/forensic reasons in drug-related fatalities, we studied possible changes in alprazolam distribution after death in a rat model. Rats were sacrificed 30 minutes after alprazolam administration. Blood and tissue samples from 8 animals per sampling time were collected at 0, 2, 6, and 24 h after death. The experimental samples were assayed for alprazolam using validated UHPLC-PDA method. Median blood alprazolam concentrations increased approximately 2 times compared with ante-mortem levels due to the redistribution during early post-mortem phase and then slowly decreased with a half-life of 60.7 h. The highest alprazolam tissue concentrations were found in fat and liver and the lowest levels were observed in lungs and brain. The median amount of alprazolam deposited in the lungs was relatively stable over the 24-h post-mortem period, while in heart, liver and kidney the deposited proportion of administered dose increased by 43–48% in comparison with ante-mortem values indicating continuous accumulation of alprazolam into these tissues. These results provide evidence needed for the interpretation of toxicological results in alprazolam-related fatalities and demonstrate modest alprazolam post-mortem redistribution.

This study was supported by the Charles University Project Progres Q25, Research Centre program No. UNCE/SCI/014, and a grant No. SVV 260523.

Mailing Address: Martin Šíma, PharmDr., PhD., Institute of Pharmacology, First Faculty of Medicine, Charles University and General University Hospital in Prague, Albertov 4, 128 00 Prague 2, Czech Republic; Phone: +420 224 968 161; e-mail: martin.sima@lf1.cuni.cz

https://doi.org/10.14712/23362936.2020.21

Introduction

Drug overdose belongs among common causes of death worldwide with mortality rate of approximately 22.6 and 217 cases per million inhabitants in the EU and USA, respectively (European Monitoring Centre for Drugs and Drug Addiction, 2019). Although the majority of drug-related deaths in Europe occur in men, suicidal drug overdoses are more frequent in women. Most fatal drug overdoses are linked to the use of opioids, central nervous system depressants including benzodiazepines or polydrug use. Alprazolam itself was the fifth most common drug detected in 6,209 drug-related deaths in the USA in 2016 (Hilberg et al., 1999). Alprazolam is therefore frequently evaluated for legal/forensic reasons in drug-related fatalities.

The post-mortem toxicological findings may be misinterpreted if the drug undergoes substantial post-mortem redistribution, which is mainly expected for basic, lipophilic compounds widely distributed into peripheral compartments (Kugelberg et al., 2004; Castaing et al., 2006). The mechanisms of post-mortem redistribution have not been fully characterized, but leakage of intracellular content after cellular death (Musther et al., 2014), disruption of physiological barriers (Banks et al., 1992), degradation of the compounds by gut microorganisms and their diffusion from gastrointestinal content into the body tissues belong among known causes contributing to this phenomenon (European Monitoring Centre for Drugs and Drug Addiction, 2019). Moreover, metabolism may also continue during the first few hours after death (Jonsson et al., 2004).

Post-mortem redistribution has been described for number of drugs involved in fatal drug-related overdoses including haloperidol, morphine, citalopram, triazolam or diazepam (Koren and MacLeod, 1985; Shiota et al., 2004; Kposowa and McElvain, 2006).

Alprazolam with log P of 2.12 belongs among lipophilic compounds; it has apparent volume of distribution of approximately 1 l/kg in man (Greenblatt and Wright, 1993). These characteristics suggest possible role of post-mortem redistribution for this drug. Reports that evaluated central to peripheral blood concentrations ratios in human have suggested that alprazolam may exhibit a modest post-mortem redistribution (Hargrove and McCutcheon, 2008; Han et al., 2012). However, there are no data on post-mortem redistribution from direct measurement of alprazolam concentrations in particular tissues available. Therefore, the aim of our study was to describe possible changes in alprazolam distribution after death in rats.

Methods

Chemicals

Alprazolam was purchased from Sigma-Aldrich (Saint Louis, USA). The drug was then dissolved in a mixture of 70% ethanol and saline (1:1; v/v) for the purpose of intraperitoneal application. Isoflurane was used as IsoFlo 250 ml (Zoetis, Parsippany, USA).

Animals

Female Wistar rats (Velaz, Prague, Czech Republic) were used throughout the study. They were maintained under standard conditions (12-h light-dark cycle, 22 ± 2 °C temperature and 50 ± 10% relative humidity) and fed on water and standard granulated diet *ad libitum*. All experiments were performed in accordance with the Guiding Principles in the Use of Animals in Charles University, First Faculty of Medicine, and every effort was made to minimize animal suffering. The experimental animal project was approved by the Ministry of Education, Youth and Sports of the Czech Republic under the number MSMT-9445/2018-8.

Experimental procedure

Rats were randomly divided into four groups: (1) immediate autopsy, (2) autopsy 2 hours after death, (3) autopsy 6 hours after death, and (4) autopsy 24 hours after death. All animals were anesthetized by inhalation of 2–5% isoflurane and anaesthesia was maintained throughout the procedure. Following anesthetization, rats were injected alprazolam intraperitoneally at a dose of 4 mg or 6 mg for animals weighting ≤ 250 g or more, respectively. Thirty minutes after alprazolam administration, an ante-mortem blood sample was taken via cardiac puncture from each rat. Immediately following the sampling, rats were sacrificed by cervical dislocation and death was confirmed by the lack of a heartbeat. Following death, rats in groups 2–4 were left lying on their backs at room temperature (22 ± 2 °C) for the defined time to autopsy. Post-mortem aortic blood samples were drawn and the following tissue samples were also collected at the time of autopsy: liver (left lateral lobe), left kidney, heart, left lung, brain and abdominal fat. The tissue samples were cleaned with tissue paper, weighted and immediately homogenized with Tissue-Tearor homogenizer model 985-370 (BioSpec Products, Inc., Bartlesville, USA) in two volumes of 80% acetonitrile and then vortexed for 30 s. Both blood samples and tissue homogenates were centrifuged for 10 minutes at 2,500× *g* (4 °C). Blood samples and tissue supernatants were then stored at –80 °C before further processing. Before the chromatography analysis, the blood samples and tissue supernatants were deproteinized by acetonitrile, adding 60 µl of 100% acetonitrile to 20 µl of sample and performing deproteinization in an Eppendorf tube by vortexing for 15 s. Then, both blood and tissue samples were centrifuged at 16,500× *g* for 6 min, and 50 µl of supernatant was transferred into LC vials.

Analysis of alprazolam

Determination of alprazolam in different tissues and blood samples was carried out using Acquity UPLC H-class equipment (Waters Corporation, Milford, MA). LC column Poroshell HPH C18 (3.00 mm i.d. × 100 mm, 2.7 µm) from Agilent Technologies (Waldbronn, Germany), thermostatted at 30 °C, was used for the analysis. The mobile phase consisted of 10 mM ammonium phosphate, pH 2.80 (Solvent A) and acetonitrile (Solvent B). The flow rate of the mobile phase

was maintained at 0.5 ml/min. The optimized gradient program (min/% B) was 0/30, 1/30, 3.5/60, 4/80, 7/80, 7.5/30, and 10/30. The injection volume was 1 µl, and samples were kept at 10 °C. Detection was performed by diode array detector, and the wavelength was set to 245 nm.

The method was validated according to the FDA guidance on analytical procedures and method validation to demonstrate that it is suitable for its intended purpose (U. S. Food and Drug Administration, 2015). The selectivity of the method was verified by mass spectrometry operated in the scan mode (Triple Quad 6460 mass spectrometer; Agilent Technologies, Waldbronn, Germany).

Selectivity was monitored by injecting all studied tissue extracts. These chromatograms showed no interfering compound (no *m/z* was observed except *m/z* corresponding to alprazolam) within the retention time window of alprazolam. Moreover, the DAD peak purity test of all analysed samples was successfully met for the alprazolam peak, which ensures high selectivity. Selectivity was thus confirmed independently by DAD and mass spectrometry. The calibration curve was constructed in the 80% acetonitrile with nine concentration levels (0.1; 0.2; 0.5; 1; 2; 5; 10; 50; 100 µg/ml) by plotting the peak area of alprazolam against its concentration. Calibration was performed before each batch of samples. Standard plots were constructed and linearity was evaluated statistically by linear regression analysis using the least-squares regression method. To confirm the reliability of our results derived from the calibration curve, we performed determination using the standard addition method with selected samples of different tissue extracts and blood. The standard was added into blood and tissue extract samples before deproteinization to include the potential effect of deproteinization. No significant difference in concentration means was observed between results obtained using both methods. This result proved that tissue and blood matrices have no effect on the reliable quantification of alprazolam. The linearity was evaluated through the calibrations providing coefficients of determination (R^2) higher than 0.9997 which indicate excellent linearity. Limit of detection value was 0.02 µg/ml, determined as $3.3 \times \sigma/S$ ratio, where σ is the highest baseline noise obtained from the blank blood/tissue extracts, and S is the slope of the regression line (based on peak heights). Limit of quantification was the lowest point of the calibration (0.1 µg/ml).

Method accuracy and precision were evaluated by measuring 5 replicates at four different concentrations (0.1; 1; 5, and 50 µg/ml) prepared by spiking alprazolam into blank tissue extracts and blood. The accuracy (relative error, %) was within ± 3.0%, and the inter- and intra-day precisions (RSD, %) were within ± 2.5%. These samples were also used as quality control (QC) samples. QC samples were injected after each 7th sample to assess the validity of the analytical method. Recovery was evaluated by comparing the area of the alprazolam standard peak of the pre-protein-precipitation spiked blood sample with that of the corresponding post-protein-precipitation spiked sample at three concentrations (0.1; 10, and 50 µg/ml). Since there is no reference material of different tissues containing alprazolam, the recovery

was simulated by fortifying of different tissue homogenates with the standard of alprazolam at three concentrations (0.1; 10, and 50 μg/ml). Extraction and protein precipitation was performed with 80% acetonitrile and vortexed for 30 s. The recovery ranged from 96.8 to 100.9%.

Data analysis and statistics

Tissue concentrations (μg/g) were calculated from measured supernatant concentrations (μg/ml), used amounts of solvent (ml) and weights of homogenized tissues (g). Subsequently, both tissue and blood concentrations were normalized per dose of 20 mg/kg.

Distribution half-life was calculated as $(t \times \ln 2)/\ln(C_2/C_{24})$, where C_2 and C_{24} are median alprazolam blood concentration 2 and 24 h after death, respectively, and t is 22 h as the time between C_2 and C_{24}.

Median and interquartile range (IQR) values were calculated using MS Excel 2010 (Microsoft Corporation, Redmond, USA). Significance of differences in alprazolam concentrations/tissue distribution between group 1 and the other groups was determined by the Mann-Whitney test, while potential differences in weights and weight-normalized doses between study groups were examined by the Kruscal-Wallis test using GraphPad Prism 8.2.1 (GraphPad Software, Inc., La Jolla, USA). Statistical significance was considered at $p \leq 0.05$.

Results

Thirty-two female rats weighing 162–365 g were enrolled in this study; eight rats per group. Administered alprazolam doses ranged from 16.4 to 24.7 mg/kg. There were no significant differences in animal weight ($p=0.97$) or administered alprazolam doses ($p=0.96$) between study groups.

Post-mortem changes in dose-normalized blood and tissue concentrations of alprazolam are presented in Figure 1. All post-mortem groups showed significantly increased blood drug concentrations compared with ante-mortem alprazolam blood levels. The ratio between median post-mortem and ante-mortem alprazolam blood concentrations were 1.78, 1.54 and 1.39 at 2, 6 and 24 hours after death, respectively. Thus, steep rise in alprazolam blood levels during early post-mortem phase was followed by slow decrease with a half-life of 60.7 h.

Distribution of alprazolam into the tissues expressed as percentages of the total administered alprazolam dose are showed in Table 1.

Discussion

This study was designed to describe possible post-mortem alprazolam redistribution in rat in order to improve our understanding and interpretation of the toxicological findings in alprazolam related fatalities that belong among frequent intentional drug overdoses world-wide. We conducted the study in female rats, since women are 4 times more likely to die from drug poisoning than men (Kposowa and McElvain,

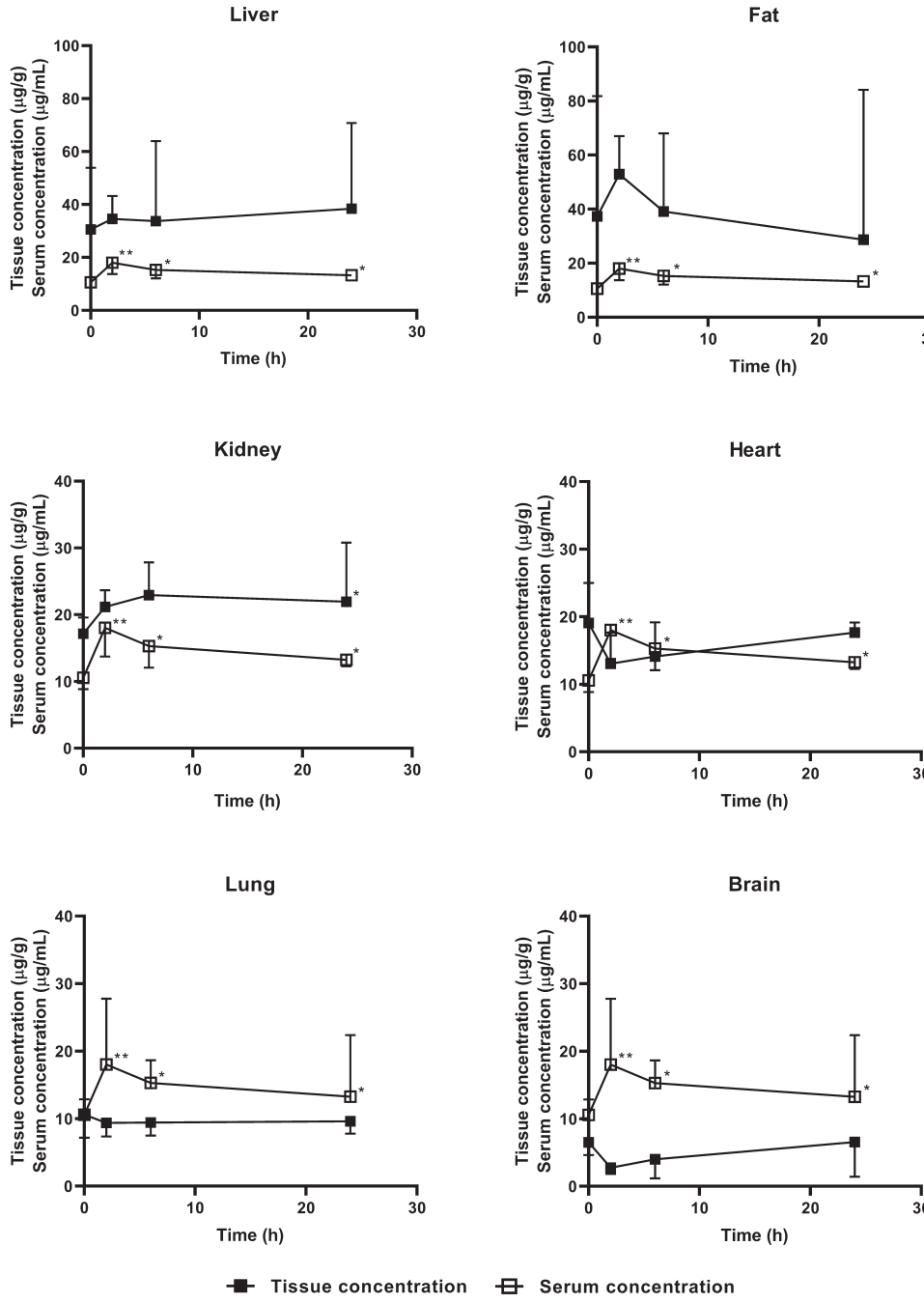

*Figure 1 – Post-mortem changes of alprazolam concentrations normalized per dose of 20 mg/kg in the rat blood and tissues. Values are represented as median (interquartile range); n=8; *p<0.05; **p<0.005 vs. 0 h after death.*

Table 1 – Alprazolam tissue distribution expressed as median percentages of total administered alprazolam dose (%) at time after death

	Group 1 0 h	Group 2 2 h	Group 3 6 h	Group 4 24 h
Liver	5.17	7.11	8.17*	7.38
Kidney (left)	0.29	0.34	0.42	0.43*
Heart	0.21	0.22	0.23	0.32
Lung (left)	0.08	0.08	0.09	0.10
Brain	0.32	0.10	0.14	0.24

*p<0.05 vs. 0 h after death

2006). A fix dose of 4 or 6 mg was administered to each animal with respect to its actual body weight in order to reach approximate dose of 20 mg/kg for each animal, which corresponds to human equivalent dose of 3.3 mg/kg (rat/human dose conversion factor of 6 has been reported) (Nair and Jacob, 2016). The actual doses ingested are usually unknown in human alprazolam-related fatalities, however, the drug has been reported among compounds with the most frequent toxic levels detected in forensic analyses in drug related fatalities (Jonsson et al., 2004). A study in 131 deliberate alprazolam self-poisoning cases reported that the median (IQR) alprazolam dose was 23 defined daily doses (10–40) (Isbister et al., 2004), which is less in comparison with the dose we used. However, other individual case reports have shown high plasma and tissue levels indicating that the dose ingested must have been considerably higher (Jenkins et al., 1997). Since the doses ingested in an intentional overdose are in reality highly uncertain, we have chosen the human equivalent dose for our study corresponding to the possible worst case scenario for acute intoxication after ingestion of whole alprazolam high strength package (100 tablets, 2 mg).

Alprazolam blood levels reported for human fatal intoxications are extremely variable. While some repots mention plasma levels within the toxic range of 0.1–0.4 μg/ml (Jones et al., 2016; McIntyre et al., 2017), Jenkins et al. (1997) detected plasma levels in a human alprazolam fatality of 2.1–2.3 μg/ml that is approximately 20% of the ante-mortal levels seen in our study.

We observed significantly increased blood drug concentrations at all sampling times post-mortem. This phenomenon has been previously described for some other lipophilic drugs, e.g. thioridazine, morphine or citalopram (Koren and Klein, 1992; Kugelberg et al., 2004; Castaing et al., 2006). However, the interindividual variability of the drug concentration increase after death is high, in a few animals the post-mortem increase of alprazolam blood levels was as large as 6-fold. This is again comparable to the previous observations for morphine with up to 5-fold drug level increase (Koren and Klein, 1992).

The highest alprazolam tissue concentrations were found in fat and liver in group 1 (autopsy 30 min after intraperitoneal administration), whereas the lowest levels were observed in lungs and brain. These findings follow a similar distribution pattern described for ^{14}C-alprazolam 30 min after intravenous administration (Banks et al., 1992) and correspond also to distribution of diazepam and triazolam that both belong among benzodiazepines (Shiota et al., 2004). Although alprazolam concentration in the brain was low, the percentual distribution of the administered dose was similar to that found in left kidney at the time of death (Table 1). The highest percentage of alprazolam dose were accumulated in the liver. It can be expected that largest proportion of alprazolam dose accumulates in adipose tissue, however, as the total body fat is unknown the distribution could not be estimated.

The amount of alprazolam deposited in the lung tissue was relatively stable over the 24-h post-mortem period, while in heart, liver and kidney the deposited proportion of administered dose increased by 43–48% at 24 h after death in comparison with pre-mortem values indicating continuous accumulation of alprazolam into these tissues. The tissue concentrations tended to increase correspondingly to the percentage of the dose deposited in liver and kidney, while the drug tissue concentration dropped in the heart early after death contrary to the increasing drug accumulation in the tissue. This was likely caused by an increased intramyocardial water content that may be seen after death especially in females (Boyd and Knight, 1963). On the other hand, both brain alprazolam content and brain tissue concentrations decreased early after death with subsequent tendency to reach equilibrium with blood concentrations. Due to the high variability of tissue concentrations obtained, the differences of tissue concentrations from the post-mortem sample only reached statistical significance for kidney at 24 h.

The clinical data on alprazolam distribution post-mortem are extremely limited. In a single fatal overdose, the ratios between tissue and plasma drug levels in kidney and liver were approximately 1.7 and 4.2, respectively (Jenkins et al., 1997), which well corresponds to the individual tissue to plasma ratios seen in our study ranging from 0.2 to 4.1 for kidney and from 0.9 to 9.2 for liver samples. The anatomical proximity between the different organs in rats in our model thus did not result in unrealistically overestimated post-mortem redistribution values for the human toxicological findings. In case there is an unabsorbed drug in the stomach or gastrointestinal tract at the time of death, this may be redistributed to surrounding tissues (Pounder et al., 1996). In order to eliminate this phenomenon, we administered alprazolam intraperitoneally in this study. Although the most alprazolam overdoses are expected to follow oral ingestion of the drug in humans, the absorption is fast and complete with T_{max} of 1 h and absolute bioavailability 80–100% (Greenblatt and Wright, 1993). Therefore, substantial alprazolam redistribution from the gastrointestinal tract is not expected in clinical settings.

Conclusion

Median central blood alprazolam concentrations increased approximately 1.5–2 times due to the redistribution over the 24-h post-mortem period and there was a substantial variability of the extent of alprazolam redistribution (0.9–6.1 fold).

The median amount of alprazolam deposited in the lung tissue was relatively stable over the 24-h post-mortem period, while in heart, liver and kidney the deposited proportion of administered dose increased by 43–48% at 24 h after death in comparison with pre-mortem values indicating continuous accumulation of alprazolam into these tissues.

These results demonstrate modest alprazolam redistribution post-mortem. However, due to the high variability of alprazolam blood and tissue concentrations seen, the estimation of drug exposure or time from death can't be reliably done based on these pharmacokinetic data.

References

Banks, W. R., Yamakita, H., Digenis, G. A. (1992) Metabolism and distribution of 1-[14C]alprazolam in rats. *J. Pharm. Sci*. **81**, 797–801.

Boyd, E. M., Knight, L. M. (1963) Postmortem shifts in the weight and water levels of body organs. *Toxicol. Appl. Pharmacol*. **5**, 119–128.

Castaing, N., Titier, K., Canal-Raffin, M., Moore, N., Molimard, M. (2006) Postmortem redistribution of two antipsychotic drugs, haloperidol and thioridazine, in the rat. *J. Anal. Toxicol*. **30**, 419–425.

European Monitoring Centre for Drugs and Drug Addiction (EMCDDA) (2019) *European Drug Report: Trends and Developments*. Available at: http://www.emcdda.europa.eu/system/files/publications/11364/20191724_TDAT19001ENN_PDF.pdf

Greenblatt, D. J., Wright, C. E. (1993) Clinical pharmacokinetics of alprazolam. Therapeutic implications. *Clin. Pharmacokinet*. **24**, 453–471.

Han, E., Kim, E., Hong, H., Jeong, S., Kim, J., In, S., Chung, H., Lee, S. (2012) Evaluation of postmortem redistribution phenomena for commonly encountered drugs. *Forensic Sci. Int*. **219**, 265–271.

Hargrove, V. M., McCutcheon, J. R. (2008) Comparison of drug concentrations taken from clamped and unclamped femoral vessels. *J. Anal. Toxicol*. **32**, 621–625.

Hilberg, T., Ripel, A., Slordal, L., Bjorneboe, A., Morland, J. (1999) The extent of postmortem drug redistribution in a rat model. *J. Forensic Sci*. **44**, 956–962.

Isbister, G. K., O'Regan, L., Sibbritt, D., Whyte, I. M. (2004) Alprazolam is relatively more toxic than other benzodiazepines in overdose. *Br. J. Clin. Pharmacol*. **58**, 88–95.

Jenkins, A. J., Levine, B., Locke, J. L., Smialek, J. E. (1997) A fatality due to alprazolam intoxication. *J. Anal. Toxicol*. **21**, 218–220.

Jones, A. W., Holmgren, A., Ahlner, J. (2016) Post-mortem concentrations of drugs determined in femoral blood in single-drug fatalities compared with multi-drug poisoning deaths. *Forensic Sci. Int*. **267**, 96–103.

Jonsson, A., Holmgren, P., Ahlner, J. (2004) Fatal intoxications in a Swedish forensic autopsy material during 1992–2002. *Forensic Sci. Int*. **143**, 53–59.

Koren, G., MacLeod, S. M. (1985) Postmortem redistribution of digoxin in rats. *J. Forensic Sci*. **30**, 92–96.

Koren, G., Klein, J. (1992) Postmortem redistribution of morphine in rats. *Ther. Drug Monit*. **14**, 461–463.

Kposowa, A. J., McElvain, J. P. (2006) Gender, place, and method of suicide. *Soc. Psychiatry Psychiatr. Epidemiol*. **41**, 435–443.

Kugelberg, F. C., Druid, H., Carlsson, B., Ahlner, J., Bengtsson, F. (2004) Postmortem redistribution of the enantiomers of citalopram and its metabolites: an experimental study in rats. *J. Anal. Toxicol*. **28**, 631–637.

McIntyre, I. M., Gary, R. D., Joseph, S., Stabley, R. (2017) A fatality related to the synthetic opioid U-47700: Postmortem concentration distribution. *J. Anal. Toxicol*. **41**, 158–160.

Musther, H., Olivares-Morales, A., Hatley, O. J., Liu, B., Rostami Hodjegan, A. (2014) Animal versus human oral drug bioavailability: do they correlate? *Eur. J. Pharm. Sci*. **57**, 280–291.

Nair, A. B., Jacob, S. (2016) A simple practice guide for dose conversion between animals and human. *J. Basic Clin. Pharm*. **7**, 27–31.

Pounder, D. J., Fuke, C., Cox, D. E., Smith, D., Kuroda, N. (1996) Postmortem diffusion of drugs from gastric residue: an experimental study. *Am. J. Forensic Med. Pathol*. **17**, 1–7.

Shiota, H., Nakashima, M., Terazono, H., Sasaki, H., Nishida, K., Nakamura, J., Taniyama, K. (2004) Postmortem changes in tissue concentrations of triazolam and diazepam in rats. *Leg. Med. (Tokyo)* **6**, 224–232.

U. S. Food and Drug Administration; Department of Health and Human Services (2015) *Analytical Procedures and Methods Validation for Drugs and Biologics: Guidance for Industry*. Available at: https://www.fda.gov/files/drugs/published/Analytical-Procedures-and-Methods-Validation-for-Drugs-and-Biologics.pdf